

**FAST FOURIER TRANSFORM AND FORMULATION OF
ECONOMIC RECESSION INDUCED STOCHASTIC VOLATILITY
MODELS FOR AMERICAN OPTIONS COMPUTATION**

BY

Philip Ajibola BANKOLE

Matric No.: 128309

B.Sc. Mathematics (Ibadan), M.Sc. Mathematics (Ibadan)

A Thesis in the Department of Mathematics
Submitted to the Faculty of Science in partial fulfilment of the
requirements for the Degree of

DOCTOR OF PHILOSOPHY

of the

UNIVERSITY OF IBADAN

8 DECEMBER, 2022

CERTIFICATION

I certify that this study was carried out by Philip Ajibola BANKOLE with Matriculation Number 128309 in the Department of Mathematics, Faculty of Science, University of Ibadan under my supervision

.....

Supervisor

Professor Olabisi O. Ugbebor,

B.Sc. (Ibadan), Ph.D. (London)

Department of Mathematics,

University of Ibadan, Nigeria.

.....

Co-Supervisor

Dr M. E. Egwe,

B.Sc., M.Sc., Ph.D. (Ibadan)

Department of Mathematics,

University of Ibadan, Nigeria.

DEDICATION

I dedicate this thesis to the Almighty God.

ACKNOWLEDGEMENTS

All glory be to God for making this study a success. Without Him, I am nobody. May His name be praised forever.

Finally, many thanks to all whose names were not mentioned here. God bless you all.

Philip Ajibola BANKOLE

ABSTRACT

Economic recession has become a global and recurring phenomenon which poses worrisome uncertainties on assets' returns in financial markets. Various stochastic models have been formulated in response to price instability in financial markets. However, the existing stochastic volatility models did not incorporate the concept of economic recession and induced volatility-uncertainty for options price valuation in a recessed economic setting. Therefore, this study was geared towards the formulation of economic recession-induced stochastic models for price computation.

Stochastic modelling methods with probabilistic uncertainty measure were used to formulate two new volatility models incorporating economy recession volatility uncertainties. The Feynman-Kac formula was applied to derive the characteristic functions for the two novel models. The derived characteristic functions were used to obtain an inverse-Fourier analytic formula for European and American-style options. A modified Carr and Madan Fast-Fourier Transform (FFT)-algorithm was used to obtain an approximate solution for the American-call option, and a class of Multi-Assets option in multi-dimensions. Itô Calculus was used to obtain an explicit formula for a Factorial function Black-Scholes Partial Differential Equations (BS-PDE) for American options subject to moving boundary conditions. The FFT call-prices accuracy test at varied fineness grid points N was investigated using an FFT-algorithm via Maple, taking BS-prices as benchmark. Sample paths and numerical simulations were generated via software codes for the control regime-switching Triple Stochastic Volatility Heston-like (TSVH) model.

The derived Uncertain Affine Exponential-Jump Model (UAEM) with recession, induced stochastic-volatility and stochastic-intensity, and a control regime-switching Triple Stochastic Volatility Heston-like (TSVH) formulated with respect to economy recession volatility uncertainties are:

$$\begin{cases} d \ln S(t) = (r - q - \lambda(t)m)dt + \sqrt{\sigma(t)}dW_s(t) + (e^\nu - 1)dN(t), & S(0) = S_0 > 0 \\ d\sigma(t) = \kappa_\sigma(\beta^* + \beta^{rec} - \sigma(t))dt + \xi_\sigma\sqrt{\sigma(t)}dW_\sigma(t), & \sigma(0) = \sigma_0 > 0 \\ d\lambda(t) = \kappa_\lambda(\theta - \lambda(t))dt + \xi_\lambda\sqrt{\lambda(t)}dW_\lambda(t), & \lambda(0) = \lambda_0 > 0. \end{cases}$$

and

$$\begin{cases} dy_t = (r - q)dt + \sqrt{v_1(t)}dW_1(t) + \sqrt{v_2(t)}dW_2(t) + \alpha(\sqrt{v_3(t)}dW_3(t)), & S(0) = S_0 > 0 \\ dv_1(t) = \kappa_1(\theta_1 - v_1(t))dt + \sigma_1\sqrt{v_1(t)}d\widehat{W}_1(t), & v_1(0) = v_{1_0} > 0. \\ dv_2(t) = \kappa_2(\theta_2 - v_2(t))dt + \sigma_2\sqrt{v_2(t)}d\widehat{W}_2(t), & v_2(0) = v_{2_0} > 0. \\ dv_3(t) = \alpha(\kappa_3(\theta_3 - v_3(t))dt + \sigma_3\sqrt{v_3(t)}d\widehat{W}_3(t))_{recession}, & v_3(0) = v_{3_0} > 0 \end{cases}$$

respectively, where α was a binary control parameter defined as:

$$\alpha := \begin{cases} 0, & \text{if the economy is not in recession;} \\ 1, & \text{if the economy is in recession.} \end{cases}$$

The inverse-Fourier analytic formulae for European-style and American-style call-options obtained for the UAEM-process are:

$$E_T^{call}(k) = \frac{\exp(-\alpha k)}{\pi} \int_0^\infty e^{-(rT+iu k)} \varphi_\tau(u - (\alpha + 1)i) \times \left(\frac{\alpha^2 + \alpha - u^2 - i(2\alpha + 1)u}{\alpha^4 + 2\alpha^3 + \alpha^2 + (2(\alpha^2 + \alpha) + 1)u^2 + u^4} \right) du$$

$$\text{and } A_t(k) = \frac{\exp(-\alpha k)}{\pi} \int_0^\infty e^{-(rT+iu_k)} \times \left(\frac{\varphi_\tau(u - (\alpha + 1)i) (\alpha^2 + \alpha - u^2 - i(2\alpha + 1)u)}{\alpha^4 + 2\alpha^3 + \alpha^2 + (2(\alpha^2 + \alpha) + 1)u^2 + u^4} \right) du + P_t,$$

respectively where P_t is premium price. The approximate solution obtained for American-call option via FFT-algorithm for the UAEM-process was:

$$A_\tau(k_u) \approx \frac{\exp(-\alpha k)}{\pi} \sum_{j=1}^N e^{-iu_j \zeta \eta (j-1)(u-1)} e^{i\varpi u_j} \psi_T(u_j) \eta + P_t, \quad \text{where } 1 \leq u \leq N \text{ and } \zeta \eta = \frac{2\pi}{N}.$$

The derived multi-Assets options prices formula in n-dimension was:

$$V_T(k_{1,p_1}, k_{2,p_2}, \dots, k_{n,p_n}) \approx \frac{e^{-(\alpha_1 k_{1,p_1} + \alpha_2 k_{2,p_2} + \dots + \alpha_n k_{n,p_n})}}{(2\pi)^n} \Omega(k_{1,p_1}, k_{2,p_2}, \dots, k_{n,p_n}) \prod_{j=1}^n h_j,$$

where $0 \leq p_1, p_2, \dots, p_n \leq N - 1$ and

$$\begin{aligned} \Omega(k_{1,p_1}, k_{2,p_2}, \dots, k_{n,p_n}) &= \sum_{m_1=1}^{N_1-1} \sum_{m_2=1}^{N_1-1} \dots \sum_{m_n=1}^{N_1-1} e^{-\frac{2\pi}{N} \left((m_1 - \frac{N}{2})(p_1 - \frac{N}{2}) + (m_2 - \frac{N}{2})(p_2 - \frac{N}{2}) + \dots + (m_n - \frac{N}{2})(p_n - \frac{N}{2}) \right)} \\ &\times \psi_T(u_1, u_2, \dots, u_n). \end{aligned}$$

The derived explicit formula for the Factorial function BS-PDE was:

$$S(T) = S(t_0) \exp \left[n! \left(r + \frac{1}{2}(n-1)\sigma^2 \right) (T - t_0) + n! \sigma \left(W(t) - W(t_0) \right) \right], \quad S(t_0) \neq 0,$$

and the TSVH call pricing formula derived was:

$$C(K) = S_t e^{-q\tau} P_1 - K e^{-r\tau} P_2$$

such that

$$\begin{aligned} P_1 &= \frac{1}{2} + \frac{1}{\pi} \int_0^\infty \Re \left[\frac{\exp(-i\omega \ln K) f(\omega - i; y_t, v_1(t), v_2(t), v_3(t))}{i\omega S_t e^{(r-q)\tau}} \right] d\omega \\ P_2 &= \frac{1}{2} + \frac{1}{\pi} \int_0^\infty \Re \left[\frac{\exp(-i\omega \ln K) f(\omega; y_t, v_1(t), v_2(t), v_3(t))}{i\omega} \right] d\omega, \end{aligned}$$

and $f(\omega - i; y_t, v_1(t), v_2(t), v_3(t)) = \exp(A(\tau, \omega) + B_0(\tau, \omega)y_t + B_1(\tau, \omega)v_1(t) + B_2(\tau, \omega)v_2(t) + B_3(\tau, \omega)v_3(t))$ where A, B_0, B_1, B_2, B_3 are coefficient terms of the stochastic processes $y_t, v_1(t), v_2(t), v_3(t)$.

The options prices obtained from *An Uncertain Affine Exponential-Jump Model with Recession, induced stochastic-volatility and stochastic-intensity* and a control regime-switching *Triple Stochastic Volatility Heston-like* model, were efficient in terms of probable future payoffs and applicable in financial markets, for options valuation in recessed and recession-free economy states.

Keywords: Fast Fourier Transform, Recession induced-volatility, Economic uncertainties

Word count: 425

Contents

Title Page	i
Certification	i
Dedication	ii
Acknowledgements	iii
Abstract	v
Contents	vi
List of Tables	xi
List of Figures	xiii
Basic Notations	xiv
CHAPTER ONE	1
1 INTRODUCTION	1
1.1 Background to the study	1
1.2 Statement of the Problem	4
1.3 Motivation for the Study	5
1.4 Objectives of the Study	5
1.5 Significance of the study	6
1.6 Structure and arrangement of the thesis	7
CHAPTER TWO	9
2 LITERATURE REVIEW	9
2.1 Chapter Overview	9
2.2 Options Pricing	10
2.3 Economy recession effects on investment	11

2.4	Simple Economy recession decay model	11
2.5	Review on Stochastic Volatility Models	12
2.5.1	The Detemple - Tian model (DTM)	12
2.5.2	Constant Elasticity of Variance (CEV) model	13
2.5.3	The Stochastic α, β, ρ (SABR) - model	13
2.5.4	Grzelak Oosterlee Van Veeren (GOVV)-model	14
2.5.5	Schöbel - Zhu - Heston model	15
2.5.6	Schöbel - Zhu model	15
2.5.7	Heston Model	16
2.5.8	Double Heston Model (DHM)	16
2.6	Review on Fast Fourier Transform (FFT)	17
CHAPTER THREE		19
3 MATERIALS AND METHODS		20
3.1	Chapter Overview	20
STUDY ONE		21
3.2	Probability Distribution Theory	21
3.2.1	Measurability	21
3.2.2	Stochastic Process	22
3.2.3	Itô Calculus	23
3.2.4	Characteristic Function	25
3.2.5	Some Axioms of Characteristic Functions	26
3.2.6	Moments and Cumulants for a distribution function	27
3.2.7	Inversion Theorem	28
3.2.8	Gaussian Densities	29
3.2.9	Moment Generating Function	35
STUDY TWO		36
3.3	Fourier Transform Methodology	36
3.3.1	Fourier and Inverse Fourier Transform	37
3.3.2	Example of Fourier Transform	38
3.3.3	Some Essential Properties of Fourier Transform	44
3.3.4	The Fast Fourier Transform (FFT)	47
3.3.5	Symmetric Property of characteristic function for Fourier In- tegrals simplification	48
STUDY THREE		49
3.4	Uncertainty theory	49
3.4.1	Uncertain Measure	50

CHAPTER FOUR	51
4 RESULTS AND DISCUSSIONS	52
4.1 Chapter Overview	52
RESULT 1	54
4.2 STUDY ONE	54
4.2.1 Preamble	54
4.2.2 Justification for recession causing Jumps in the asset's price associated with Economic Recession	55
4.2.3 An Underlying Stock price jump	56
4.2.4 Some factors causing Stock's price Jumps	56
4.3 The Roadmap to the first model formulation	58
4.3.1 The Model Assumptions	58
4.3.2 Uncertain variable with respect to Recession	58
4.4 The first Model	60
4.4.1 Characteristic function	63
4.4.2 The Feynman-Kac formula	64
4.5 STUDY TWO	66
4.5.1 The Model Solution	66
4.5.2 Further Results from the model (4.5.2) Solution	72
4.6 STUDY THREE	75
4.6.1 Numerical Fourier based Transform of the UAEM to European- style option	75
4.6.2 Extension of the formulation to American-type options	79
4.7 STUDY FOUR	81
4.7.1 Numerical Experiment	81
4.8 Discussion of Result 1	91
4.9 Conclusion	92
RESULT 2	93
4.10 STUDY FIVE	93
4.10.1 An overview of the Result 2	93
4.10.2 Introduction	93
4.10.3 The Fast Fourier Transform (FFT) Algorithm	96
4.10.4 Fast Fourier Transform of a class of correlated multi-assets in finite dimension	96
4.10.5 Application on three correlated stocks Assets.	101
4.11 STUDY SIX	105
4.11.1 Application of the method to three correlated stocks assets.	105

4.11.2	Tables of Result 2	107
4.12	Conclusion	109
RESULT 3		110
4.13	An overview of Result 3	110
4.13.1	Introduction	111
4.14	STUDY SEVEN	112
4.14.1	Factorial function Black - Scholes PDE formulation for Option Pricing	112
4.14.2	Moving Boundary for American Options	118
4.14.3	Determination of Optimal Exercise Boundaries for American Put Options	118
4.15	STUDY EIGHT	120
4.15.1	Fourier transform Solution steps of the Factorial function Black-Scholes pde formulation for American Options	120
4.16	STUDY NINE	132
4.16.1	Valuation of a dividend paying American put option under Economy recession induced Volatility uncertainty	132
4.16.2	Fourier Transform of Ordinary Differential Equations	137
4.16.3	Fourier Transform of Partial Differential Equation	138
4.17	Numerical Results	142
4.17.1	American call Option Payoffs with Dividend	143
4.17.2	Non-dividend paying American call Option Payoffs	148
4.18	The Result 3 Analysis	150
4.19	Conclusion	150
RESULT 4		151
4.20	An Overview of the Result 4	151
4.21	STUDY TEN	151
4.21.1	Introduction	151
4.21.2	Preliminaries to the model formulation	152
4.21.3	The control regime-switching Triple Stochastic Volatility Heston-like (TSVH) model formulation	153
4.22	Options computation in the control regime-switching Triple Stochastic Volatility Heston-like model (TSVH)	155
4.23	A control regime-switching Triple Stochastic Volatility Heston-like model (TSVH) PDE form	159
4.24	Characteristic function derivation for the TSVH model	160
4.25	STUDY ELEVEN	168

4.25.1 Numerical discretisation and Simulation schemes for the TSVH model	168
4.26 Sample paths of the stochastic volatility processes $v_1(t), v_2(t)$ & $v_3(t)$	173
4.27 Simulations and Sample paths of the TSVH-model	178
CHAPTER FIVE	188
5 SUMMARY, CONCLUSION AND RECOMMENDATIONS	189
5.1 Introduction	189
5.2 Summary	189
5.3 Conclusion	192
5.4 Recommendations	192
5.5 Contributions to knowledge	193
5.6 Suggestions for further research	194
REFERENCES	195
APPENDICES	201

List of Tables

3.1	Characteristic function and Density function for selected Continuous distributions	33
3.2	Characteristic function and Density function for selected Discrete Distributions	34
4.1	The Options value comparison via FFT method versus BSM & American option Pricing solver	82
4.2	A dividend compensating (paying) multi-assets European-type call options returns under double source of volatility	107
4.3	Non-dividend paying multi-assets European call options returns under double source of volatility	108
4.4	A dividend paying American call Option prices under variant Grid points	144
4.5	The Option prices comparison at specified grid points for FFT method with BSM price as the benchmark price.	145
4.6	The Option prices at various grid points using integrability parameter $\alpha = 4.9$	146
4.7	The Option prices at various grid points using integrability parameter $\alpha = 2.5$	147
4.8	The Option prices at various grid points using integrability parameter $\alpha = 2.5$	149
4.9	Monte Carlo Simulation of Bonds Price under the TSVH model . . .	186
4.10	Table of Parameters used for the simulation of the TSVH model . . .	187
4.11	Comparison Stocks output based on Trapezoidal and Gauss-Laguerre for TSVH model	188

List of Figures

3.1	2D plot of the Fourier transform $\hat{f}(\omega)$ of the piecewise function $f(x)$.	40
3.2	3D-plot of the Fourier transform $\hat{f}(\omega)$ of the piecewise function $f(x)$.	41
3.3	Fast Fourier transform speed based on the order of computation. . . .	43
4.1	The Call options values from FFT versus BSM & American-style option pricing Solver in recession-free state.	83
4.2	The call options output of FFT versus BSM & American-style option pricing solver under recession induced volatility change.	84
4.3	The Nigerian Flourmill stock price dynamics under economy recession outbreak in 2016 and the Recovery year 2017	85
4.4	The Stock price performance in the time of Nigeria Economy Recession 2016 & Recovery year 2017 of Flourmill stock.	87
4.5	The Bar charts presentation of Nigerian Flourmill stock price performance during economy recession in 2016 & economy recovery in 2017	88
4.6	Nigerian Fourmill stock prices performance in the period of Economy Recession 2016 & Recovery year 2017	89
4.7	Surface plot of Flourmill stock data during Nigerian 2016 recession. .	90
4.8	Plots of Probability density function $f(S_\tau)$ for a shorter range of Options prices.	126
4.9	Probability density function $f(S_\tau)$ plots wrt variants of Options prices.	127
4.10	Plots of Probability density function $f(S_\tau)$ for range of Options prices.	129
4.11	Plots of Probability density functions $f(S_\tau)$ for range of Option prices with respect to time variation.	130
4.12	Three Sample paths for the stochastic process $v_1(t)$	174
4.13	A sample path for the stochastic volatility process $V_2(t)$	175
4.14	A sample path for the stochastic volatility process $V_3(t)$ due to recession	176
4.15	TSVH sample path at $N = 10000$	178
4.16	TSVH sample path at $N = 5000$	179
4.17	TSVH sample path at $N = 1000$	180

4.18	Stocks values Sample path generated under the TSVH- model at $N =$ 500	182
4.19	The TSVH-model Surface plot at $N = 5000$	183
4.20	Stocks returns listplot with $N = 1000$ under TSVH-model	184

BASIC NOTATIONS

PROBABILITY AND STOCHASTIC PROCESSES

a.s.	:- Almost surely.
\mathbb{P}	:- Probability measure (i.e the market measure).
Q	:- Probability measure (i.e an equivalent martingale measure).
$(\Omega, \mathcal{F}, \mathbb{P})$:- a complete probability space.
$(\Omega, \mathcal{F}, \mathbb{P}, \mathbb{F})$:- a filtered complete probability space.
$\mathbb{F} \equiv (\mathcal{F}_t), t \in [0, \infty]$:- Filtration.
$\mathcal{B}(H)$:- Borel σ -algebra of H .
$\mathbb{1}_H$:- Indicator function on a set H .
DFT	:- Discrete Fourier Transform.
IFT	:- Inverse Fourier Transform.
FFT	:- Fast Fourier Transform.
$TSVH$:- A control regime-switching Triple Stochastic Volatility Heston-like model
NBER	:- National Bureau of Economic Research
PIDE	:- Partial Integro-Differential Equation

FINANCIAL INSTRUMENTS AND DYNAMICS

t	:- time.
T	:- Options maturity date
\mathbb{T}	:- trading dates.
μ	:- the drift term.
σ	:- the volatility.
σ^*	:- Economy recession induced volatility.
δ or q	:- as dividend rate.
K	:- strike price.
$A^{call}(t)$:- An American call price at a time t .
$A^{put}(t)$:- American put price at a time t .
$E^{call}(t)$:- European call price at a time t .
P_t	:- Premium price at time t .
$S(t)$:- Spot price of a unit of an underlying asset at time t .
BS	:- Black - Scholes.

CHAPTER ONE

INTRODUCTION

1.1 Background to the study

This thesis examines uncertainties in options payoff with respect to economic recession among other risk factors in option pricing in an unstable economy not limited to Nigeria but with more emphasis on Nigerian economic recession in recent time. The negative effect of Nigeria economic recession eruption in the year 2016 on the uncertainty in investments payoffs as well as the standard of living of Nigerians during the recession period cannot be over emphasized. Many businesses, trades, and productions crumbled. It is saddening that many people lost their jobs as some companies in the country could not withstand the shock and as a result liquidated. It worths noting that Economic recession is almost surely becoming a global problem and a re-occurring phenomenon in most parts of the world. The United States of America (USA) takes the lead in economic recession history. They are known to have experienced a sequence of economic recession outbreaks. As a result, the United States of America (USA) established the National Bureau of Economic Research (NBER) to be responsible for disseminating timely economic recession information to general public in 1929. The NBER defined economic recession as “a substantial decline in the activities of the economy which spreads across and lasts over a few months, revealed in production, real income, employment, and other indicators” (HSU, 2016).

Diverse economic recession definitions found in the press stressed that an economic recession usually commences after two successive declines in GDP. However, the NBER is not in total agreement of using GDP fall as the only yardstick for measuring

the entire economic activities, and therefore sees the GDP definition to be insufficient for measuring economic activities. Hence, the GDP value should not be the sole consideration while predicting the economic recession date of upsurge. There are scenarios whereby economic recession emergence may not need to be comprised of two successive quarters of economy decay. The economic recession outbreak of 2001 in United States of America is an example. With reference to Hsu (2016), the declinations in GDP are closely correlated to recession period.

Consequently, the declaration of economic recession outbreak of Nigeria in 2016 by his Excellency, the President of Nigeria, Mr. Muhammadu Buhari, was hinged on the outrageous decline in the GDP of the country and other macroeconomic indicators to include high rate of unemployment, high rate of inflation, etc after two consecutive quarters.

However, following the financial crises arising based on some economy factors such as economic meltdown, economic recession, there is need for strategies diversification put in place by financial institutions, investors, policymakers, and all other players in the financial markets in order to circumvent or reduce the risk of loss in investment returns. Future returns of an investment and various financial securities have been tailored to the application of mathematical models formulation suitable in predicting or forecasting possible assets' returns, especially risky assets such as stocks. The various mathematical models formulation follow assumptions suitable for simulating stochastic processes in which the models themselves are stochastic due to the observable characteristic of stock prices.

However, one of the formulated mathematical models which had gained ground in mathematical finance especially in options pricing is popularly called Black - Scholes model or simply Black-Scholes equation (Black & Scholes, 1973). The model was formulated using a mathematical concept of Partial Differential Equations (PDEs).

A version of the model is of the form:

$$\frac{\partial A^{put}}{\partial t}(S(t), T) + \frac{1}{2}\sigma^2 S^2 \frac{\partial^2 A^{put}}{\partial S^2(t)}(S(t), T) + rS \frac{\partial A^{put}(S(t), T)}{\partial S(t)} = rA^{put}(S(t), T). \quad (1.1.1)$$

for a put option A^{put} on an underlying asset $S(t)$, the term σ , is the constant volatility in the model and r , is the risk-neutral interest rate with constant value.

The Black-Scholes model has some shortcomings which render the model unsuitable for valuation of financial assets in an unstable economy especially in a recessed economy. Among the identified shortcomings observed in classical Black-Scholes model (1973) is the issue of constant volatility assumption in the model knowing fully that asset's prices, especially stock assets, are risky assets. The prices of such assets cannot be stable or constant since various factors responsible for price fluctuations in financial markets are not stable too and reflect in the stochastic dynamic nature of assets' returns.

The quest to unravel the identified shortcomings of Black-Scholes model has motivated researchers in mathematical finance as well as those in financial engineering, among other related fields of studies, to concentrate on the formulation of other models for valuation of assets and options on risky assets. Among the models that researchers have successfully developed whereby a stochastic term structure of volatility was considered are: Heston (1993) model, Stochastic $\alpha\beta\rho$ (SABR)- model, Grzelak - Oosterlee-Vann Veeren (GOVV)-model, Schöbel-Zhu-Heston model, Schöbel - Zhu model, Double Heston model by Christoffersen, Heston, and Jacobs (2009), and Da Fonseca, (2008), to mention but a few.

The state of financial market volatility is of keen interest to investors, policymakers, financial institutions, and every other player in the financial market. Among various stochastic volatility models available, the concept of economic recession induced stochastic volatility uncertainty is yet to be introduced by other researchers. A very sound knowledge of uncertainty studies in terms of economy recession stochastic

volatility by most practitioners especially the investors in financial markets, will surely assist them in decision making throughout recession periods and beyond. Following the fact that an economy downturn affects investment, economy activities and human endeavours generally, it is therefore worthy of paying attention to, while formulating models for investment analysis or options valuation.

In the field of Financial mathematics, options valuation has become an indispensable and crucial focus of many academic researchers and practitioners. It connects various mathematical fields of studies. It depends on the use of some mathematical tools and concepts which include: Probability and measure theory, Stochastic differential equations (SDEs), Optimization theory, partial differential equations (PDEs), integral representations, numerical analysis, integral transforms, Ordinary Differential Equations (ODEs), and other relevant mathematical concepts.

However, in this thesis, studies on options pricing in relation to economic recession, fast Fourier transform and stochastic volatility models formulation are subjects of our study focus.

1.2 Statement of the Problem

Economic recession has become a global and recurring phenomenon which poses worrisome uncertainties on assets' returns in financial markets. Following the observed limitations of deterministic volatility models such as the Black-Scholes model 1973, there has been a paradigm shift to stochastic volatility models formulation and application in financial markets. The various stochastic models formulated in response to price instability in financial markets are not limited to the popular Heston model 1993 and Double Heston model 2009. However, the existing stochastic volatility models did not incorporate the concept of economic recession and induced volatility-uncertainty for options price valuation in a recessed economic setting. Therefore, this study was designed to develop economic recession-induced stochastic models for option price computation, provide investors some useful infor-

mation on uncertainty effects of recession on investment payoff, for decision making and Fourier transform solution of the related stochastic models.

1.3 Motivation for the Study

The Nigeria economic recession eruption of the year 2016 and its contributory effects on the level of uncertainty felt in the Nigerian Stocks Exchange (NSE) payoffs forms the core motivating issues among others which compelled us to propose an economic recession induced volatility concept in valuation of options prices. There were huge volatility variation effects caused by economic recession on economic activities, financial engagements and standard of living generally during the period of recession observed in Nigeria. However, an economic recession stochastic volatility uncertainty concept was first conceived following the overwhelming volatility variation observed during economic recession period in comparison with the period of non-economic recession.

The motivation of this research study is to establish the concept of economic recession volatility in the valuation of options. Formulate economic recession induced stochastic volatility models for Options price computation. Introduce an economic recession induced volatility uncertainty concept in an uncertain exponential - jump model which features stochastic volatility as well as stochastic intensity, and deriving the characteristic function. To carry out fast Fourier Transform computation for the model and applications in options pricing. We also wish to propose a form of control regime - switching Triple Stochastic Volatility Heston-like model for Options valuation under economic recession induced uncertainty.

1.4 Objectives of the Study

The objectives of this research study are to:

- (i) incorporate the concept of economic recession induced stochastic volatility in options valuation.

- (ii) present fast-Fourier Transform of American-style option prices computation using a newly formulated Uncertain affine exponential-jump model (UAEM) with respect to stochastic volatility (SV) and stochastic intensity (SI) based on economic recession induced volatility uncertainty concept.
- (iii) carry out fast-Fourier Transform of a class of correlated multi-assets option with respect to economic recession inducing uncertainties and show a framework for extending the fast-Fourier Transform of the options to multi-dimensions.
- (iv) propose Factorial function Black-Scholes PDE for options valuation.
- (v) obtain Fourier Transform of the Factorial function Black-Scholes PDE model for computation of options prices.
- (vi) investigate the accuracy of Fast-Fourier Transform method with control fineness of integration grid points, N , for Valuation of American-style Options.
- (vii) propose control regime-switching Triple Stochastic Volatility Heston-like (TSVH) model for pricing Option with economic recession induced stochastic volatility.
- (viii) To investigate simulation of sample paths and volatility surface for the proposed control regime-switching Triple Stochastic Volatility Heston-like (TSVH) model for pricing Options with economic recession induced stochastic volatility.
- (ix) Present some numerical schemes for a control regime-switching Triple Stochastic Volatility Heston-like (TSVH) model for pricing Options with economic recession induced stochastic volatility.

1.5 Significance of the study

This study shows model formulation that incorporate economic recession induced stochastic volatility uncertainty for options pricing. Two models are formulated for options pricing with a rapt focus on economy recession factors. The first and the second model are presented in Chapter 4 of this study under Result 1 and Result 4

respectively. It is believed that this study will be very informative to various financial institutions, investors, researchers in the field of financial mathematics, financial engineering, economics, optimization theory, stochastic modelling, computational mathematics, and partial differential equations. It is hoped the study will also draw more attention of various researchers to options pricing in relation to economy recession.

1.6 Structure and arrangement of the thesis

This thesis is structured as follows. Chapter 1 is introduction. There are various sections which include: Motivation for the research, Statement of the Problem, the study objectives, and the significance of the study. Chapter 2 is titled Review of Literature, with some sections to include: Review on stocks payoff uncertainty, Economy recession effect on investment, stochastic volatility models. Chapter 3 is titled “Methodology”. Chapter 4 is titled “ Results and Discussions”. We present Four Results.

Result 1 is titled “FFT Computation of American Options prices with Economy Recession induced Stochastic Volatility”. The sections and some of the subsections in this chapter are: Introduction to the Result 1, Justification for Jumps on Asset Prices associated with Economy Recession, Jumps of the Underlying Stock price, The Model Assumptions, The Model formulation, the UAEM model characteristic function derivation, the model solution, Numerical Fourier based Transform of Options, Numerical Experiment, and Conclusion.

The Result 2 is titled “FFT Computation of a class of Multi-assets Option with Economic Recession Induced Uncertainties”. The sections include: An overview of Result 2, Introduction, The FFT of a class of finite dimension correlated multi-assets, Application on three correlated assets, and Conclusion.

The Result 3 is: “Accuracy of Fast Fourier Transform Method with Control Fineness of Integration grid for Valuation of American Option”. The sections are: Overview of

the Result 3, Introduction, Factorial function Black - Scholes PDE, Moving Boundary for American Options, Fourier transform solution step for the Factorial function Black-Scholes PDE for American Options, Valuation of dividend paying American put option under Economic recession induced volatility uncertainty, Numerical Results, and Conclusion.

The Result 4 is titled “A control regime - switching triple stochastic volatility Heston-like model for Options valuation in a Recessed Economy”. The sections are: An Overview of Result 4, Introduction, Preliminaries to the model formulation, The Triple Stochastic Volatility Heston (TSVH) model formulation, Options computation in control regime-switching Triple Stochastic Volatility Heston-like (TSVH) model, control regime-switching Triple Stochastic Volatility Heston (TSVH) model PDE form, Some numerical discretization schemes for the TSVH model, Simulations and sample paths generation for the TSVH-model, and Conclusion.

The last chapter of the thesis is chapter Five titled “Summary and Conclusion”.

CHAPTER TWO

LITERATURE REVIEW

2.1 Chapter Overview

In this section, we present the review of relevant existing literature on this study. The chapter consists of the following sections: Stocks payoff uncertainty, Economic recession effects on investment, Simple economic recession decay model, Review on stochastic volatility models to include; The Detemple - Tian model (DTM), Constant-Elasticity-of-Variance (CEV) models, The Stochastic $\alpha\beta\rho$ (SABR)- model, Grzelak Oosterlee Vann Veeren (GOVV)-model, Schöbel-Zhu-Heston model, Schöbel - Zhu model, Heston model, and Double Heston model. We further review Fast Fourier Transform. In the financial market, the concept of uncertainty theory could vividly be attributed to research studies of Baoding Liu (2010).

There are numerous definitions of *uncertainty* obtainable in literature. The following definitions of uncertainty were given by several authors in their peculiar scenarios. Dungan, Gao and Pang (2001) has defined uncertainty as “a multi-faceted description about data or predictions made from data involving several concepts such as: error, accuracy, validity, quality, noise, confidence and reliability”. It was stressed further that “uncertainty seems to endogenously increase throughout economy recessions, for the fact that lower economy growth results to a greater micro uncertainty level as well as macro level of uncertainty” (Nicholas, 2014). During the time - period of economy crisis, the prices of assets undergo stochastic form of variation in the financial market most especially stock assets being a very risky asset type. There exists much tendency for stock assets price fluctuations whenever the underlying terms structures undergo some variations no matter how stereotypically such vari-

ation may be, most especially the volatility term variation. However, the volatility study in terms of stock prices is indispensable as a result of the effect it has on the stocks prices in financial market.

Owing to uncertainty in financial market, authors have formulated some realistic models which have come to stay because the models show an anticipated random movement of tradeable instruments in the financial market. Stein and Stein (1991) studied stock price distribution with respect to stochastic volatility, adopting analytic approach. Other stochastic volatility models are properly presented under the review of stochastic volatility models section.

2.2 Options Pricing

As far as the history of option valuation is concerned, the popular Black - Scholes model (Black & Scholes, 1973) which encouraged constant interest rate of return as well as constant volatility has been criticized by various researchers. The fact is that the classical Black-Scholes model could not wholly reflect the stochastic behaviour anticipated in financial markets. The underlying deficiency observed in the classical B-S model has prompted researchers to come out with other realistic models capable of showing better random movement of tradeable assets prices in financial markets. The example of the models include: single stochastic volatility Heston model (Heston, 1993), Double Heston model (Christoffersen et al., 2009), Regime switching models, the Double exponential jump models, etc. In the research study of Song-Ping, Alexander and Xianoping (2012), it was stressed that “regime - switching behaviour is able to capture changing preferences as well as the investors’ beliefs about asset prices whenever there exists a change in the financial market state”. The concept of regime switching model for option value computation was known to have been presented in the study by Hamilton (1998). Since then, a good number of outstanding developments have taken place through the consideration of his submission.

2.3 Economy recession effects on investment

The price of stock market volatility or Gross Domestic Product has been mostly used to determine the measure of uncertainty. This is due to the fact that a data series forecast becomes more difficult if its volatility becomes very high, beyond a considerable moderate level. According to Nicholas (2014), other common measures of uncertainty consist of the pronouncement of uncertainties in news, productivity shocks to firms' dispersion or spreads, and forecaster disagreement. In the particular study of Nicholas (2014), it was stressed further that “stock markets volatility, the exchange rates, the bond markets as well as growth in the GDP usually increase swiftly during economy recession”.

Bankole et al. (2017) emphasises “the negative growth in investment under economy recession exposure”. However, this invariably poses challenges to investors in the financial market because the decision of investors is also dependent on the daily inflow of information into the financial market concerning the economy state.

2.4 Simple Economy recession decay model

Growth or decay modeling often involves exponential functions. If economy decay of a nation under the threat of Economy recession is considered, the dynamics of such economy could be modeled to include an exponential function. Suppose E_n^{rec} denotes the value (i.e worth) of an economy under the threat of economy recession. Applying the knowledge of recurrence relation (Bankole et al., 2017), we gave a simple decay model of the economy as follows:

$$E_{n+1}^{rec} = r^n E_n, \quad n \in \mathbb{N}, \quad 0 < r < 1, \quad E_n = \text{the economy decay at } n \text{ - months.} \quad (2.4.1)$$

As an improvement on the simple economy decay model given above in (2.4.1), it is worth noting that the trajectory of an economy wealth decay may be stochastic in nature at times since the various factors for recession are stochastic in nature, hence, we intend to add the noise term as an improvement on the above model. The

equation (2.4.1) is then given as:

$$E_{n+1}^{rec} = r^n E_n + \sigma dW(t), \quad n \in \mathbb{N}, \quad 0 < r < 1, \quad t \in \mathbb{T} \quad (2.4.2)$$

where the time t is within the time-horizon, the parameter σ is the instantaneous volatility term of the recession aided by the white noise $W(t)$ or simply the Brownian motion.

2.5 Review on Stochastic Volatility Models

In literature, various stochastic volatility models have been formulated by researchers as a swift correction of the shortcomings observed in invariant volatility term models. Some researchers, in their models formulation, considered the dynamics of an asset price determined by a single stochastic volatility process, others with two stochastic volatility processes in addition to random variables such as stochastic intensities, stochastic interest rate, jump processes such as the Poisson process.

A reasonable number of such stochastic models in existence are reviewed in this section. They include: the Detemple-Tian model (DTM), the SABR model, the Constant-Elasticity-of-Variance (CEV) model, Grzelak Oosterlee Van Veeren (GOVV) model, Heston model, Schöbel - Zhu model, Schöbel - Zhu - Heston model; while we also considered two stochastic volatilities models structure popularly referred to as Double Heston model (Christoffersen et al., 2009; Schöbel & Zhu, 1999).

2.5.1 The Detemple - Tian model (DTM)

In the DTM model (Detemple & Tian, 2002), the authors assumed that the dynamics of a dividend paying asset price, S_t , is driven by stochastic interest rate at constant volatilities, σ_i , $i = 1, 2$.

The model is given below as:

$$\begin{cases} \frac{dS_t}{S_t} = (r_t - \delta)dt + \sigma_1 dW_1(t) \\ dr_t = a(r - r_t)dt + \sigma_2 dW_2(t) \equiv (\theta(t) - ar_t)dt + \sigma_2 dW_2(t) \end{cases} \quad (2.5.1)$$

where $a, \delta, \sigma_1, \sigma_2$ are all constants, dividend rate is δ , the asset price volatility is σ_1 , the interest rate speed of the model mean reversion is a with volatility σ_2 . W_1 and

W_2 are standard Brownian motions furnished with a correlation coefficient denoted by ρ , and $\theta(t)$ being a deterministic function. The authors applied the model in valuation of American options price in which the exercise region depends on the interest rate, likewise the dividend return. In the research study of Murara et al., (2016), a review on selected stochastic volatility models including the Detemple - Tian model was done.

2.5.2 Constant Elasticity of Variance (CEV) model

The constant elasticity of variance (CEV) is a model in the form:

$$dS_t = \mu S_t dt + \sigma S_t^\beta dW_t \quad (2.5.2)$$

where the μ is a constant drift term and the other term structure $\beta \geq 0$ and volatility $\sigma \geq 0$ are both real-valued constants. The elasticity factor β distinguishes (CEV)-model from Black-Scholes Merton model of 1973 (Black & Scholes, 1973). The parameter β serves as a control factor between the asset price and its volatility in the above (CEV)-model. The modifications in the value assumed by β results in the evolution of other models. For example, if $\beta = 0$ in (2.5.2), the resulting model is the Bachelier model (Bachelier, 1964) while $\beta = 1$ leads to Black-Scholes-Merton model of 1973 (Black and Scholes, 1973). In the recent time, year 2019 precisely, Satoshi, (2019) derived another option pricing formula which was based on the model of Bachelier whereby comparisons with other prior researches include the studies of Haug, (2007) was done. Some results were presented on page 24 of the research study of Satoshi, (2019).

2.5.3 The Stochastic $\alpha.\beta.\rho$ (SABR) - model

The SABR model is a form of stochastic volatility model widely used in Mathematical finance as one of the models in an effort to capture volatility smile in financial market dealing with derivatives securities. The model was formulated and shown in the research study by Hagan, Kumar, Lesniewski, and Woodward (2002). The acronym SABR simply refers to the stochastic parameters, “*alpha, beta, rho* (α, β, ρ)”, in the models as applicable in derivatives pricing especially in interest

rate derivative markets. The authors stressed that the evolution of a single forward $F(t)$, such as: a forward swap rate, a LIBOR forward rate, or simply a forward stock price, could be described by the given stochastic differential equations (2.5.3) of the form:

$$\begin{cases} dF(t) = \alpha(t)(F(t))^\beta dW_1(t), & F(0) = F_0 > 0, \\ d\alpha(t) = v(t)\alpha(t)dW_2(t), & \alpha(0) = \alpha_0 > 0; \end{cases} \quad (2.5.3)$$

where the parameter β satisfies the condition $0 \leq \beta \leq 1$. $v(t)$ is an instantaneous variance parameter for the volatility process. ρ represents the instantaneous correlation which exists between the underlying asset and the volatility process $\alpha(t)$, while $W_i(t)$, $i = 1, 2$ are two correlated Wiener processes driving the SABR model. The role of $v(t)$ is to control the height of the implied volatility level for the *forward stock price* when it is at the money (ATM). In the case of forward stock price $S(t)$, the variable $F(t)$ could be replaced in the model (2.5.3). Various extensions of the SABR model have been considered by other researchers, the bottom line is that the model, among other stochastic volatility models, has immensely attracted the attention of many practitioners in the financial market trading derivatives securities.

2.5.4 Grzelak Oosterlee Van Veen (GOVV)-model

The authors of GOVV-model (Grzelak et al, 2008) extend stochastic volatility models by choosing the interest rate process to satisfy that of Hull-White interest rate process. In their formulation, an asset (stock) price $S(t)$ at an arbitrary time, t , is assumed governed by an SDE, that is, stochastic differential equation possessing stochastic interest rate $r(t)$, and stochastic volatility $v(t)$. The GOVV- model is expressed in the form:

$$\begin{cases} \frac{dS(t)}{S(t)} = r(t)dt + v^p(t)dW_1(t), & S(0) = S_0 > 0, \\ dr(t) = \lambda(\theta(t) - r(t))dt + \eta dW_2(t), & r(0) = r_0 > 0, \\ dv(t) = \kappa(\bar{v} - v(t))dt + \gamma v^{1-p}(t)dW_3(t), & v(0) = v_0 > 0; \end{cases} \quad (2.5.4)$$

where p is constant, λ and κ denote the speed of the model mean reversion processes, η denotes the volatility of the stochastic interest rate, γ denotes the volatility of

volatility parameter, $\theta(t)$ denotes the model long run mean for the stochastic interest rate, \bar{v} denotes the model long run mean for the stochastic volatility while the $W_i(t)$, $i = 1, 2, 3$ are correlated Brownian motions. The correlation factor of the W_i , $i = 1, 2, 3$ are defined by

$$dW_i(t)dW_j(t) = \rho_{ij}, \quad i, j = 1, 2, 3.$$

A rigorous demonstration on the application of GOVV model in pricing European style options was presented in Murara, et al., (2016). The result shows that the stochastic volatility model is able to give better structure of the behaviour of asset prices in comparison with deterministic terms structure options pricing models.

2.5.5 Schöbel - Zhu - Heston model

In their model formulation, the stochastic term structure of the underlying asset (stock) price is governed by systems of stochastic differential equations (2.5.5) on setting $p = 1$ in the model of (2.5.4) presented above. The Schöbel - Zhu - Heston model is given as:

$$\begin{cases} \frac{dS(t)}{S(t)} = r(t)dt + v(t)dW_1(t), & S(0) = S_0 > 0, \\ dv(t) = \kappa_H(\bar{v}_H - v(t))dt + \gamma_H dW_3(t), & v(0) = v_0 > 0; \end{cases} \quad (2.5.5)$$

where $\kappa_H, \bar{v}_H, \gamma_H$ denote the speed of mean reversion processes, the long-run mean, and variance of the volatility (**vol. of vol**) constants respectively while the H is an indicator that the parameters are Heston type. In Murara et al., (2016), the Schöbel - Zhu - Heston model was given in an expanded form. Other parameters are of same interpretation as obtainable in GOVV model 2.5.4.

2.5.6 Schöbel - Zhu model

A modified Schöbel - Zhu - Heston model by transforming the instantaneous stocks variance parameter yielded another stochastic volatility model popularly referred to as Schöbel - Zhu model. The model is given in an expanded form as:

$$\begin{cases} \frac{dS(t)}{S(t)} = r(t)dt + \nu(t)dW_1(t), & S(0) = S_0 > 0, \\ d\nu(t) = 2\kappa\left(\nu(t) + v(t)\bar{v} + \frac{\gamma^2}{2\kappa}\right)dt + 2\gamma\sqrt{\nu(t)}\left(\rho_{12}dW_1(t) + \sqrt{1 - \rho_{12}^2}dW_2(t)\right), \\ \nu(0) = \nu_0 > 0, \end{cases} \quad (2.5.6)$$

where r denotes the constant interest rate, $v(t) = \sqrt{\nu(t)}$ represents the instantaneous stock variance, 2κ denotes the *mean reverting rate* of the stochastic volatility process, $-\left(v(t)\bar{v} + \frac{\gamma^2}{2\kappa}\right)$ the mean in the long run, γ denotes the volatility of volatility parameter, and the $W_i(t)$, $i = 1, 2$ are correlated Brownian motions. The correlation factor of the W_i , $i = 1, 2$ are defined by

$$dW_i(t)dW_j(t) = \rho_{ij}, \quad i, j = 1, 2.$$

2.5.7 Heston Model

In Heston (1993), a single factor Stochastic volatility model was formulated to show realistic behaviour of financial derivatives. The model is able to take care of the slope of option smile but does not vividly capture largely independent fluctuations that arise in the up and down stochastic movement due to risk associated with stocks over time. The single factor Heston model is given by:

$$\begin{cases} \frac{dS(t)}{S(t)} = (r - q)dt + \sqrt{v(t)}dW(t), & S(0) = S_0 > 0 \\ dv(t) = \kappa(\theta - v(t))dt + \sigma\sqrt{v(t)}d\widehat{W}(t), & v(0) = v_0 > 0, \end{cases} \quad (2.5.7)$$

where the parameters; r , is the *riskless interest rate*, q denotes the *dividend rate*, κ is the *mean reverting rate*, and θ , being the *volatility of variance* constant.

Other authors have extended the Heston, (1993) model to accommodate some other variables such as jumps in asset price, parameter uncertainties etc. In the next subsection, we consider two-factor stochastic volatility model popularly referred to as “Double Heston Model”.

2.5.8 Double Heston Model (DHM)

In an attempt to improve the Steve Heston (1993) single-factor stochastic volatility model, the authors: Christoffersen, Heston, and Kris (2009) introduced the double

Heston model which is a two-factor stochastic volatility model.

The double Heston model is given by:

$$\begin{cases} \frac{dS(t)}{S(t)} = (r - q)dt + \sqrt{v_1(t)}dW_1(t) + \sqrt{v_2(t)}dW_2(t), & S(0) = S_0 > 0 \\ dv_1(t) = \kappa_1(\theta_1 - v_1(t))dt + \sigma_1\sqrt{v_1(t)}d\widehat{W}_1(t), & v_1(0) = v_{1_0} > 0. \\ dv_2(t) = \kappa_2(\theta_2 - v_2(t))dt + \sigma_2\sqrt{v_2(t)}d\widehat{W}_2(t), & v_2(0) = v_{2_0} > 0. \end{cases} \quad (2.5.8)$$

where the parameters in the above model have the following denotation: r is the given *interest rate*, q denotes the *dividend rate*, $\kappa_j, j = 1, 2$ are the *mean reverting rate*, $\theta_j, j = 1, 2$ are the *volatility of variance (vol of vol)* constant.

Rouah, (2013) provided Matlab and C# codes for option pricing in the Heston model and double Heston model. Such models are solved in affine form involving characteristic function derivation. We shall see the derivation of a characteristic function in affine form for an affine model under the “Result 1” and “Result 4” in chapter four for our models formulated in this study.

2.6 Review on Fast Fourier Transform (FFT)

Fourier transform approach for pricing options especially in the sense of European-style have caught the attention of many authors. The one with tremendous value known to us among the various formulations by other researchers was the Carr and Madan (1999) model for pricing European call and put options. However, mathematical formulations for European options with respect to Fourier transform has been well established in literature. Much attention of authors in studying FFT method for options pricing has been devoted to European style options. The study of Oleksandr (2010) stood out as FFT approach was extended to American put option valuation with stochastic volatility. Kazuhisa (2004) provides a more simplified introduction to understanding the technique of Fourier transform for options price computation. Among the prerequisite knowledge required to understand the application of Fourier transform method in options computation is the characteristic function. In the theory of probability, characteristic functions and moment gener-

ating functions are among the crucial topics discussed at the elementary level up to advanced level especially while dealing with stochastic processes. It is suggested that the readers who doesn't have broad knowledge of probability and stochastic processes consult elementary level textbooks on probability theory with *MAT 352* by Ugbebor (2011a) in order to have the better understanding of this study. The study of Kazuhisa (2004) is also recommended for the basic understanding of Fourier Transform technique as used in this study.

However, to the best of our knowledge, the concept of economy recession factor is yet to be incorporated in option computation. A limited number of authors have carried out studies with respect to Fourier Transform for computing American option values. Much attention has been devoted to pricing European options probably owing to the complexity of American-style. The prominent study known to us is the research study by Oleksandr in (2010) on American options valuation using Fast Fourier Transform method. The author used the Geske Johnson scheme and Richardson extrapolation type in order to extend FFT algorithm to American-type financial security numerically. This was done by introducing varieties of probable exercising times up to the time of the option maturity. Jiexiang, Wenli, and Xinfeng (2014) used FFT technique to estimate options price in a stochastic volatility with stochastic intensity model driven by double exponential jumps. They made comparison between the options values obtained via fast Fourier Transform and Monte Carlo simulation method. Their findings revealed that fast Fourier method has speed advantage over the popular Monte Carlo method.

Zhao, (2016) also contributed to Stochastic volatility models with applications in finance showing some computational methods. Ricardo Crisóstomo investigated speed and biases of Fourier-based options pricing choices using numerical analysis. His findings show that the strike optimized version of Carr and Madan's formula is simultaneously faster and more accurate than the direct fast Fourier transform (Ricardo, 2017). The framework of economy recession prompted volatility uncertainty

effect is missing in their formulation.

Samuel and Martin, (2018) considered “European option pricing with stochastic volatility model”. An issue of parameter uncertainty was discussed in their study. Uncertainty theory is considered crucial, as the behaviour of stocks generally exhibit such feature. The notion of Uncertainty of volatility estimates following Heston Greeks point of view was studied by PFante, and Bertschinger, (2018). However, we are not aware of the notion of uncertainty in options pricing with respect to economy recession in the formulation of various authors except economy recession probability prediction study using probit model and ARCH-GARCH model. The predictions may not be accurate at times and therefore cannot be guaranteed. That’s exactly what uncertainty is all about. The good side of it is that it provides the investors and all practitioners in financial markets information on forecasting what the end product is likely to be from the present.

Nevertheless, formulation based on option valuation with economy recession uncertainty or economy recession volatility uncertainty has not been modeled by authors cited nor others as far as we know. Also, option valuation based on the framework of economy recession has not been studied and such framework with fast Fourier Transform technique of European-type and American-type option computation. Hence, the concept of economy recession induced volatility in options valuation models, Fourier transformation of the models to be formulated, derivation of characteristic function for the models and computational issues are our priority in this study.

CHAPTER THREE

MATERIALS AND METHODS

3.1 Chapter Overview

This chapter presents the methodology adopted in solving the models formulated in this study. The following three major mathematical theories are used to drive the solution of our models in this study. Probability distribution theory, Fast Fourier transform, and Uncertainty theory. Under probability distribution theory, the following concepts were presented: Measurability, Stochastic process, Itô Calculus, Characteristic functions, Axioms of characteristic functions, Moments and Cumulants for a distribution function, Inversion theorem, Gaussian process, and Moment generating functions.

Under Fast Fourier Transform (FFT), we consider definition of Fourier transform technique, Inverse Fourier transform, Examples of Fourier transform, Essential properties of Fourier transforms, and Symmetric property of characteristic functions for Fourier integrals simplification.

We further present uncertainty theory in the sense of Baoding Liu (2010). As this study deals with the concept of uncertainty studies under the exposure of economy recession, we consider uncertainty measures in addition to other forms of uncertainties in financial stock market valuation.

STUDY ONE

3.2 Probability Distribution Theory

Probability theory has been seen as a fundamental support for modern mathematics by means of relations to other mathematical study areas such as analysis, algebra, topology, geometry or dynamical systems. Probability theory includes a measure theoretical structure on a given nonempty set Ω .

3.2.1 Measurability

Definition 3.2.1. Given a sample space Ω , the σ -algebra defined on Ω is a class \mathcal{F} comprising subsets of Ω , in such way that \mathcal{F} is closed under complements and countable intersections (also under countable union) and $\emptyset \in \mathcal{F}$, (hence, $\Omega \in \mathcal{F}$).

Definition 3.2.2. A measurable map say X , from (Ω, \mathcal{F}) to a measurable space (M, ε) is a map from Ω to M such that for any $B \in \varepsilon$, the set

$$X^{-1}(B) := \{\omega \in \Omega : X(\omega) \in B\}$$

belongs to \mathcal{F} .

Note: For any given class \mathcal{H} of subsets of Ω , we denote $\sigma(\mathcal{H})$ the smallest σ -algebra which contains \mathcal{H} (\equiv intersection of all the σ -algebras containing \mathcal{H}). Let \mathbb{T} be some interval in \mathbb{R}_+ . $\mathcal{B}(\mathbb{T})$ denotes the σ -algebra of Borel subsets of \mathbb{T} .

Definition 3.2.3. A real valued random variable, X , defined on (Ω, \mathcal{F}) is a measurable map from (Ω, \mathcal{F}) to $(\mathbb{R}, \mathcal{B})$ where \mathcal{B} is the Borel σ -algebra, the smallest σ -algebra containing open intervals in \mathbb{R} and this implies closed, half open, semi-infinite, belong to \mathcal{B} .

Definition 3.2.4. A probability measure \mathbb{P} defined on a measurable space (Ω, \mathcal{F}) is a mapping from \mathcal{F} to $[0, 1]$ such that:

(i) $\mathbb{P}(\Omega) = 1,$

(ii) $\mathbb{P}\left(\bigcup_{i=1}^{\infty} H_i\right) = \sum_{i=1}^{\infty} \mathbb{P}(H_i)$ for any given countable family of disjoint sets $H_i \in \mathcal{F}$,
i.e. such that

$$H_i \cap H_j = \emptyset \quad \text{for } i \neq j.$$

Note: Whenever there is $H \in \mathcal{F}$, $\mathbb{P}(H) = 1 - \mathbb{P}(H^c)$ where H^c is the complement set of H , which implies that $\mathbb{P}(\emptyset) = 0$.

3.2.2 Stochastic Process

Definition 3.2.5. A stochastic process \mathcal{H} is said to be a Poisson process with parameter λ if the following holds:

(i) $\mathcal{H}_0 = 0$

(ii) for $0 \leq s \leq t$, $\mathcal{H}_t - \mathcal{H}_s$ is $P_0(\lambda(t-s))$ -distributed.

(iii) For $0 = t_0 < t_1 < \dots < t_m$, we have that $\{\mathcal{H}_{t_k} - \mathcal{H}_{t_{k-1}} : k = 1, \dots, m\}$

is a set of variables evolving independently.

Definition 3.2.6. A stochastic process X such that:

(i) $X_0 = 0$ a.s.

(ii) almost all paths $t \rightarrow X_t(\omega)$

(iii) for $0 \leq s \leq t$, $X_t - X_s$ is $\mathcal{N}(0, t-s)$ -distributed.

(iv) for $0 = t_0 < t_1 < \cdots < t_m$, we have $\left\{ X_{t_k} - X_{t_{k-1}} : k = 1, \dots, m \right\}$ represent a set of random variables whose evolution is independent of each other, called *Brownian motion process*, also popularly known as Wiener process.

Definition 3.2.7. Two processes say $(X_t, t \geq 0)$ and $(Y_t, t \geq 0)$, possess the same law if given any n and (t_1, t_2, \dots, t_n) , $(X_{t_1}, X_{t_2}, \dots, X_{t_n}) \stackrel{\text{law}}{=} (Y_{t_1}, Y_{t_2}, \dots, Y_{t_n})$. We hereby write in short $X \stackrel{\text{law}}{=} Y$, or $X \stackrel{\text{law}}{=} \mu$ for a given probability law, say, μ on the canonical space.

Definition 3.2.8. A stochastic process, f , on a filtered complete probability space $(\Omega, \mathcal{F}, \mathbb{P}, \mathbb{F})$ is said to be simple if it is possible to express f in the form

$$f(t, \omega) = f_0(\omega)\mathbb{I}_{\{0\}}(t) + \sum_{j=0}^{\infty} f_j(\omega)\mathbb{I}_{(t_j, t_{j+1}]}(t) \quad (3.2.1)$$

$t \in \mathbb{R}_+$, $\omega \in \Omega$ for some strictly increasing sequence, $\{t_j\}_{j=0}^{\infty} \in \mathbb{R}$, such that $t_0 = 0$ and $\lim_{j \rightarrow \infty} t_j = \infty$, and a sequence $\{f_j\}_{j=0}^{\infty}$ of random variables satisfying $\sup_{j \geq 0} |f_j(\omega)| < c$, a positive constant with f_j being \mathcal{F}_{t_j} -measurable for $j \geq 0$.

3.2.3 Itô Calculus

Definition 3.2.9. Let X be a stochastic process defined on a filtered probability space $(\Omega, \mathcal{B}, \mathbb{P}, \mathbb{F}(\mathcal{B}))$. Then the quadratic variation $\langle X \rangle$ on $[0, t]$, $t > 0$ is the stochastic process $\langle X \rangle$ defined as:

$$\langle X \rangle(t) = \lim_{|\mathcal{P}| \rightarrow 0} \sum_{j=0}^n |X(t_{j+1}) - X(t_j)|^2$$

where $\mathcal{P} = \{0 = t_0 < t_1 < t_2 < \cdots < t_n = t\}$ is any partition of $[0, t]$, and

$$\mathcal{P} = \max_{0 \leq j \leq n-1} |t_{j+1} - t_j|.$$

Theorem 3.2.1. Itô Formula: (Kloeden & Platen, 1992; Chiarella, He & Nikitopoulos, 2015):

Let $(\Omega, \mathcal{F}, \mathbb{P}, \mathbb{F}(\mathcal{F}))$ be a filtered probability space and $X = \{X_t : t \geq 0\}$ be an adapted stochastic process on $(\Omega, \mathcal{F}, \mathbb{P}, \mathbb{F}(\mathcal{F}))$ possessing a quadratic variation $\langle X \rangle$, with a stochastic differential equation defined as:

$$dX(t) = g(t, X(t))dt + f(t, X(t))dW(t), \quad t \in \mathbb{R}_+ \quad (3.2.2)$$

and let $w = u(t, X(t)) \in C^{1 \times 2}(\mathbb{T} \times \mathbb{R})$, then

$$du(t, X(t)) = \frac{\partial u}{\partial t}dt + \frac{\partial u}{\partial x}dX(t) + \frac{1}{2} \frac{\partial^2 u}{\partial x^2} (dX(t))^2 \quad (3.2.3)$$

By substituting (3.2.2) into (3.2.3) gives:

$$du(t, X(t)) = \frac{\partial u}{\partial t}dt + \frac{\partial u}{\partial x} \left[g(t, X(t))dt + f(t, X(t))dW(t) \right] + \frac{1}{2} \frac{\partial^2 u}{\partial x^2} (dX(t))^2$$

or

$$du(t, X(t)) = \left[\frac{\partial u}{\partial t} + g \frac{\partial u}{\partial x} + \frac{1}{2} f^2 \frac{\partial^2 u}{\partial x^2} \right] dt + f \frac{\partial u}{\partial x} dW(t). \quad (3.2.4)$$

The equation (3.2.4) is equivalently expressed in integral form as:

$$u(t, X(t)) = u(s, X(s)) + \int_s^t \left[\frac{\partial u}{\partial t} + g \frac{\partial u}{\partial x} + \frac{1}{2} f^2 \frac{\partial^2 u}{\partial x^2} \right] d\tau + \int_s^t f \frac{\partial u}{\partial x} dW(\tau) \quad (3.2.5)$$

Lemma 3.2.1. Itô's Lemma: (Chiarella, He & Nikitopoulos, 2015; Ekhaguere, 2010):

Let $X = \{X_t, t \geq 0\}$ be such that $X = W$ in the above Lemma, then $g \equiv 0$ and $f \equiv 1$, on $\mathbb{T} \times \mathbb{R}$. Then,

$$u(t, W(t)) = u(s, W(s)) + \int_0^t \left[\frac{\partial u}{\partial \tau} + \frac{1}{2} \frac{\partial^2 u}{\partial \tau^2} \right] ds + \frac{\partial u}{\partial x} dW(\tau). \quad (3.2.6)$$

The above expression is called Itô's Lemma.

3.2.4 Characteristic Function

The concept of characteristic function is crucial while dealing with random variables with respect to Fourier transform. The closed form formula for the distribution function of some jump diffusion processes is not readily available, perhaps the characteristic function could be explicitly determined. However, there exists “a one to one relationship between the probability density and a characteristic function” (Schmelzle, 2010). It is very interesting to know that the characteristic function is determinable even if a particular random variable does not have a known analytical expression in closed form, it is certain that the characteristic function exists for any random variable.

Definition 3.2.10. *Let X be an arbitrary random variable. The characteristic function of X , is given by:*

$$\varphi_X(\omega) = \mathbb{E}(e^{i\omega X}) = \int_{-\infty}^{\infty} f_X(x) e^{i\omega x} dx, \quad \omega \in \mathbb{R}, \quad (3.2.7)$$

where $f_X(x)$ is the probability density function (pdf) of the random variable X . The above definition is similar to the inverse Fourier Transform of functions given in equation (3.3.6) and equal if $\frac{1}{2\pi}$ is excluded. For instance, let N_t be a Poisson process with parameter λ , then the characteristic function is expressed as:

$$\varphi_N(\omega) \equiv \mathbb{E}(e^{i\omega N_t}) = \exp\{\lambda t(e^{i\omega} - 1)\}. \quad (3.2.8)$$

The concept of moment generating function is related to characteristic function. The popular Euler's Identity empowers us to express the term $e^{i\omega X}$ of the characteristic function in (3.2.7) in terms of trigonometric functions; sine and cosine, for the random variable, say X as:

$$e^{i\omega X} = \cos(\omega X) + i \sin(\omega X) \quad (3.2.9)$$

where $i = \sqrt{-1}$ is the imaginary unit.

3.2.5 Some Axioms of Characteristic Functions

The following highlighted axioms of characteristic functions are interesting to us in this study. Suppose a characteristic function $\varphi_X(\omega)$ of an arbitrary random variable X is absolutely integrable over the whole real line \mathbb{R} . Then the variable X possesses almost surely an absolutely continuous probability distribution which obeys Lebesgue integrability belonging to $L^1(\mathbb{R})$. With reference to Schmelzle (2010) and Ugbebor (2011a), we consider the following axioms for $\varphi_X(\omega)$:

- $\varphi_X(\omega)$ often exists surely as far as the expression $|e^{i\omega X}|$ is absolutely continuous and bounded function on \mathbb{R} and by extension, we have an absolutely convergence in integral for the pdf $f_X(x)$ given by

$$\left| \int_{-\infty}^{\infty} f_X(x) dx \right| \leq \int_{-\infty}^{\infty} |f_X(\omega)| dx \quad (3.2.10)$$

- $\varphi_X(\omega = 0) \equiv \mathbb{E}(e^{i \cdot 0 \cdot X}) = 1$ for any arbitrary distribution.
- $|e^{i\omega X}| \leq 1$.

- $\overline{\varphi_X(\omega)} = \varphi_X(-\omega)$ where $\overline{\varphi_X(\omega)}$ denotes the complex conjugate of the characteristic function $\varphi_X(\omega)$.

-

$$\begin{aligned}
|\mathbb{E}[\varphi_X(t)]| &= |\mathbb{E}[\cos tX + i \sin tX]| \\
&\leq \mathbb{E}|\cos tX + i \sin tX| \\
&= \mathbb{E}(\cos tX + i \sin tX)(\overline{Z}) \\
&= \sqrt{\cos^2(tX) + \sin^2(tX)} \\
&= 1.
\end{aligned}$$

- Let Y be another random variable such that $Y := \alpha + \beta X$ for $\alpha, \beta \in \mathbb{R}$, takes real values. $\varphi_Y(\omega) = e^{i\omega\alpha} \varphi_X(\beta\omega)$.

- For sequence of stochastic independent variables $X_1, X_2, X_3, \dots, X_n$ well defined such that $Z := \sum_{i=1}^n X_i$ is another random variable, the sum of the random variables $X_i, i = 1, 2, \dots, n$, then the characteristic function for the new random variable Z is given by

$$\varphi_Z(\omega) = \varphi_{X_1}(\omega) \cdot \varphi_{X_2}(\omega) \cdot \varphi_{X_3} \dots \varphi_{X_n}(\omega) \quad (3.2.11)$$

with $n \in \mathbb{N}$.

- Suppose that $\mathbb{E}(|X^n|) < \infty$ for some n , then $\mathbb{E}(|X|^k) < \infty \forall k \leq n$. See Ugbebor, (2011a).

3.2.6 Moments and Cumulants for a distribution function

Let X be a random variable. Suppose the characteristic function is differentiable to order k at the origin of ω . Then the k -th moment $\mathbb{E}(X^k)$ of the distribution function

provided it exists is given by:

$$\mathbb{E}(X^k) = \frac{d^k \varphi_X(\omega)}{i^k d\omega^k}, \quad \text{at } \omega = 0. \quad (3.2.12)$$

From the above equation, it is easy to see that the characteristic function is a generator of the moments. In a similar way, the characteristic function could be used to generate the cumulants denoted $c_k(X)$. This is made possible by taking the logarithm of the characteristic function. The formula is expressed as:

$$c_k(X) = \frac{d^k \ln \varphi_X(\omega)}{i^k d\omega^k}, \quad \text{at } \omega = 0 \quad (3.2.13)$$

where $\ln \varphi_X(\omega)$ is referred to as cumulant characteristic function. Next, we are ready to give the inverse theorem in the next subsection. The “Inversion Theorem has been taken as the Fundamental Theorem of the Theory of Characteristic Functions because it connects the characteristic function to its probability distribution through an inverse Fourier transform” (Ugbebor, 2011a; Schmelzle, 2010).

3.2.7 Inversion Theorem

We consider the fundamental theorem of the Theory of Characteristic functions in probability distribution linking inverse Fourier Transformation in the sense of Gil-Pelaez (1951). Several authors had given various representations. For a review of inversion theorem, see Waller (1995) and Schmelzle (2010).

We consider the inversion algorithm of Gil-Pelaez for cumulative distribution function (CDF) $\int_{-\infty}^x f_X(x)dx$ whereby the distribution function $F_X(x)$ is expressed as:

$$F_X(x) = \mathbb{P}(X \leq x) = \frac{1}{2} - \frac{1}{2\pi} \int_{-\infty}^{\infty} \frac{e^{-i\omega x} \varphi_X(\omega)}{i\omega} d\omega. \quad (3.2.14)$$

By differentiating the distribution function $F_X(x)$ in (3.2.14), we have the probability density function $f_X(x)$ given by:

$$f_X(x) \equiv \mathcal{F}^{-1}(\varphi_X(\omega)) = \frac{1}{2\pi} \int_{-\infty}^{\infty} e^{-i\omega x} \varphi(\omega) d\omega. \quad (3.2.15)$$

Remark 3.2.1. It is easy to see that the equations (3.2.14) and (3.2.15) are the inverse of each other showing the relationship in distribution function and the probability density function of a random process.

3.2.8 Gaussian Densities

Definition 3.2.11. The *Gaussian density* equipped with variance τ is

$$g_\tau(x) = \left(\frac{1}{2\pi\tau} \right)^{d/2} e^{-|x|^2/2\tau}.$$

Equivalently, the density of $\sqrt{\tau}Z$, where $Z = (Z_1, \dots, Z_d)$ with $Z_i \sim N(0, 1)$ independent.

To compute the Fourier transformation directly, as well as showing that Fourier inversion formula is valid. We start off with the case $d = 1$ and $Z \sim N(0, 1)$. The computation of the Fourier transform for the characteristic function of the Gaussian density follows.

Proposition 3.2.1. (Gordan, 2013)

Let $Z \sim N(0, 1)$. Then

$$\phi_Z(a) = e^{-a^2/2}.$$

It is not difficult to see that the above is Gaussian up to a factor of 2π .

Proof. We have

$$\begin{aligned}\phi_Z(u) &= \mathbb{E}[e^{iuZ}] \\ &= \frac{1}{\sqrt{2\pi}} \int e^{iux} e^{-x^2/2} dx.\end{aligned}$$

By the boundedness of the function, differentiation is possible under the integral sign. This yields:

$$\begin{aligned}\phi'_Z(u) &= \mathbb{E}[iZ e^{iuZ}] \\ &= \frac{1}{\sqrt{2\pi}} \int ix e^{iux} e^{-x^2/2} dx \\ &= -u\phi_Z(u),\end{aligned}$$

the last equality is come by through integrating by parts. Hence, $\phi_Z(u)$ is a solution of

$$\phi'_Z(u) = -u\phi_Z(u).$$

Through integration, we see that

$$\log \phi_Z(u) = -\frac{1}{2}u^2 + C.$$

Therefore, we have

$$\phi_Z(u) = Ce^{-u^2/2}.$$

We know that $C = 1$, since $\phi_Z(0) = 1$. So we have

$$\phi_Z(u) = e^{-u^2/2}. \quad \square$$

Michaelmas (2016) presented a general case which is synonymous to what follows:

Proposition 3.2.2. *Let $Z = (Z_1, \dots, Z_d)$ with $Z_j \sim N(0, 1)$ independent. Then $\sqrt{\tau}Z$ has density*

$$g_t(x) = \frac{1}{(2\pi\tau)^{d/2}} e^{-|x|^2/(2\tau)}.$$

with

$$\hat{g}_\tau(u) = e^{-\frac{|u|^2\tau}{2}}.$$

Proof. We have

$$\begin{aligned} \hat{g}_t(u) &= \mathbb{E}[e^{i(u, \sqrt{\tau}Z)}] \\ &= \prod_{j=1}^d \mathbb{E}[e^{i(u_j, \sqrt{\tau}Z_j)}] \\ &= \prod_{j=1}^d \phi_Z(\sqrt{\tau}u_j) \\ &= \prod_{j=1}^d e^{-\tau u_j^2/2} \\ &= e^{-|u|^2\tau/2}. \quad \square \end{aligned}$$

Similarly, g_τ and \hat{g}_t are almost surely the same, the only difference is the factor of $(2\pi\tau)^{-d/2}$ attached and the shifting of τ 's position. Hence, it is written as:

$$\hat{g}_\tau(u) = (2\pi)^{d/2} \tau^{-d/2} g_{1/\tau}(u).$$

It shows that

$$\hat{\hat{g}}_\tau(u) = (2\pi)^d g_\tau(u).$$

However, the symmetry property of the Gaussian distribution empowers us to obtain

$$g_\tau(x) = g_\tau(-x) = (2\pi)^{-d} \hat{g}_\tau(-x) = \left(\frac{1}{2\pi}\right)^d \int \hat{g}_\tau(u) e^{-i(u,x)} du.$$

The Summary of characteristic functions and density function for some processes as retrieved from Gordan (2013) is presented both in continuous and discrete distribution in the following tables [3.1](#) and [3.2](#) respectively.

Table 3.1: Characteristic function and Density function for selected Continuous distributions

S/N	Name	Parameters	Density $f_X(x)$	Char. function $\varphi_X(t)$
1	Uniform	$a < b$	$\frac{1}{b-a} \mathbb{I}_{[a,b]}(x)$	$\frac{e^{-ita} - e^{itb}}{it(b-a)}$
2	Symmetric Uniform	$a > 0$	$\frac{1}{2a} \mathbb{I}_{[-a,a]}(x)$	$\frac{\sin(at)}{at}$
3	Normal	$\mu \in \mathbb{R}, \sigma > 0$	$\frac{1}{\sqrt{2\pi\sigma^2}} \exp\left(-\frac{(x-\mu)^2}{2\sigma^2}\right)$	$\exp\left(i\mu t - \frac{1}{2}\sigma^2 t^2\right)$
4	Exponential	$\lambda > 0$	$\lambda \exp(-\lambda x) \mathbb{I}_{[0,\infty)}(x)$	$\frac{\lambda}{\lambda - it}$
5	Double Exponential	$\lambda > 0$	$\frac{1}{2} \lambda \exp(-\lambda x)$	$\frac{\lambda^2}{\lambda^2 + t^2}$
6	Cauchy	$\mu \in \mathbb{R}, \gamma > 0$	$\frac{\gamma}{\pi(\gamma^2 + (x-\mu)^2)}$	$\exp(i\mu t - \gamma t)$

Source: Gordan, (2013).

The table 3.1 shows the characteristic function and density function summary for some selected continuous distributions. The distributions are: Uniform distribution, Symmetric Uniform, Normal distribution, Exponential distribution, Double exponential distribution, and Cauchy distribution. Each of the distributions depends on the specified parameters and conditions for their derivation as shown under the column for parameters in the table above. The characteristic functions and the density functions for the specified processes are already available in literature. In the case whereby a process has no already available density function, it is almost sure that the corresponding characteristic function is derivable. The derivation may follow an affine characteristic function derivation process. It is common to combine more than one distribution in the formulation of a more complex model, especially in Financial Mathematics modeling, which could lead to an affine process. The characteristic function derivation for such an affine model follows an affine procedure as the case may be.

Table 3.2: Characteristic function and Density function for selected Discrete Distributions

S/N	Name	Parameters	Density μ_X	Char. function $\varphi_X(t)$
7	Dirac	$c \in \mathbb{R}$	δ_c	$\exp(itc)$
8	Biased Coin-toss	$p \in (0, 1)$	$p\delta_1 + (1-p)\delta_{-1}$	$\cos(t) + (2p-1)i\sin(t)$
9	Geometric	$p \in (0, 1)$	$\sum_{n \in \mathbb{N}_0} p^n (1-p) \delta_n$	$\frac{1-p}{1-e^{it}p}$
10	Poisson	$\lambda > 0$	$\sum_{n \in \mathbb{N}_0} e^{-\lambda} \frac{\lambda^n}{n!} \delta_n, n \in \mathbb{N}_0$	$\exp(\lambda(e^{it} - 1))$

Source: Gordan, (2013)

The table 3.2 shows the characteristic function and density function summary for some selected discrete distributions. The distributions are: Dirac distribution, Biased Coin-toss, Geometric distribution, and Poisson distribution. Each of the distributions depends on the specified parameters and conditions for their derivations as shown under the column for parameters in the table. The variants of the above characteristic functions and Density functions for the specified processes are available in literature.

3.2.9 Moment Generating Function

The moment generating function (MGF) of an arbitrary real-valued random variable has an application in probability theory. It serves as alternate specification for the probability distribution of any arbitrary random variable, X_t .

Definition 3.2.12. The MGF of an arbitrary random variable, X , is mathematically expressed as:

$$M(t) = \mathbb{E}(e^{tX}), \quad t \in \mathbb{R}, \quad (3.2.16)$$

if the expectation exists.

Example 3.2.1. Consider a Poisson distribution with parameter λ , the moment-generating function $M(t) = e^{\lambda(e^t-1)}$ while its characteristic function $\varphi(t) = e^{\lambda(e^{it}-1)}$.

In the case of a continuous type probability density function, we define the MGF as:

$$M(t) = \int_{-\infty}^{\infty} e^{tx} f(x) dx \quad (3.2.17)$$

where $f(x)$ represents the probability density function.

Definition 3.2.13. Consider a vector of stochastic variables $\mathbf{X} = (X_1, \dots, X_d)$ on a probability space $(\Omega, \mathcal{F}, \mathbb{P})$ with \mathbb{P} a risk-neutral probability measure (i.e. *equivalent martingale measure*). Let the filtration $\{\mathcal{F}_t : 0 \leq t \leq T\}$ be generated by a standard d -dimensional Wiener process \mathbf{W}_t and suppose that \mathbf{X} under the risk-neutral measure \mathbb{P} satisfies the stochastic differential equation:

$$d\mathbf{X}_t = \mu(t, \mathbf{X}_t)dt + \zeta(t, \mathbf{X}_t)d\mathbf{W}_t, \quad (3.2.18)$$

where $\mu : [0, T] \times \mathbb{R}^m \rightarrow \mathbb{R}^m$ and $\zeta : [0, T] \times \mathbb{R}^m \rightarrow \mathbb{R}^{m \times d}$ are the drift and diffusion

term respectively.

Suppose further that the payoff of a financial asset is $f(x)$ at a maturity time $T \in \mathbb{R}^+ \setminus \{0\}$ with a riskless interest rate $(r(t), \mathbf{X}_t)$. Then the asset price $V(t, \mathbf{x})$ under the risk-neutral measure is given by:

$$V(t, \mathbf{x}) = \mathbb{E} \left[\exp \left(- \int_0^T r(s, \mathbf{x}) ds \right) f(\mathbf{X}_T) \middle| \mathcal{F}_t, \mathbf{X}_t = \mathbf{x} \right]. \quad (3.2.19)$$

According to Andersen and Piterbarg, (2010), the asset price $V(t, \mathbf{x})$ in equation (3.2.19) with respect to the terminal value condition that $V(t, \mathbf{x}) = f(x)$, satisfies the following partial differential equation:

$$\frac{\partial V}{\partial t} + \sum_{i=1}^m \mu_i(t, \mathbf{x}) \frac{\partial V}{\partial x_i} + \frac{1}{2} \sum_{i=1}^m \sum_{j=1}^m \sum_{k=1}^d \zeta_{ik}(t, \mathbf{x}) \zeta_{kj}(t, \mathbf{x}) \frac{\partial^2 V}{\partial x_i \partial x_j} - r(t, \mathbf{x})V = 0. \quad (3.2.20)$$

STUDY TWO

3.3 Fourier Transform Methodology

Fourier transform in financial mathematics was first applied to estimate asset price distribution employing inversion techniques for a class of stochastic volatility model” (Stein and Stein, 1991). We consider the definitions, basic conditions sufficient for existence of Fourier transform and inverse Fourier transform as follows.

Definition 3.3.1. Given a Lebesgue measurable function $f(x)$ for $x \in \mathbb{R}$, the L^2 -norm of the function, f , is expressed as:

$$\|f\| = \left(\int_{-\infty}^{\infty} |f(x)|^2 dx \right)^{\frac{1}{2}} \quad (3.3.1)$$

where

$$L^2 = \{f : \|f\| < \infty\}. \quad (3.3.2)$$

Alternatively, the piecewise integrable real-valued function, $f(x)$, satisfies the condition:

$$\int_{-\infty}^{\infty} |f(x)| dx < \infty. \quad (3.3.3)$$

The existence of the Fourier transform as well as inverse Fourier transform of a function demands absolute integrability over \mathbb{R} , and in addition, the function should have finite value as given in the equation (3.3.3). An absolutely integrable function defined on an interval (a, b) is said to be on $L^1(a, b)$ space. However, the concept of Fourier transform is extendable to the functions that are square integrable.

Definition 3.3.2. A square integrable functions is defined as:

$$\int_{-\infty}^{\infty} |f(x)|^2 dx < \infty. \quad (3.3.4)$$

The square integrable functions space denoted by $L^2(\mathbb{R})$ is defined over the entire real line, or simply on an open interval $(a, b) \subseteq \mathbb{R}$.

Remark 3.3.1. We shall limit ourselves to L^1 -space.

3.3.1 Fourier and Inverse Fourier Transform

There are some conventional representations of Fourier transform found in use depending on various fields of application. For instance, in Physics, Fourier transform of a given function say, $f(t)$, is done moving from time, t , domain into an angular frequency, ω , domain measured in (*radians/second*), while in the case of Signal Processing as a field of study, Fourier transform is done moving from time, t , domain into frequency (cycles /second) domain in place of angular frequency, ω - domain. Nevertheless, there is a relation between the transition from one domain to the other

and both measure the same thing or yield similar results. The relation between the frequency, f , and angular frequency, ω , is given by: $\omega = 2\pi f$.

Definition 3.3.3. Let $f : \mathcal{D} \subset \mathbb{R} \rightarrow \mathbb{R}$ be a real-valued function. Then for $x \in \mathcal{D} \subset \mathbb{R}$, the Fourier transform (FT) of the function f is given by:

$$\mathcal{F}(f(x); \omega) = \hat{f}(\omega) = \int_{-\infty}^{\infty} f(x)e^{i\omega x} dx, \quad \omega \in \mathbb{R}, \quad (3.3.5)$$

with $i = \sqrt{-1}$, ω is a parameter.

By inverse Fourier transform, it is possible to recover $f(x)$ from $\hat{f}(\omega)$.

Definition 3.3.4. An *inverse Fourier transform* (IFT) of a real-valued function, $\hat{f}(\omega)$, is given as:

$$\mathcal{F}^{-1}(\hat{f}(\omega); x) = f(x) = \frac{1}{2\pi} \int_{-\infty}^{\infty} \hat{f}(\omega)e^{-i\omega x} d\omega, \quad x \in \mathbb{R} \quad (3.3.6)$$

which belongs to L^1 - spaces.

3.3.2 Example of Fourier Transform

Example 1: Consider a piecewise function $f(x)$ defined below:

$$f(x) = \begin{cases} \frac{1}{4}, & \text{for } -2 \leq x < 0; \\ -\frac{1}{4}, & \text{for } 0 < x \leq 2. \\ 0; & \text{otherwise} \end{cases} \quad (3.3.7)$$

Compute the Fourier transform for $f(x)$.

Solution:

$$\mathcal{F}(f(x); \omega) = \hat{f}(\omega) = \int_{-2}^0 \frac{1}{4} e^{i\omega x} dx - \int_0^2 \frac{1}{4} e^{i\omega x} dx \quad (3.3.8)$$

$$\begin{aligned}
\hat{f}(\omega) &= \frac{1}{4} \left(\frac{e^{i\omega x}}{i\omega} \right) \Big|_{-2}^0 - \frac{1}{4} \left(\frac{e^{i\omega x}}{i\omega} \right) \Big|_0^2 \\
&= \frac{1}{4i\omega} \left(e^{i\omega(0)} - e^{i\omega(-2)} \right) - \frac{1}{4i\omega} \left(e^{i\omega(2)} - e^{i\omega(0)} \right) \\
&= \frac{1}{4i\omega} \left(1 - e^{-2i\omega} \right) - \frac{1}{4i\omega} \left(e^{2i\omega} - 1 \right) \\
&= \frac{1}{4i\omega} \left(1 - e^{-2i\omega} - e^{2i\omega} + 1 \right) \\
&= \frac{1}{4i\omega} \left(-e^{2i\omega} - e^{-2i\omega} + 2 \right) \\
&= -\frac{1}{4i\omega} \left(e^{i\omega} - e^{-i\omega} \right)^2
\end{aligned}$$

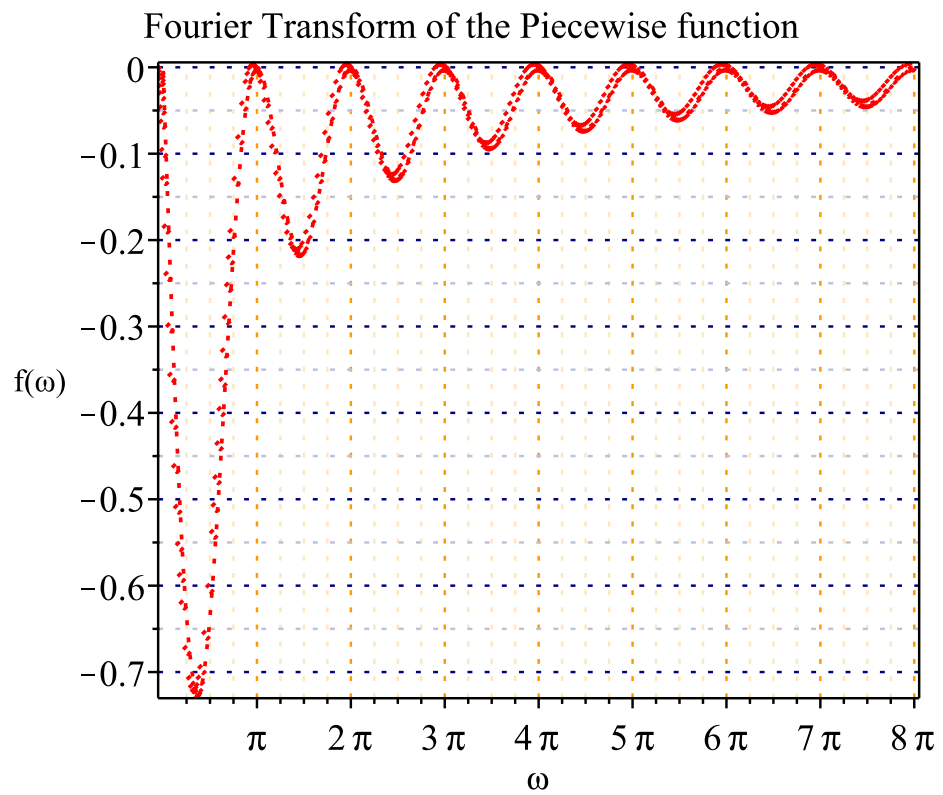
Applying Euler's identity

$$e^{i\omega} = \cos \omega + i \sin \omega, \quad e^{-i\omega} = \cos \omega - i \sin \omega$$

We have:

$$\hat{f}(\omega) = -\frac{1}{4i\omega} (2i \sin \omega)^2 = -\frac{i \sin^2 \omega}{\omega}.$$

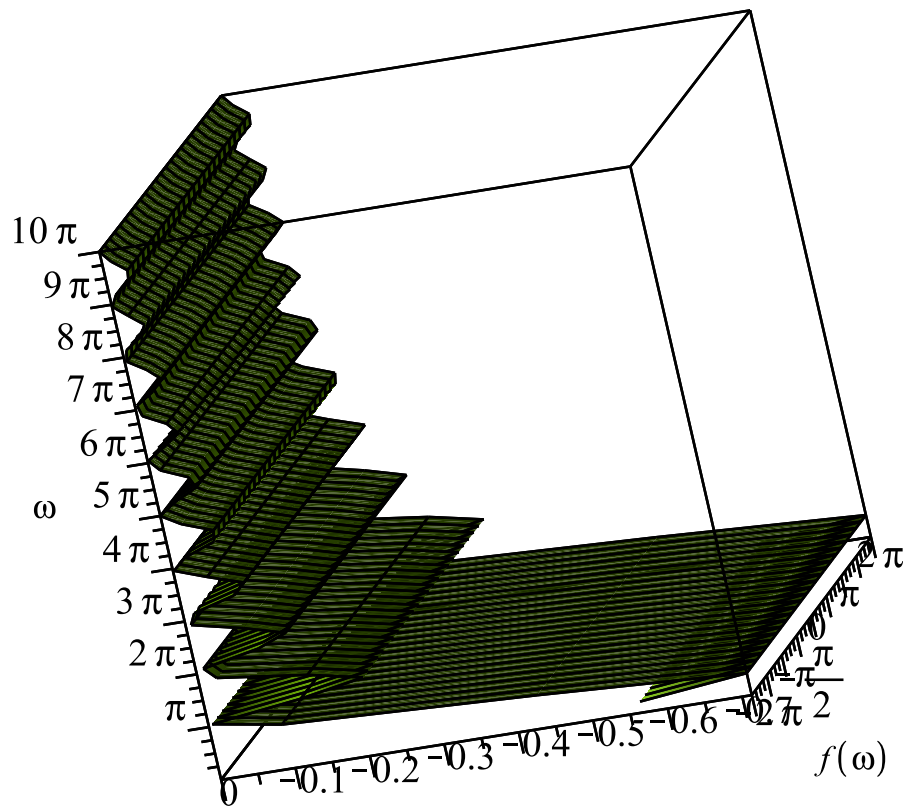
We give the graphical representation in 2-dimension and 3-dimension of the $\hat{f}(\omega) = -\frac{i \sin^2 \omega}{\omega}$ respectively in sequel.



Source: Author's self plotted graph via Maple 2017

Figure 3.1: 2D plot of the Fourier transform $\hat{f}(\omega)$ of the piecewise function $f(x)$

3D plot of Fourier Transform of the piecewise function

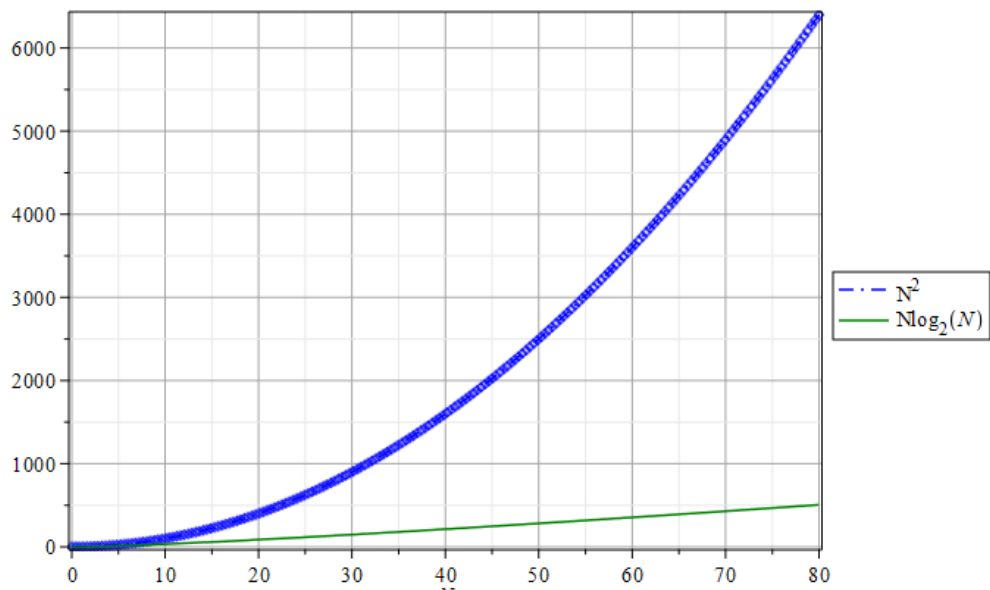


Source: Author's self plotted graph via Maple 2017

Figure 3.2: 3D-plot of the Fourier transform $\hat{f}(\omega)$ of the piecewise function $f(x)$

The figure 3.1 is the 2-dimensional graph of the Fourier transform $\hat{f}(\omega)$ of the piecewise function in equation (3.3.7). It was observed that the graph behaves like signal processing. At a uniform spacing of the Fourier-based argument ω taking interval of 20 each up to 120 points, the corresponding Fourier transform $\hat{f}(\omega)$ were obtained from 0.0 – 0.7. From the graph, $\hat{f}(\omega)$ was at its peak when the argument $\omega = 0$. There was contraction in value for increase in the argument ω up to 120. In other words, the signal plots converges to zero for sufficient ω -values greater than or equal to 120.

The figure 3.2 is the 3-dimensional plot of Fourier transform $\hat{f}(\omega)$ of the piecewise constant function given in equation (3.3.7). The graph was like a signal processing in nature. The argument ω - follows uniform spacing of $\frac{\pi}{2}$ in radians. By symmetric property of Fourier transform, the graph of the Fourier transformed function, $\hat{f}(\omega)$, shows equal visualisation for both the negative and positive values of the argument, ω , in radians. In other words, the 3D-plot above verifies the symmetric property of Fourier transform of an arbitrary piece-wise constant function. By extension, the property holds for square integrable functions.



Source: Author's self plotted graph via Maple 2017.

Figure 3.3: Fast Fourier transform speed based on the order of computation.

The figure 3.3 above shows computational complexities reduction based on the order of fast-Fourier transformation. Various studies has proved that fast-Fourier transform helps in reducing computational tussles of direct computation of the integrals of functions in Fourier transform which operates on power of 2 for the grid points N , that is N^2 , but through FFT-algorithm implementation on the Discrete Fourier transform (DFT), the order computation is $N \log_2 N$, that is $O(N \log_2 N)$, which makes the computational burden less. In other words, FFT-algorithm increases the speed of computation of the corresponding Discrete Fourier Transform faster than the Direct Computation which operates on order $O(N^2)$. The blue curve shows how slower the direct computation of the integrals was to the FFT computation of the corresponding DFT of the function. That is, the plot in orange colour shows the speed advantage of the FFT over direct computation.

3.3.3 Some Essential Properties of Fourier Transform

We maintained our representation of Fourier transform of a function $f(x)$ denoted as:

$$\hat{f}(\omega) = \mathcal{F}(f(x); \omega) = \int_{-\infty}^{\infty} f(x)e^{i\omega x} dx. \quad (3.3.9)$$

- Translation property:

$$\mathcal{F}(f(x - x_0); \omega) = e^{i\omega x_0} \hat{f}(\omega) \quad (3.3.10)$$

where x_0 is a constant.

- Linear property: Let $f(x)$ and $g(x)$ be any two arbitrary piecewise continuous functions in either L^1 -space or in square integrable space L^2 . The Fourier transform of the linearity of f and g is expressed as:

$$\mathcal{F}(af(x) + bg(x); \omega) = \int_{-\infty}^{\infty} (a(f(x); \omega) + b(f(x); \omega)) e^{i\omega x} dx \quad (3.3.11)$$

$$= a \int_{-\infty}^{\infty} f(x) e^{i\omega x} dx + b \int_{-\infty}^{\infty} g(x) e^{i\omega x} dx \quad (3.3.12)$$

$$= a\mathcal{F}(f(x); \omega) + b\mathcal{F}(g(x); \omega) \quad (3.3.13)$$

$$= a\hat{f}(\omega) + b\hat{g}(\omega) \quad (3.3.14)$$

where a and b are arbitrary non-zero numbers.

- Convolution property: This property is essential as convolution of any arbitrary well- defined two functions is mapped into the multiplication inside the Fourier space. Suppose $f, g \in L^1$ -space. The convolution of the two functions is defined by:

$$(f \star g)(x) = \int_{-\infty}^{\infty} f(x-y)g(y)dy = \int_{-\infty}^{\infty} f(y)g(x-y)dy \quad (3.3.15)$$

The Fourier transform of convolution of the given functions, f , and g , with convolution operator \star is given as:

$$\mathcal{F}((f \star g); \omega) = \int_{-\infty}^{\infty} [f(x-y)g(y)dy] e^{i\omega x} dx = \hat{f}(\omega)\hat{g}(\omega) \quad (3.3.16)$$

The equation (3.3.16) proof follows.

Proof:

$$\mathcal{F}((f \star g); \omega) = \int_{-\infty}^{\infty} \left[\int_{-\infty}^{\infty} f(x-y)g(y)dy \right] e^{i\omega x} dx \quad (3.3.17)$$

$$= \int_{-\infty}^{\infty} \left[\int_{-\infty}^{\infty} f(x-y)g(y)e^{i\omega x} dy \right] dx \quad (3.3.18)$$

$$= \int_{-\infty}^{\infty} \left[\int_{-\infty}^{\infty} f(x-y)g(y)e^{i\omega x} dx \right] dy \quad (3.3.19)$$

$$= \int_{-\infty}^{\infty} g(y) \left[\int_{-\infty}^{\infty} f(x-y)e^{i\omega x} dx \right] dy \quad (3.3.20)$$

We then have:

$$\mathcal{F}((f \star g); \omega) = \int_{-\infty}^{\infty} g(y) e^{i\omega y} \left[\int_{-\infty}^{\infty} f(\zeta) e^{i\omega(\zeta+y)} d\zeta \right] dy \quad (3.3.21)$$

$$= \int_{-\infty}^{\infty} g(y) e^{-i\omega y} \left[\int_{-\infty}^{\infty} f(\zeta) e^{i\omega\zeta} d\zeta \right] dy \quad (3.3.22)$$

$$= \hat{f}(\omega) \int_{-\infty}^{\infty} g(y) e^{i\omega y} dy \quad (3.3.23)$$

$$= \hat{f}(\omega) \hat{g}(\omega). \quad (3.3.24)$$

In similar way,

$$\mathcal{F}(fg; \omega) = \mathcal{F}(f(x; \omega)) \star \mathcal{F}(g(x; \omega)) \quad (3.3.25)$$

$$= \int_{-\infty}^{\infty} f(x) e^{i\omega x} \star \int_{-\infty}^{\infty} g(x) e^{i\omega x} \quad (3.3.26)$$

$$= \hat{f}(\omega) \star \hat{g}(\omega). \quad (3.3.27)$$

- Differentiation property: Let f be a piecewise n -times continuously differentiable function such that $f^{(n)}$ is the derivative of order $n \in \mathbb{N}$. Suppose each of the derivative is absolutely integrable on the whole real line, the Fourier transform of the derivative is then given by:

$$\mathcal{F}(f^{(n)}(x); \omega) = \int_{-\infty}^{\infty} f^{(n)}(x) e^{i\omega x} dx \quad (3.3.28)$$

$$= (i\omega)^n \int_{-\infty}^{\infty} f(x) e^{i\omega x} dx \quad (3.3.29)$$

$$= (i\omega)^n \mathcal{F}(f(x); \omega) \quad (3.3.30)$$

$$= (i\omega)^n \hat{f}(\omega). \quad (3.3.31)$$

- Symmetric property:

$$\mathcal{F}(f(x); \omega) = \hat{f}(\omega) \implies \mathcal{F}(f(-x); \omega) = \hat{f}(-\omega). \quad (3.3.32)$$

There is a very close relation between Fourier transform and characteristic function.

Definition 3.3.5. *Let $\mathbb{P}(x)$ denote the probability distribution function (pdf) for $x \in \mathbb{R}$. The definition of characteristic function $\phi(\omega)$, for $\omega \in \mathbb{R}$, coincides with the Fourier transform of $\mathbb{P}(x)$ expressed as:*

$$\mathcal{F}(\mathbb{P}(x); \omega) \equiv \hat{\phi}(\omega) \equiv \int_{-\infty}^{\infty} \mathbb{P}(x) e^{i\omega x} d\omega = \mathbb{E}[e^{i\omega x}] \quad (3.3.33)$$

It is possible to recover the pdf (probability distribution function) $\mathbb{P}(x)$, this is done through the reverse process of Fourier transform of the characteristic function analogous to the inverse Fourier transform (IFT) definition in (3.3.6).

This we defined by:

$$\mathbb{P}(x) = \mathcal{F}^{-1}(\hat{\phi}(\omega)) = \frac{1}{2\pi} \int_{-\infty}^{\infty} \hat{\phi}(\omega) e^{-i\omega x} d\omega. \quad (3.3.34)$$

3.3.4 The Fast Fourier Transform (FFT)

The Fast Fourier transform is a mathematical powerful algorithm for computing the Discrete Fourier Transform (DFT) of a sequence. The algorithm is capable of predicting future values in diverse of fields ranging from physics data, weather forecast data, environmental data to financial data. The FFT method of valuation is often applied by quantitative finance employing complex algorithmic trading strategies.

Definition 3.3.6. *(Schmelzle, 2010):*

The FFT has been reckoned with as a highly efficient implementation of discrete

Fourier transform mapping a vector $\mathbf{h} = (h_j)_{j=0}^{N-1}$ onto some vector $D_k(\mathbf{h})$ such that

$$D_k(\mathbf{h}) = \sum_{j=0}^{N-1} e^{-i\frac{2\pi}{N}jk} h_j, \quad k = 0, \dots, N-1. \quad (3.3.35)$$

In applications, N is usually expressed as power of 2. This is so in order to reduce the complexity of the FFT algorithm from an order of N^2 for direct numerical integration methods to that of $N \log_2 N$ operations to compute N values.

3.3.5 Symmetric Property of characteristic function for Fourier

Integrals simplification

In the complex plane, the real part of the characteristic function denoted by: $\Re[\varphi_X(\omega)]$ is given by:

$$\Re[\varphi_X(\omega)] = \frac{\varphi_X(\omega) + \varphi_X(-\omega)}{2} \quad (3.3.36)$$

and the imaginary part, $\Im[\varphi_X(\omega)]$ is given by:

$$\Im[\varphi_X(\omega)] = \frac{\varphi_X(\omega) - \varphi_X(-\omega)}{2i}, \quad i = \sqrt{-1} \quad (3.3.37)$$

showing that the real part $\Re[\varphi_X(\omega)]$ of the characteristic function is even but the imaginary part is odd for all ω . By the unique property of an even function, the negative and positive halves are the same, it is easy to express probability density function $f_X(x)$ in the simplification of Fourier integrals as shown in what follows:

$$f_X(x) = \frac{1}{2\pi} \Re \left[\int_{-\infty}^0 e^{-i\omega x} \varphi_X(\omega) d\omega \right] + \frac{1}{2\pi} \Re \left[\int_0^{\infty} e^{-i\omega x} \varphi_X(\omega) d\omega \right], \quad (3.3.38)$$

$$= \frac{1}{2\pi} \Re \left[\int_{-\infty}^0 \overline{e^{-i\omega x} \varphi_X(\omega)} d\omega \right] + \frac{1}{2\pi} \Re \left[\int_0^{\infty} e^{-i\omega x} \varphi_X(\omega) d\omega \right], \quad (3.3.39)$$

$$= \frac{1}{2\pi} \Re \left[2 \int_0^{\infty} e^{-i\omega x} \varphi_X(\omega) d\omega \right], \quad (3.3.40)$$

$$= \frac{1}{\pi} \Re \left[\int_0^{\infty} e^{-i\omega x} \varphi_X(\omega) d\omega \right]. \quad (3.3.41)$$

The cumulative distribution function CDF is calculated similarly as follows:

$$F_X(x) = \frac{1}{2} + \frac{1}{2\pi} \int_0^\infty \frac{e^{i\omega x} \varphi_X(-\omega) - e^{-i\omega x} \varphi_X(\omega)}{i\omega} d\omega, \quad (3.3.42)$$

$$= \frac{1}{2} + \frac{1}{2\pi} \int_0^\infty \frac{-e^{-i\omega x} \varphi_X(\omega) - e^{-i\omega x} \varphi_X(\omega)}{i\omega} d\omega, \quad (3.3.43)$$

$$= \frac{1}{2} - \frac{1}{\pi} \int_0^\infty \Re \left[\frac{e^{i\omega x} \varphi_X(\omega)}{i\omega} \right] d\omega, \quad (3.3.44)$$

$$= \frac{1}{2} - \frac{1}{\pi} \int_0^\infty \Im \left[\frac{e^{i\omega x} \varphi_X(\omega)}{\omega} \right] d\omega \quad (3.3.45)$$

The complementary cumulative distribution function denoted $F'_X(x)$ follows using the probability relation, $F'_X(x) + F_X(x) = 1$, with the probability,

$$\mathbb{P}(X > x) := \int_x^\infty f_X(x) dx \equiv F'_X(x).$$

We thus obtain:

$$F'_X(x) = \frac{1}{2} + \frac{1}{\pi} \int_0^\infty \Re \left[\frac{e^{i\omega x} \varphi_X(\omega)}{i\omega} \right] d\omega, \quad (3.3.46)$$

$$= \frac{1}{2} + \frac{1}{\pi} \int_0^\infty \Im \left[\frac{e^{i\omega x} \varphi_X(\omega)}{\omega} \right] d\omega. \quad (3.3.47)$$

STUDY THREE

3.4 Uncertainty theory

Definition 3.4.1. (Baoding, 2010; Ugbebor, 2011): Let Γ be a non-empty set.

Then, a collection \mathcal{L} containing the subsets of Γ is said to be an algebra over Γ

whenever the following conditions are satisfied:

- (i) $\Gamma \in \mathcal{L}$;
- (ii) if $\Lambda \in \mathcal{L}$, then $\Lambda^c \in \mathcal{L}$; and

(iii) if $\Lambda_1, \Lambda_2, \dots, \Lambda_n \in \mathcal{L}$, then

$$\bigcup_{i=1}^n \Lambda_i \in \mathcal{L}.$$

Under the concept of countable union, if $\Lambda_1, \Lambda_2, \dots, \Lambda_n \in \mathcal{L}$, such that

$$\bigcup_{i=1}^{\infty} \Lambda_i \in \mathcal{L},$$

the collection \mathcal{L} is a σ - algebra over Γ .

Example 3.4.1. Suppose Λ is a proper subset of Γ . Then $\{\emptyset, \Lambda, \Lambda^c, \Gamma\}$ formed a σ -algebra on Γ .

Remark 3.4.1. The collection, Γ , is closed with respect to countable union, countable intersection, difference and limit.

Definition 3.4.2. (Ugbebor, 2011): Let $\Gamma \neq \emptyset$ be a non-empty set. Suppose \mathcal{L} is a σ -algebra over Γ . Then the pair (Γ, \mathcal{L}) is called a *measurable space* and any element or member belonging to \mathcal{L} is a measurable set.

Definition 3.4.3. (Ugbebor, 2011): A function $\xi := (\Gamma, \mathcal{L}) \rightarrow \mathbb{R}$ is *measurable* whenever

$$\xi^{-1}(\mathcal{B}) = \{\gamma \in \Gamma \mid \xi(\gamma) \in \mathcal{B}\} \in \mathcal{L} \quad (3.4.1)$$

where the space (Γ, \mathcal{L}) measurable and $\mathcal{B}(\mathbb{R})$ is a Borel set defined on entire real line \mathbb{R} .

3.4.1 Uncertain Measure

The following properties holds for an uncertain process (Baoding, 2010).

Property 1 (Normality Property): $\mathcal{M}\{\Gamma\} = 1$, for Γ being the universal set.

Property 2 (Duality Property): $\mathcal{M}(\Lambda) + \mathcal{M}(\Lambda^c) = 1$, for every event Λ .

Property 3 (Subadditivity Property): $\mathcal{M}\left\{\bigcup_{i=1}^{\infty} \Lambda_i\right\} \leq \sum_{i=1}^{\infty} \mathcal{M}\{\Lambda_i\}$ for each countable sequence of events $\Lambda_1, \Lambda_2, \dots$.

CHAPTER FOUR

RESULTS AND DISCUSSIONS

4.1 Chapter Overview

This chapter consists of results presentation and discussions of our findings in this study. We present a total of eleven (11) studies under the following tags: RESULT 1, RESULT 2, RESULT 3, and RESULT 4 respectively, in a more robust form. RESULT 1 is titled “FFT Computation of American Options Prices with Economy Recession induced Stochastic Volatility”. It consists of the following sections: Introduction, Justification for recession causing Jumps in the asset price, Jumps in an underlying stock price, Some factors liable for stock’s price jumps, the model assumptions, the model formulation, the model Solution, numerical Fourier based transform of options, numerical experiment, Discussion of result 1, and Conclusion.

The title of RESULT 2 is “FFT Computation of Multi-assets Options with Economy Recession Induced Uncertainties”. The sections involved are: An overview of the result 2, Introduction, FFT Algorithm, The FFT of a class of multi-assets in finite dimensions, Application on 3-dimensional Assets, Table of results 2, Discussion of Result 2, and Conclusion.

The tag “RESULT 3” is titled “Accuracy of Fast Fourier Transform Method with Control Fineness of Integration grid for Valuation of American Option”. It consists of the following sections and subsections: An overview of Result 3, Introduction, Factorial function based Black - Scholes PDE for option pricing, Moving boundary for American options, Determination of Optimal Exercise Boundaries for American

options, Fourier transform solution step of the Black - Scholes-like pde formulation for American options, Fast Fourier transform for non-dividend paying American call options, and Numerical results, and Result discussion.

The last result obtained tagged “Result 4” is titled “Triple Stochastic Volatility Heston-like model for option valuation in a Recessed Economy”. The sections involved are: An overview of the result 4, Introduction, Preliminaries to the model formulation, A control regime-switching Triple Stochastic Volatility Heston-like (TSVH) model, The PDE representation for TSVH model, Characteristic function derivation for the TSVH model, Numerical discretisation and Simulation schemes for the TSVH model, Simulations and sample paths of the TSVH-model, and Discussion of result 4.

RESULT 1

FFT Computation of American Options Prices with Economic Recession induced Stochastic Volatility

4.2 STUDY ONE

4.2.1 Preamble

Financial Mathematics applies many mathematical concepts and tools. The concepts include the following but not limited to: Probability theory, partial differential equations, Uncertainty theory, Control theory, Optimization theory, Ordinary Differential Equations (ODEs), numerical analysis, Stochastic Differential Equations (SDEs), transformation and many more. Mathematical consistency is required while formulating mathematical models in mathematical finance. Among numerous mathematical transformation techniques are: Laplace transform, Mellin transform, Hankel transform, Hilbert and Fourier transform. We apply fast Fourier transform computational method to options on financial assets with focus on uncertainty induced by economic recession on the option's payoff or returns.

In recent time, Pfante, and Bertschinger, (2018) carried out research on “Uncertainty of volatility estimates from the perspective of Heston Greeks”. Volatility has been verified to be the major cause of numerous statistical properties of observed stock price processes”. A variation in assets stochastic term structure such as volatility poses a serious challenge on assets' prices stability. In other words, stock asset price instability is a function of uncertainty term structure associated with the stock asset valuation in the financial markets. Hence, there is need for responsive study of stocks prices volatility.

However, our stated objectives (i) and (ii) in chapter 1 were achieved under this RESULT 1. Our contribution to knowledge on options valuation under the “Result 1” are highlighted in what follows:

(i) We incorporated the notion of volatility uncertainty with respect to economy re-

cession in exponential jump model driven by stochastic volatility and intensity. The proposed economy recession induced volatility is reckoned as an uncertain variable.

(ii) Characteristic function derivation of the affine model is carried out to involve recession uncertainty effect.

(iii) Fourier transform of the proposed affine model.

(iv) The affine model characteristic function is extended to Carr & Madan (1999) - type fast Fourier transform algorithm used in European options pricing. This algorithm was extended to American style options valuation through the inclusion of *time premium* in which its limit value goes to zero at the options expiration.

(v) The affine model volatility surface with respect to economy recession induced uncertainty.

4.2.2 Justification for recession causing Jumps in the asset's price associated with Economic Recession

There are some major market parameters paramount to financial modelers in financial models formulation. These include: price, riskless interest rate, volatility, dividend rate and time. Asset prices undergo lots of fluctuations during recession period. Assets such as stocks are never seen to be stable. Due to the behaviour exhibited by stocks or risky assets generally, the interest rate and volatility parameter ought to be considered as stochastic in nature. In some exceptional cases, a constant value is assigned to the interest rate, r , but in reality, stochastic volatility should be considered because the market volatility behaviour does not seem to be constant. The volatility of Stock is taken as a measure of uncertainty on the stock asset's returns or payoff which investors use in decision taking. The volatility variation during economy recession period is considered higher than when the economy is in recession-free state. However, recession factor is taken into consideration in our model formulations in this study.

4.2.3 An Underlying Stock price jump

Let the stock price $S(t)$ possesses dynamics given by

$$\frac{dS(t)}{S(t)} = \left(r - q - \lambda(t)m \right) dt + \sqrt{\sigma(t)} dW_s(t) + (e^\nu - 1) dN(t) \quad (4.2.1)$$

where r is taken as the risk-neutral interest rate, q as the dividend yield rate, the $N(t)$ is a Poisson process equipped with stochastic intensity parameter $\lambda(t)$, and the average jump amplitude is expressed as $m = \mathbb{E}^{\hat{P}}(e^\nu - 1)$ where the jump size ν varies randomly. The equation consists of two processes, that is, the *diffusion process* and the *jump process*. The stock price is governed by two sources of fluctuations, and we grouped them as “*changes in the state of the economy*” and “*changes arising from supply and demand factors*”. However, the jump process in the model caters for the arrival of some information into the stock market which could affect the performance of stock price negatively.

4.2.4 Some factors causing Stock’s price Jumps

Among the factors responsible for stock asset price jumps highlighted in the study by Matthew (2007), we include economy recession. However, the factors are hereby grouped as follows:

- (a) **Firm specific jumps:** These category of jumps arises due to news inflow to the stock markets from time to time on firm’s profit/loss report.
- (b) **Industrial sector specific jumps:** These arise as a result of unfavourable news affecting specific company/ industry to include the news on sudden *holiday* declaration.
- (c) **Market specific jumps:** These type of jumps evolve if there is breaking news on either rising or down trend of events, say the oil prices, the credit spreads, etc which invariably could affect the stock market performance.

(d) **Economy recession jumps:** The economy state news inflow to the stock market including events such as economy crisis coupled with economy recession probability indicators. Other forms of sudden events is the Corona virus pandemic (Covid-19) outbreak in the year 2019 which emanated from Wuhan in China. The latter has affected the whole world health wise and by extension, affected the global economy including Nigeria. These are some of the factors that can lead to stock price uncertainties induced by economy recession jumps.

In the model formulation of our financial assets (stocks) price which focuses on economy recession induced stochastic volatility effect on stocks, the highlighted factors above are further grouped as we can see as follows. The first three factors, “(a)-(c)” were grouped into *other sources* and setting its volatility to be σ_t^* , while σ_t^{rec} is assigned to the economy recession induced volatility source in the specified factor in (d).

Let $N(t)$ be a well-defined *Poisson process* subject to the probability density function (pdf) given by the equation:

$$P(N_t = \nu) = \frac{(\lambda t^\nu)}{\nu!} e^{-\lambda t}, \quad \nu = 0, 1, 2, \dots \quad (4.2.2)$$

where λ denotes the intensity parameter. With reference to Matthew (2007), we propose that whenever economy recession information and the likes from other sources enter the stock market, there exists an instantaneous jump in the price of the stocks from $S(t) \rightarrow \nu_t S(t)$ where ν_t is the absolute magnitude of the jump. Then the relative price change is given as:

$$\frac{dS(t)}{S(t)} = \frac{\nu_t S(t) - S(t)}{S(t)} = \frac{S(t)(\nu_t - 1)}{S(t)} = \nu_t - 1. \quad (4.2.3)$$

4.3 The Roadmap to the first model formulation

4.3.1 The Model Assumptions

Assumption 1: Let X_t be an asset under the influence of two sources of volatility. That is, $\sigma_{X_t}^{rec}$ and $\sigma_{X_s}^{os}$, which are respectively the market volatility prompted by economy recession, and the market volatility from other sources such that

$$\sigma_{X_s}^{market} = \sigma_t^{rec} + \sigma_s^{os}. \quad (4.3.1)$$

Assumption 2: The economy state is assumed unique always, uniqueness in the sense that the economy is never seen to be in two states at a time concurrently. Hence, the volatility parameter is ‘economy state dependent’ while pricing in the stock market. For instance, during economy recession period, the volatility of the stock is taken as $\sigma^{market} = \sigma_t^{rec} + \sigma_s^{os}$, due to the effect of economy recession on the market price but during recession-free state, the stock market volatility $\sigma_t^{market} = \sigma_s^{os}$ that is the volatility from other sources, since $\sigma_s^{rec} = 0$. Hereafter, we define $\sigma_s^{os} := \sigma_s^*$.

4.3.2 Uncertain variable with respect to Recession

Suppose $\xi(\gamma)$ is an economy recession variable defined over an uncertain space, $(\Gamma, \mathcal{L}, \mathcal{M})$, where $\gamma = \{\gamma_1, \gamma_2\}$ such that

$$\mathcal{M}\{\gamma_1\} = \alpha, \quad \mathcal{M}\{\gamma_2\} = \beta.$$

Then

$$\xi(\gamma) = \begin{cases} 0, & \text{if } \gamma = \gamma_1 \\ 1, & \text{if } \gamma = \gamma_2 \end{cases} \quad (4.3.2)$$

is an uncertain variable. The following holds

$$\mathcal{M}\{\xi = 0\} = \mathcal{M}\{\gamma \mid \xi(\gamma) = 0\} = \mathcal{M}\{\gamma_1\} = \alpha$$

and

$$\mathcal{M}\{\xi = 1\} = \mathcal{M}\{\gamma \mid \xi(\gamma) = 1\} = \mathcal{M}\{\gamma_2\} = \beta$$

such that $\mathcal{M}\{\gamma_1\} + \mathcal{M}\{\gamma_2\} \equiv \alpha + \beta = 1$.

Example 4.3.1. Suppose the economy recession-induced variation process $\xi(\gamma)$ given above is defined on the uncertain space, $(\Gamma, \mathcal{L}, \mathcal{M})$, where $\gamma = \{\gamma_1, \gamma_2\}$ such that

$$\mathcal{M}\{\gamma_1\} = 0.41, \quad \mathcal{M}\{\gamma_2\} = 0.59$$

which satisfies equation (4.3.2), then

$$\mathcal{M}\{\xi = 0\} = \mathcal{M}\{\gamma \mid \xi(\gamma) = 0\} = \mathcal{M}\{\gamma_1\} = 0.41$$

and

$$\mathcal{M}\{\xi = 1\} = \mathcal{M}\{\gamma \mid \xi(\gamma) = 1\} = \mathcal{M}\{\gamma_2\} = 0.59$$

Suppose $(\Omega, \mathcal{F}_t, \hat{\mathcal{P}}, \mathbb{F})$ is a filtered probability space such that $\mathcal{F}_t := \mathcal{F}_t^{eco} \subseteq \mathcal{F}_t^{mkt}$ with \mathcal{F}_t^{mkt} and \mathcal{F}_t^{eco} describing the market filtration and the economy in which the market activities takes place respectively. \mathcal{F}_t^{mkt} and \mathcal{F}_t^{eco} are the market and the economic filtration at a given time $t \in (0, T]$ respectively.

Definition 4.3.1. (Wei-yin, 2014): “An uncertain random variable is defined as a measurable function, say $\xi \in \mathbb{R}^p$ (resp. $\mathbb{R}^{p \times m}$), emanating from an uncertainty probability space, $(\Gamma \times \Omega, \mathcal{L} \otimes \mathcal{F}, \mathcal{M} \times P)$, to a nonempty set in \mathbb{R}^p (resp. $\mathbb{R}^{p \times m}$),

for any Borel set $A \in \mathbb{R}^p$ (resp, $\mathbb{R}^{p \times m}$), the given set

$$\{\xi \in A\} = \{(\gamma, \omega) \in \Gamma \times \Omega : \xi \in (\gamma, \omega) \in A\} \in \mathcal{L} \otimes \mathcal{F}.$$

The mathematical expectation (i.e the expected value) of such uncertain random variable, ξ , is defined by:

$$\mathbb{E}[\xi] = \mathbb{E}_p[\mathbb{E}_{\mathcal{M}}[\xi]] = \int_{\Omega} \left[\int_0^{\infty} \mathcal{M}\{\xi \geq r\} dr \right] P(d\omega) - \int_{\Omega} \left[\int_0^{\infty} \mathcal{M}\{\xi \leq r\} dr \right] P(d\omega) \quad (4.3.3)$$

where \mathbb{E}_p and $\mathbb{E}_{\mathcal{M}}$ represent the expected values under the uncertainty space and the probability space, respectively”.

The definition given above shows the connection between the concept of probability and uncertainty theory in the sense that a random variable is defined from a probability space to an uncertainty space. An introduction of the concept of uncertainty theory into financial model formulation makes sense taking into consideration stock asset valuation during economy recession period or other forms of financial crisis arising in the market.

Some authors such as Erik Lindström and Johan Strålfors, (2012) in their research studies considered parameter uncertainty in financial models, but to the best of our knowledge the concept of economy recession induced uncertainty has not been introduced by any of the authors. Consequently, we therefore introduced the concept of economy recession induced uncertainty to the stochastic volatility term structure in our model formulation for option pricing.

4.4 The first Model

The first model is formulated as follows ‘an Uncertain Affine Exponential-Jump Model (UAEM) with recession induced stochastic - volatility and stochastic - intensity’. Let an asset, X , at a time, t , be a two-state regime switching process such

that the asset prices could switch within the given two states defined as:

$$X_t = \begin{cases} 1, & \text{if the economy is in the state of Expansion;} \\ 2, & \text{if the economy is in the state of Recession.} \end{cases} \quad (4.4.1)$$

Suppose there exists a flow from one state to the other which follows a Poisson process such that

$$P(t_{lm}^* > t) = \exp(-\lambda_{lm}^* t), \quad l, m = 1, 2; \quad (4.4.2)$$

where λ_{lm}^* is the transition rate from state l , to state m , while the time spent in the state, l , prior to the transition to state, m , is t_{lm}^* .

Let the price of the asset, X , be defined on a filtered probability space $(\Omega, \mathcal{F}_t^{mkt}, \mathcal{P}, \mathbb{F})$ and assume the filtration of the market is generated by both standard Wiener process and jump process in a specified time, $t \in [0, T]$. Take P to be a risk-neutral probability measure or an equivalent Martingale measure. The anticipating model (*UAEM*) which governs the dynamics of the underlying stock price, $S(t)$, is given as:

$$\begin{cases} dS(t) = (r - q - \lambda(t)m)S(t)dt + \sqrt{\sigma(t)}dW_s(t) + (e^\nu - 1)S(t)dN(t), & S(0) = S_0 > 0 \\ d\sigma(t) = \kappa_\sigma(\beta^* + \beta^{rec} - \sigma(t))dt + \xi_\sigma\sqrt{\sigma(t)}dW_\sigma(t), & \sigma(0) = \sigma_0 > 0 \\ d\lambda(t) = \kappa_\lambda(\theta - \lambda(t))dt + \xi_\lambda\sqrt{\lambda(t)}dW_\lambda(t), & \lambda(0) = \lambda_0 > 0. \end{cases} \quad (4.4.3)$$

where, r is a risk-neutral interest rate, q is a dividend rate for a dividend paying stock, $N(t)$ is Poisson process subject to a stochastic intensity $\lambda(t)$, and an average jump amplitude is given as $m = \mathbb{E}^P(e^\nu - 1)$ with jump size ν , which is a random variable. The other parameters, $\xi_\sigma > 0$, and $\xi_\lambda > 0$, are specified constants with mean - reverting rates, κ_σ , and κ_λ , which are all positive constants.

The stochastic volatility, $\sigma(t)$, of the stock market is given by:

$$\sigma(t) = \begin{cases} \sigma^{rec} + \sigma^*, & \text{when the economy is under recession ;} \\ \sigma^*, & \text{when the economy is in expansion state (i.e recession-free state).} \end{cases} \quad (4.4.4)$$

where σ^{rec} is the economy recession-induced volatility arising as a result of information inflow into the stock market from the recessed economy, and σ^* is the stock market volatility from other sources. Moreover, the constants β^* and β^{rec} are referred to as the other sources long term volatility, and economy recession-induced long term volatility during economy recession period respectively while θ denotes the intensity constant.

The β^{rec} is the economy recession-induced long-run volatility emanating from the recessed economy complementing the usual long-run volatility, throughout the life-span of the stocks' option valuation. The $W_s(t)$ and $W_\sigma(t)$ are Wiener processes whereby $W_\lambda(t)$ evolves independent of the correlation of the Wiener processes $W_s(t)$ and $W_\sigma(t)$ in the given model presented above. The correlation of $W_s(t)$ and $W_\sigma(t)$ is such that $\langle W_s(t), W_\sigma(t) \rangle = \rho dt$ and $|\rho|$ is necessarily less than 1. The parameter, m , has been taken to be an average jump amplitude as the stock price jumps could either be upward or downward. Thus, we have

$$m = \frac{p}{1 - \xi_u} + \frac{q}{1 + \xi_d} - 1 \equiv \int_{-\infty}^{\infty} e^\nu f(\nu) d\nu - 1 \quad (4.4.5)$$

where p denotes the probability of the upward jumps and q , the downward jumps respectively such that $p + q = 1$.

Jiexiang et al. (2014) gave the mean positive jumps and negative jumps in their model as $\frac{1}{\xi_u}$ and $\frac{1}{\xi_d}$, respectively. The solution and some analysis of “double exponential jump model with respect to stochastic-volatility and stochastic-intensity” was presented in their study (Jiexiang et al., 2014). The uniqueness of our own model is the concept of economy recession stochastic volatility inclusion which was

not in their own model.

Remark 4.4.1. *The stochastic volatility, $\sigma(t)_{x_t}$, in our model includes recession-induced volatility uncertainties of stock prices.*

4.4.1 Characteristic function

Definition 4.4.1. Let X be an arbitrary random variable. The characteristic function of X , is given as:

$$\varphi_X(\omega) = \mathbb{E}(e^{i\omega X}) = \int_{-\infty}^{\infty} f_X(x)e^{i\omega x} dx, \quad \omega \in \mathbb{R}, \quad (4.4.6)$$

where $f_X(x)$ denotes the probability density function (pdf) of the random variable X . The above definition is similar to inverse Fourier Transform of function given in equation (3.3.6) if $\frac{1}{2\pi}$ is excluded. For instance, let N_t be a Poisson process with parameter λ , then the characteristic function in discrete form is expressed as:

$$\varphi_N(\omega) \equiv \mathbb{E}(e^{i\omega N_t}) = \exp\{\lambda t(e^{i\omega} - 1)\}. \quad (4.4.7)$$

However, the concept of moment generating function is related to characteristic function. The moment generating function say, \mathbf{M} , of an arbitrary real valued random variable has applications in probability theory. One important difference is that for characteristic function, $|\varphi_x(t)| \leq 1$ whereas moment generating function may not exists outside a small interval including zero (Ugbebor, 2011).

Definition 4.4.2. The moment generating function (MGF) of an arbitrary random variable, X , is mathematically expressed as:

$$M(t) = \mathbb{E}(e^{tX}), \quad t \in \mathbb{R}, \quad (4.4.8)$$

if the expectation exists.

Example 4.4.1. Let $P(\lambda)$ be a Poisson distribution. Then, the moment-generating function $M(t) = e^{\lambda(e^t-1)}$ while its characteristic function $\varphi(t) = e^{\lambda(e^{it}-1)}$.

In the case of continuous probability density function, we define the moment-generating function as:

$$M(t) = \int_{-\infty}^{\infty} e^{tx} f(x) dx \quad (4.4.9)$$

where $f(x)$ represents the probability distribution function.

However, setting $x(\tau) := \ln S(\tau)$, and $\tau = T - t$ or $\tau = t^* - t$ depending on the consideration at hand where $x(\tau)$ is taken as the log stock asset price in the model (4.4.3) and τ denotes the time difference in the option's expiration time and the present time or the time difference in the optimal time to exercise the option and the present time. The latter is valid for early exercise possibility in American - type option if the optimal exercise time for the option is determined or known. The Feynman-Kac Formula is applied while deriving the characteristic function for the UAEM in 4.4.3 as follows.

4.4.2 The Feynman-Kac formula

This formula makes it possible to obtain the probabilistic expectation with respect to an Itô-diffusion process as a solution of the related partial differential equation. As an illustration, consider a d -dimensional stochastic process, $X(t) = (X_t^1, \dots, X_t^d)$, a solution of the stochastic differential equation

$$dX_t^i = \mu_i(t, X_t)dt + \sigma_i(t, X_t)dW_t^i$$

where W_t^i , $i = 1, \dots, d$, are Wiener's process equipped with the correlation given by $\langle dW_t^i, dW_t^j \rangle = \rho_{ij}dt$. Let $\mathcal{Z}(x) = \mathcal{Z}(x_1, \dots, x_d)$ be some payoffs. Then the function

$$g(t, x) := \mathbb{E}[\mathcal{Z}(X_T) | X_t = x] \quad (4.4.10)$$

is a solution of the partial differential equation

$$\frac{\partial g}{\partial t} + \sum_{i=1}^d \mu(t, x) \frac{\partial g}{\partial x_i} + \frac{1}{2} \sum_{i,j=1}^d \rho_{ij} \sigma_i(t, x) \sigma_j(t, x) \frac{\partial^2 g}{\partial x_i \partial x_j} = 0 \quad (4.4.11)$$

subject to the terminal condition $g(t, x) = \mathcal{Z}(x)$. In the case of a 1-dimensional stochastic process, X_t . Suppose X_t is the solution of the stochastic differential equation:

$$dX_t = \mu(t, X_t)dt + \sigma(t, X_t)dW_t. \quad (4.4.12)$$

The Feynman-Kac formula for an arbitrary function say

$$g(t, X_t) = \mathbb{E}[g(t, X_t) | X(t)] \quad (4.4.13)$$

is the solution to the partial differential equation

$$\frac{\partial g}{\partial t} + \mu(t, X_t) \frac{\partial g}{\partial x} + \frac{1}{2} \sigma^2(t, X_t) \frac{\partial^2 g}{\partial x^2} = 0. \quad (4.4.14)$$

The equation (4.4.13) can be extended to the concept of *characteristic function* as:

$$g(\tau, X_\tau) = \varphi(\omega, X_\tau, \tau) = e^{i\omega X_\tau}. \quad (4.4.15)$$

Similarly,

$$g(\tau, X_t) = \varphi(\omega, X_t, t) = e^{i\omega X_t} = \mathbb{E}[e^{i\omega X_\tau} | X_t]. \quad (4.4.16)$$

Remark 4.4.2. (i) $\varphi(\omega, X_\tau, \tau)$ represents the characteristic function of X_τ .

(ii) The moment generating function $M(\omega) = \varphi(-i\omega)$.

In the next study, we present the solution of the UAEM model for options valuation.

4.5 STUDY TWO

4.5.1 The Model Solution

We present the solution of the first formulated model UAEM as follows.

Theorem 4.5.1. Let a stock asset under economic recession be driven by the formulated model in equation (4.4.3). Then the closed form solution of the model for the stock asset via characteristic function is given as:

$$M(\omega, x(\tau), \sigma(\tau), \lambda(\tau), \tau) = e^{(r-q)\tau\omega + \omega x(\tau) + A(\omega, \tau) + B(\omega, \tau)\sigma(\tau) + C(\omega, \tau)\lambda(\tau)} \quad (4.5.1)$$

where

$$\begin{aligned} A(\omega, \tau) &= -\left\{ \frac{\kappa_\sigma(\beta^* + \beta^{rec})}{\xi_\sigma^2} \left[\psi_{+\tau} + 2 \ln \left(\frac{\psi_- + \psi_+ e^{-\varsigma\tau}}{2\varsigma} \right) \right] + \frac{\kappa_\lambda \theta}{\xi_\lambda^2} \left[\psi_{+\tau} + 2 \ln \left(\frac{\chi_- + \chi_+ e^{-\epsilon\tau}}{2\epsilon} \right) \right] \right\} \\ B(\omega, \tau) &= -(\omega - \omega^2) \frac{1 - e^{-\varsigma\tau}}{\psi_- + \psi_+ e^{-\varsigma\tau}} \\ C(\omega, \tau) &= 2\Lambda \left(\frac{1 - e^{-\epsilon\tau}}{\psi_- + \psi_+ + e^{-\varsigma\tau}} \right) \\ \Lambda(\omega) &= \int_{-\infty}^{\infty} e^{\nu\omega} f(\nu) d\nu - 1 - \omega \left(\int_{-\infty}^{\infty} e^\nu f(\nu) d\nu - 1 \right), \\ \epsilon &= \sqrt{\kappa_\lambda^2 - 2\xi_\lambda^2 \Lambda(\omega)} \\ \chi_\pm &= \epsilon \mp \kappa_\lambda \\ \psi_\pm &= \mp \left(\kappa_\sigma - \rho \xi_\sigma \omega \right) + \sqrt{(\kappa_\sigma - \rho \xi_\sigma \omega)^2 - \xi_\sigma (\omega - \omega^2)} \\ \varsigma &= \sqrt{(\kappa_\sigma - \rho \xi_\sigma \omega)^2 - \xi_\sigma (\omega - \omega^2)}. \end{aligned}$$

Proof:

Consider the model in equation (4.4.3) rewritten in the form:

$$\begin{cases} \frac{dS(t)}{S(t)} = \left(r - q - \lambda(t)m \right) dt + \sqrt{\sigma(t)} dW_s(t) + (e^\nu - 1) dN(t), & S(0) = S_0 > 0 \\ d\sigma(t) = \kappa_\sigma \left(\beta^* + \beta^{rec} - \sigma(t) \right) dt + \xi_\sigma \sqrt{\sigma(t)} dW_\sigma(t), & \sigma(0) = \sigma_0 > 0 \\ d\lambda(t) = \kappa_\lambda (\theta - \lambda(t)) dt + \xi_\lambda \sqrt{\lambda(t)} dW_\lambda(t), & \lambda(0) = \lambda_0 > 0. \end{cases} \quad (4.5.2)$$

where $\langle dW_s(t), dW_\sigma(t) \rangle = \rho dt$ and $\langle dW_s(t), dW_\lambda(t) \rangle = 0 = \langle dW_\sigma(t), dW_\lambda(t) \rangle$ and the volatility is $\sigma(t) = \sigma^* + \sigma^{rec}$ as defined in equation (4.4.4).

The partial integro-differential equation (PIDE) for the moment generating function, $M(\omega)$ of $x_\tau := \ln S_\tau$ for the above model is expressed as:

$$\begin{aligned} & M_\tau + \left(r - q - \frac{1}{2}\sigma(\tau) - \lambda(\tau)m \right) M_x + \frac{1}{2}\sigma M_{xx} + \kappa_\sigma \left(\beta^* + \beta^{rec} - \sigma(\tau) \right) M_\sigma + \frac{1}{2}\xi_\sigma^2 \sigma(\tau) M_{\sigma\sigma} \\ & + \rho \xi_\sigma M_{x\sigma} + \kappa_\lambda (\theta - \lambda(\tau)) M_\lambda + \frac{1}{2}\xi_\lambda^2 \lambda M_{\lambda\lambda} + \lambda \int_{-\infty}^{\infty} (M(x + \nu) - M(\nu)) f(\nu) d\nu = 0 \end{aligned} \quad (4.5.3)$$

where $M_\tau = e^{x(\tau)\omega}$, is the terminal condition and $m = \int_{-\infty}^{\infty} e^\nu f(\nu) d\nu - 1$.

A guess at the solution of the PIDE (4.5.2) is of the form

$$M(\omega, x(\tau), \sigma(\tau), \lambda(\tau), \tau) = \exp \left((r-q)\tau\omega + \omega x(\tau) + A(\omega, \tau) + B(\omega, \tau)\sigma(\tau) + C(\omega, \tau)\lambda(\tau) \right). \quad (4.5.4)$$

By Substituting equation (4.5.4) into (4.5.3)

$$\begin{aligned} - \left(\frac{\partial A}{\partial \tau}(\omega, \tau) + \frac{\partial B}{\partial \tau}(\omega, \tau)\sigma(\tau) + \frac{\partial C}{\partial \tau}(\omega, \tau)\lambda(\tau) \right) &= \frac{1}{2}\sigma(\tau)(\omega^2 - \omega) - \lambda(\tau) \left(m\omega - \int_{-\infty}^{\infty} e^{\nu\omega} f(\nu) d\nu - 1 \right) \\ &+ \kappa_\sigma (\beta^* + \beta^{rec} - \sigma(\tau)) B(\omega, \tau) + \frac{1}{2}\xi_\sigma^2 \sigma(\tau) B^2(\omega, \tau) + \rho \xi_\sigma \sigma(\tau) \omega B(\omega, \tau) \\ &+ \kappa_\lambda (\theta - \lambda(\tau)) C(\omega, \tau) + \frac{1}{2}\xi_\lambda^2 \lambda(\tau) C^2(\omega, \tau) \end{aligned} \quad (4.5.5)$$

We then rearranged the equation based on the state variables; the volatility $\sigma(\tau)$,

and the intensity $\lambda(\tau)$, which leads to:

$$\begin{aligned} & \left[\frac{\partial B}{\partial \tau} + \frac{1}{2} \xi_\sigma^2 B^2(\omega, \tau) + \rho \xi_\sigma \omega B(\omega, \tau) - \kappa_\sigma B(\omega, \tau) - \frac{1}{2} \omega + \frac{1}{2} \omega^2 \right] \sigma(\tau) \\ & + \left[\frac{\partial C(\omega, \tau)}{\partial \tau} + \frac{1}{2} \xi_\lambda^2 C^2(\omega, \tau) - \kappa_\lambda C(\omega, \tau) + \left(m\omega - \int_{-\infty}^{\infty} e^{\nu\omega} f(\nu) d\nu - 1 \right) \right] \lambda(\tau) \\ & + \frac{\partial A(\omega, \tau)}{\partial \tau} + \kappa_\sigma (\beta^* + \beta^{rec}) B(\omega, \tau) + \kappa_\lambda \theta C(\omega, \tau) = 0 \end{aligned} \quad (4.5.6)$$

where

$$\int_{-\infty}^{\infty} (e^{\nu\omega} - 1) f(\nu) d\nu = \varphi_{\text{jump}}(\omega) \quad (4.5.7)$$

is the equation for the *moment generating function* of the jump-size distribution, and m is the amplitude of the average jump given earlier as

$$m = \int_{-\infty}^{\infty} e^\nu f(\nu) d\nu - 1. \quad (4.5.8)$$

Equating the term structures coefficients (= the stochastic volatility and the intensity) in equation (4.5.7) to zero, the following ODEs were obtained:

$$\frac{\partial A(\omega, \tau)}{\partial \tau} = - \left(\kappa_\sigma (\beta^* + \beta^{rec}) B(\omega, \tau) + \kappa_\lambda \theta C(\omega, \tau) \right) \quad (4.5.9)$$

$$\frac{\partial B(\omega, \tau)}{\partial \tau} = - \frac{1}{2} \xi_\sigma^2 B^2(\omega, \tau) + (\kappa_\sigma - \rho \xi_\sigma \omega) B(\omega, \tau) + \frac{1}{2} (\omega - \omega^2) \quad (4.5.10)$$

$$\frac{\partial C(\omega, \tau)}{\partial \tau} = - \frac{1}{2} \xi_\lambda^2 C^2(\omega, \tau) + \kappa_\lambda C(\omega, \tau) + \left(\int_{-\infty}^{\infty} e^{\nu\omega} f(\nu) d\nu - 1 - m\omega \right) \quad (4.5.11)$$

The systems of solutions are presented in what follows. Consider the equation (4.5.10). Firstly, it was observed that the equation (4.5.10) is a Ricatti-type differ-

ential equation. Thus setting

$$B(\omega, \tau) = 2 \frac{D'(\tau)}{\xi_\sigma^2 D(\tau)} \quad (4.5.12)$$

in equation (4.5.10), and simplifying further yields a second order differential equation which is expressed as:

$$\frac{\partial^2 D}{\partial \tau^2} + (\kappa_\sigma - \rho \xi_\sigma \omega) \frac{\partial D}{\partial \tau} + \frac{1}{4} \xi_\sigma^2 (\omega - \omega^2) D(\tau) = 0. \quad (4.5.13)$$

The general solution of the given equation (4.5.13) is expressed as:

$$D(\tau) = k_1 \exp\left(-\frac{1}{2}\psi_{-\tau}\right) + k_2 \exp\left(\frac{1}{2}\psi_{+\tau}\right) \quad (4.5.14)$$

where

$$\psi_\pm = (\kappa_\sigma - \rho \xi_\sigma \omega) \pm \sqrt{(\kappa_\sigma - \rho \xi_\sigma \omega)^2 - \xi_\sigma (\omega - \omega^2)}. \quad (4.5.15)$$

Setting time $\tau = 0$ in equation (4.5.14), the following boundary conditions are satisfied:

$$D(0) = k_1 + k_2 \quad (4.5.16)$$

$$D'(0) = \frac{1}{2}\psi_+ k_2 - \frac{1}{2}\psi_- k_1 = 0.$$

The sum

$$\psi_+ + \psi_- = 2 \sqrt{(\kappa_\sigma - \rho \xi_\sigma \omega)^2 - \xi_\sigma (\omega - \omega^2)} \equiv 2\varsigma$$

with

$$\varsigma = \sqrt{(\kappa_\sigma - \rho \xi_\sigma \omega)^2 - \xi_\sigma (\omega - \omega^2)}$$

and the product

$$\psi_- \cdot \psi_+ = -\xi_\sigma(\omega - \omega^2).$$

The constants k_1 and k_2 have values $\frac{\psi_+ D(0)}{2\varsigma}$ and $\frac{\psi_- D(0)}{2\varsigma}$ respectively by using the boundary conditions given in the equation (4.5.19) and the initial conditions,

$$A(\omega, 0) = B(\omega, 0) = C(\omega, 0) = 0.$$

By substituting the value for $D'(\tau)$ and $D(\tau)$ in equation (4.5.12)

$$B(\omega, \tau) = 2 \frac{D'(\tau)}{\xi_\sigma^2 D(\tau)}.$$

Further simplification yields:

$$B(\omega, \tau) = -(\omega - \omega^2) \frac{e^{-\frac{1}{2}\psi_+\tau} - e^{-\frac{1}{2}\psi_-\tau}}{\psi_- e^{-\frac{1}{2}\psi_+\tau} + \psi_+ e^{-\frac{1}{2}\psi_-\tau}} \quad (4.5.17)$$

$$= -(\omega - \omega^2) \frac{1 - e^{-\varsigma\tau}}{\psi_- + \psi_+ e^{-\varsigma\tau}}. \quad (4.5.18)$$

Following Artur (2003), it is possible to partition a function. Therefore, we expressed

$A(\omega, \tau)$ as the sum of two functions $E(\omega, \tau)$ and $F(\omega, \tau)$ as:

$$A(\omega, \tau) \equiv E(\omega, \tau) + F(\omega, \tau).$$

The equation (4.5.9) is rewritten as:

$$\frac{\partial A}{\partial \tau} = \frac{\partial E}{\partial \tau}(\omega, \tau) + \frac{\partial F}{\partial \tau}(\omega, \tau) \quad (4.5.19)$$

such that

$$\frac{\partial E}{\partial \tau}(\omega, \tau) = \kappa_\sigma \beta^* B(\omega, \tau) + \kappa_\sigma \beta^{rec} B(\omega, \tau) \quad (4.5.20)$$

$$\frac{\partial F}{\partial \tau}(\omega, \tau) = \kappa_\lambda \theta C(\omega, \tau). \quad (4.5.21)$$

Firstly, we integrate the equation (4.5.20) to obtain the following equations:

$$\begin{aligned}
E(\omega, \tau) &= \int_0^\tau \kappa_\sigma \beta^* B(\omega, s) ds + \int_0^\tau \kappa_\sigma \beta^{rec} B(\omega, s) ds \\
&= \kappa_\sigma \beta^* \int_0^\tau B(\omega, s) ds + \kappa_\sigma \beta^{rec} \int_0^\tau B(\omega, s) ds \\
&= \frac{-2\kappa_\sigma \beta^*}{\xi_\sigma^2} \int_0^\tau \frac{D'(s)}{D(s)} ds + \frac{-2\kappa_\sigma \beta^{rec}}{\xi_\sigma^2} \int_0^\tau \frac{D'(s)}{D(s)} ds \\
&= \frac{-2\kappa(\beta^* + \beta^{rec})}{\xi_\sigma^2} \ln D(s) \Big|_{s=0}^{s=\tau} \\
&= \frac{-2\kappa(\beta^* + \beta^{rec})}{\xi_\sigma^2} \ln \left[\frac{D(\tau)}{D(0)} \right]. \\
&= \frac{-2\kappa(\beta^* + \beta^{rec})}{\xi_\sigma^2} \ln \left[\frac{\psi_- e^{-\frac{1}{2}\psi_+\tau} + \psi_+ e^{-\frac{1}{2}\psi_-\tau}}{2\varsigma} \right].
\end{aligned}$$

The final result is given as:

$$E(\omega, \tau) = \frac{-2\kappa_\sigma(\beta^* + \beta^{rec})}{\xi_\sigma^2} \left[\psi_{+\tau} + 2 \ln \left(\frac{\psi_- + \psi_+ e^{-\varsigma\tau}}{2\varsigma} \right) \right]. \quad (4.5.22)$$

Similarly, by integrating the ordinary differential equation in (4.5.21), we obtained:

$$F(\omega, \tau) = \frac{-\kappa_\lambda \theta}{\xi_\lambda^2} \left[\psi_{+\tau} + 2 \ln \left(\frac{\chi_- + \chi_+ e^{-\epsilon\tau}}{2\epsilon} \right) \right]. \quad (4.5.23)$$

Hence, expressing the explicit solution of $A(\omega, \tau)$ as a sum of the solutions $E(\omega, \tau)$

and $F(\omega, \tau)$ given in (4.5.22) and (4.5.23) respectively leads to:

$$A(\omega, \tau) = - \left\{ \frac{\kappa_\sigma(\beta^* + \beta^{rec})}{\xi_\sigma^2} \left[\psi_{+\tau} + 2 \ln \left(\frac{\psi_- + \psi_+ e^{-\varsigma\tau}}{2\varsigma} \right) \right] + \frac{\kappa_\lambda \theta}{\xi_\lambda^2} \left[\psi_{+\tau} + 2 \ln \left(\frac{\chi_- + \chi_+ e^{-\epsilon\tau}}{2\epsilon} \right) \right] \right\}. \quad (4.5.24)$$

Similarly,

$$C(\omega, \tau) = 2\Lambda \left(\frac{1 - e^{-\epsilon\tau}}{\psi_- + \psi_+ + e^{-\varsigma\tau}} \right) \quad (4.5.25)$$

where

$$\Lambda(\omega) = \int_{-\infty}^{\infty} e^{\nu\omega} f(\nu) d\nu - 1 - \omega \left(\int_{-\infty}^{\infty} e^{\nu} f(\nu) d\nu - 1 \right) \quad (4.5.26)$$

$$\epsilon = \sqrt{\kappa_{\lambda}^2 - 2\xi_{\lambda}^2 \Lambda(\omega)} \quad (4.5.27)$$

$$\chi_{\pm} = \epsilon \mp \kappa_{\lambda} \quad (4.5.28)$$

$$\psi_{\pm} = \mp \left(\kappa_{\sigma} - \rho \xi_{\sigma} \omega \right) + \sqrt{(\kappa_{\sigma} - \rho \xi_{\sigma} \omega)^2 - \xi_{\sigma} (\omega - \omega^2)} \quad (4.5.29)$$

but $\varsigma = \sqrt{(\kappa_{\sigma} - \rho \xi_{\sigma} \omega)^2 - \xi_{\sigma} (\omega - \omega^2)}$.

The solution summary of the model (4.4.3) follows:

$$M\left(\omega, x(\tau), \sigma(\tau), \lambda(\tau), \tau\right) = e^{(r-q)\tau\omega + \omega x(\tau) + A(\omega, \tau) + B(\omega, \tau)\sigma(\tau) + C(\omega, \tau)\lambda(\tau)}. \quad (4.5.30)$$

where

$$\begin{aligned} A(\omega, \tau) &= -\left\{ \frac{\kappa_{\sigma}(\beta^* + \beta^{rec})}{\xi_{\sigma}^2} \left[\psi_{+\tau} + 2 \ln \left(\frac{\psi_{-} + \psi_{+} e^{-\varsigma\tau}}{2\varsigma} \right) \right] + \frac{\kappa_{\lambda}\theta}{\xi_{\lambda}^2} \left[\psi_{+\tau} + 2 \ln \left(\frac{\chi_{-} + \chi_{+} e^{-\epsilon\tau}}{2\epsilon} \right) \right] \right\} \\ B(\omega, \tau) &= -(\omega - \omega^2) \frac{1 - e^{-\varsigma\tau}}{\psi_{-} + \psi_{+} e^{-\varsigma\tau}} \\ C(\omega, \tau) &= 2\Lambda \left(\frac{1 - e^{-\epsilon\tau}}{\psi_{-} + \psi_{+} + e^{-\varsigma\tau}} \right) \\ \Lambda(\omega) &= \int_{-\infty}^{\infty} e^{\nu\omega} f(\nu) d\nu - 1 - \omega \left(\int_{-\infty}^{\infty} e^{\nu} f(\nu) d\nu - 1 \right), \\ \epsilon &= \sqrt{\kappa_{\lambda}^2 - 2\xi_{\lambda}^2 \Lambda(\omega)} \\ \chi_{\pm} &= \epsilon \mp \kappa_{\lambda} \\ \psi_{\pm} &= \mp \left(\kappa_{\sigma} - \rho \xi_{\sigma} \omega \right) + \sqrt{(\kappa_{\sigma} - \rho \xi_{\sigma} \omega)^2 - \xi_{\sigma} (\omega - \omega^2)} \\ \varsigma &= \sqrt{(\kappa_{\sigma} - \rho \xi_{\sigma} \omega)^2 - \xi_{\sigma} (\omega - \omega^2)}. \quad \blacksquare \end{aligned}$$

4.5.2 Further Results from the model (4.5.2) Solution

Consider a financial claim $g(x, \sigma, \lambda, \tau)$ governed by the Partial Integro-Differential Equation (PIDE) expressed in equation (4.5.2) with the payoff function, $f(e^x, K)$,

satisfied by the claim, $g(x, \sigma, \lambda, 0) = f(e^x, K)$. The *Fourier transform* of $g(x)$ simply defined on the PIDE following the equation (3.3.5) is expressed as:

$$\hat{g}(w) = \mathcal{F}(g(x); \omega) = \int_{-\infty}^{+\infty} g(x) e^{i\omega x} dx. \quad (4.5.31)$$

The corresponding *inverse-Fourier transform* which follows from the application of equation (3.3.6) is expressed as:

$$g(x) = \mathcal{F}^{-1}(\hat{g}(\omega); x) = \frac{1}{2\pi} \int_{-\infty}^{+\infty} \hat{g}(\omega) e^{-i\omega x} d\omega. \quad (4.5.32)$$

Considering Theorem 3.2 in Lewis (2001) and Theorem 3.1 on page 11 of the study by Artur Sepp (2003), we present another version in the following based on the derived characteristic function for the model studied here.

Theorem 4.5.2. : (Characteristic formula).

Suppose an asset price $x_\tau = \ln S_\tau$ has an affine analytic characteristic function, $\varphi_\tau(w)$, at a specified time, $\tau \leq T$. Define a regularity strip

$$\text{Reg } S := \{ \omega : \alpha < \Im(\omega) < \beta \}$$

where $\Im(\omega)$ denotes the imaginary part of w , which lies between α and β in the regularity strip. Let $e^{-\Im(\omega)x} g(x)$ be defined on the space of $L^1(\mathbb{R})$, such that $\hat{g}(\omega), \Im(\omega) \in S_g$, with S_g being the payoff strip and $\hat{g}(\omega)$ satisfy the Fourier transform expressed in equation (4.5.31). Then, the option value is expressed as:

$$g(x(t)) = \frac{e^{-r(T-t)}}{2\pi} \int_{i\Im(\omega)-\infty}^{i\Im(\omega)+\infty} \varphi_T(-\omega) \hat{g}(\omega) d\omega \quad (4.5.33)$$

where $\omega \in \text{Reg } S \cap S_g$.

Proof:

Consider the setting of a risk-neutral world, \mathcal{Q} , we have:

$$g(x(t)) = \mathbf{E}_{\mathcal{Q}} \left[e^{-r(T-t)} g(x(t) | \mathcal{F}_T) \right], \quad t < T. \quad (4.5.34)$$

$$\begin{aligned} g(x(t)) &= e^{-r(T-t)} \mathbf{E}_{\mathcal{Q}} [g(x(T))] \\ &= e^{-r(T-t)} \mathbf{E}_{\mathcal{Q}} \left[\frac{1}{2\pi} \int_{i\Im(\omega)-\infty}^{i\Im(\omega)+\infty} e^{-i\omega x(T)} \hat{g}(\omega) d\omega \right] \\ &= \frac{e^{-r(T-t)}}{2\pi} \int_{i\Im(\omega)-\infty}^{i\Im(\omega)+\infty} e^{-i\omega x(T)} \mathbf{E}_{\mathcal{Q}} (e^{-i\omega x(T)}) \hat{g}(\omega) \\ &= \frac{e^{-r(T-t)}}{2\pi} \int_{i\Im(\omega)-\infty}^{i\Im(\omega)+\infty} e^{-i\omega x(T)} \varphi_T(-\omega) \hat{g}(\omega) d\omega \end{aligned}$$

Corollary 4.5.1. : (Characteristic formula for an early exercise Option).

Consider an American option within the time horizon, $t \leq \tau \leq T$, with t being the initial time, τ is the early exercise time, and T is the maturity time. Suppose further that the optimal payoff time, $\tau^* < T$, is feasible within a stopping region.

The claim $g(x(\tau))$ early exercise payoff is then expressed as:

$$g(x(\tau)) = \frac{e^{-r\tau}}{2\pi} \int_{i\Im(\omega)-\infty}^{i\Im(\omega)+\infty} e^{-i\omega x(\tau)} \varphi_{\tau}(-\omega) \hat{g}(\omega) d\omega \quad (4.5.35)$$

when $\tau = \tau^*$.

Proof:

The proof follows from theorem 4.5.2 immediately with respect to optimality condition, which early exercise of American options permits each time the early exercise time, $\tau = \tau^*$. ■

The corollary is justified following the early exercise possibility of an American-type option, since one is allowed to exercise at any time, t , even up to the maturity time, $t = T$, of the option. By symmetric property as shown earlier in chapter 3, there exists $\varphi_\tau(-\omega)$ such that $\omega \in \text{Reg } S \cap S_g$, and the entire integrand holds by extension whenever $\omega \in \text{Reg } S \cap S_g$.

4.6 STUDY THREE

4.6.1 Numerical Fourier based Transform of the UAEM to European-style option

In literature including the research study of Carr & Madan (1999), it was said that “once the characteristic function of a price process furnished with a risk-neutral density is either known or derived, then an analytical representation of the process Fourier transform becomes possible”.

Theorem 4.6.1. Let the derived affine characteristic function formula for the UAEM given in theorem 4.5.2 above be valid. Then an analytic formula of a European-style option price is:

$$E_T^{call}(k) = \frac{\exp(-\alpha k)}{\pi} \int_0^\infty e^{-(rT+iu k)} \varphi_\tau(u - (\alpha + 1)i) \times \left(\frac{\alpha^2 + \alpha - u^2 - i(2\alpha + 1)u}{\alpha^4 + 2\alpha^3 + \alpha^2 + (2(\alpha^2 + \alpha) + 1)u^2 + u^4} \right) du. \quad (4.6.1)$$

Proof:

Considering the characteristic function $\varphi(iw, X_\tau, \tau)$, and from the moment-generating-

function, $M(w, X_\tau, \tau)$, derived above for the UAEM, we express:

$$\varphi_\tau(w) = \mathbb{E}(\exp(iwS_\tau)) = \int_{-\infty}^{\infty} \exp(iwS_\tau)q_\tau(S_\tau)dS_\tau \quad (4.6.2)$$

where $\tau :=$ Optimal time lying within the time horizon $\{0 = t_0 < t_1 < t_2 < \dots < t_n = T\}$.

For a European call $E_T^{call}(k)$ which will mature at time $t = T$ given the exercising price $K = e^k$ defined over an underlying stock, S , and $q_T(s)$ is the probability density function of $s_T = \ln S_T$, the fair price, $E_T^{call}(k)$, is expressed as the present value of the expected payoff function given by:

$$E_T^{call}(k) = e^{-rT} \int_k^{\infty} (e^s - e^k)q_T(s)ds. \quad (4.6.3)$$

Carr & Madan (1999) framework which initiated the concept of damping factor in FFT technique for better numerical results, we express the modified call price by using a damping factor, $\alpha \in \mathbb{R}^+$, such that $c_T(k) = e^{\alpha k} \times E_T^{call}(k)$.

To this end, we define $\psi_\tau(u)$ as the Fourier transform depiction of $c_T(k)$ and we have:

$$\psi_T(u) = \int_{-\infty}^{\infty} e^{iuk}c_T(k)dk. \quad (4.6.4)$$

Then the function describing the call option price is expressed as:

$$E_T^{call}(k) = \frac{\exp(-\alpha k)}{2\pi} \int_{-\infty}^{\infty} e^{-iuk}\psi_T(u)du \quad (4.6.5)$$

$$= \frac{\exp(-\alpha k)}{\pi} \int_0^{\infty} e^{-iuk}\psi_T(u)du. \quad (4.6.6)$$

$\psi_\tau(u)$ in (4.6.6) is nothing else but the call price Fourier transform expressed as:

$$\psi_\tau(u) = \int_{-\infty}^{\infty} \exp(iuk)c_\tau(k)dk \quad (4.6.7)$$

$$= \int_{-\infty}^{\infty} \exp(iuk) \times \exp(-rT) \int_k^{\infty} \exp(\alpha k)(e^s - e^k) q_T(s) ds dk \quad (4.6.8)$$

$$= \int_{-\infty}^{\infty} \exp(-rT) q_T(s) \int_{-\infty}^s \left(e^{s+\alpha k+iuk} - e^{(\alpha+1+iu)k} \right) dk ds \quad (4.6.9)$$

$$= \int_{-\infty}^{\infty} \exp(-rT) q_T(s) \int_{-\infty}^s \left(e^{s+(\alpha+iu)k} - e^{(1+\alpha+iu)k} \right) dk ds \quad (4.6.10)$$

By integrating the second integral term with respect to k yields:

$$\psi_\tau(u) = \int_{-\infty}^{\infty} \exp(-rT) q_T(s) \left[\frac{e^{(\alpha+1+iu)s}}{\alpha + iu} - \frac{e^{(\alpha+1+iu)s}}{\alpha + 1 + iu} \right] ds \quad (4.6.11)$$

Further simplification gives:

$$\psi_\tau(u) = \exp(-rT) \left[\frac{\varphi_\tau(u - (\alpha + 1)i)}{\alpha^2 + \alpha - u^2 + i(2\alpha + 1)u} \right] \quad (4.6.12)$$

Rationalising the base gives:

$$\psi_\tau(u) = \exp(-rT) \left[\frac{\varphi_\tau(u - (\alpha + 1)i) \times \left((\alpha^2 + \alpha - u^2) - i(2\alpha + 1)u \right)}{\underbrace{\left(\alpha^2 + \alpha - u^2 + i(2\alpha + 1)u \right)}_a \underbrace{\left(\alpha^2 + \alpha - u^2 - i(2\alpha + 1)u \right)}_b} \right] \quad (4.6.13)$$

$$= \exp(-rT) \left[\frac{\varphi_\tau(u - (\alpha + 1)i) \times \left((\alpha^2 + \alpha - u^2) - i(2\alpha + 1)u \right)}{\underbrace{\left(\alpha^2 + \alpha - u^2 + i(2\alpha + 1)u \right)}_{(a+b)} \underbrace{\left(\alpha^2 + \alpha - u^2 - i(2\alpha + 1)u \right)}_{(a-b)}} \right] \quad (4.6.14)$$

Applying the concept of factorisation by the difference of two squares implies the

denominator could reduce to:

$$\psi_\tau(u) = \exp(-rT) \times \varphi_\tau\left(u - (\alpha + 1)i\right) \left[\frac{(\alpha^2 + \alpha - u^2) - i(2\alpha + 1)u}{\underbrace{(\alpha^2 + \alpha - u^2)^2}_{a^2} - \underbrace{(i^2(2\alpha + 1)^2 u^2)}_{b^2}} \right] \quad (4.6.15)$$

The negative sign in the denominator became positive since $i^2 = -1$, thus we obtained

$$\psi_\tau(u) = \exp(-rT) \varphi_\tau\left(u - (\alpha + 1)i\right) \times \left[\frac{(\alpha^2 + \alpha - u^2) - i(2\alpha + 1)u}{\underbrace{(\alpha^2 + \alpha - u^2)^2 + (2\alpha + 1)^2 u^2}_{a^2 + b^2}} \right] \quad (4.6.16)$$

Henceforth, we suppress a and b as they were just for simplification ease purpose.

$$\psi_\tau(u) = e^{-rT} \varphi_\tau\left(u - (\alpha + 1)i\right) \times \left[\frac{(\alpha^2 + \alpha - u^2) - i(2\alpha + 1)u}{(\alpha^4 + 2\alpha^3 + \alpha^2 - 2(\alpha^2 + \alpha)u^2 + u^4) + (4\alpha^2 + 4\alpha + 1)u^2} \right] \quad (4.6.17)$$

Finally,

$$\psi_\tau(u) = e^{-rT} \varphi_\tau\left(u - (\alpha + 1)i\right) \times \left(\frac{\alpha^2 + \alpha - u^2 - i(2\alpha + 1)u}{\alpha^4 + 2\alpha^3 + \alpha^2 + (2(\alpha^2 + \alpha) + 1)u^2 + u^4} \right) \quad (4.6.18)$$

Upon the substitution of equation (4.6.18) into (4.6.7), the analytical form of the option price is given as:

$$E_T^{call}(k) = \frac{\exp(-\alpha k)}{\pi} \int_0^\infty e^{-iuk} e^{-rT} \varphi_\tau\left(u - (\alpha + 1)i\right) \times \left(\frac{\alpha^2 + \alpha - u^2 - i(2\alpha + 1)u}{\alpha^4 + 2\alpha^3 + \alpha^2 + (2(\alpha^2 + \alpha) + 1)u^2 + u^4} \right) du. \quad (4.6.19)$$

The analytic formula of the European-style option price in (4.6.19) is equivalently

stated as:

$$E_T^{call}(k) = \frac{\exp(-\alpha k)}{\pi} \int_0^\infty e^{-(rT+iu k)} \varphi_\tau(u - (\alpha + 1)i) \times \left(\frac{\alpha^2 + \alpha - u^2 - i(2\alpha + 1)u}{\alpha^4 + 2\alpha^3 + \alpha^2 + (2(\alpha^2 + \alpha) + 1)u^2 + u^4} \right) du. \quad (4.6.20)$$

This concludes the proof.

4.6.2 Extension of the formulation to American-type options

In order to extend the formulation to American-type options, we consider summing both the European call Fourier price $E_T^{call}(k)$ and the early exercise premium price $P(t)$ to attain the American call price $A_{t \leq T}$ given by:

$$A_{t \leq T} = E_T^{call}(k) + P_t, \quad \text{where } k = \log_e K. \quad (4.6.21)$$

The early premium price P_t is a well-defined determinable price function such that $\lim_{t \rightarrow T} P_t = 0$, for the American call option because at maturity time, the continuation region vanishes and therefore, there does not exist waiting time to any further extent. This implies that as the option attains its maturity date, it must be exercised at time $t = T$ if it is yet to be exercised at early time $t < T$ prior to the maturity time T . This means that American option prices will be exactly equal to the price of European option when the maturity date, T , is reached.

Therefore,

$$A_t(k) = \frac{\exp(-\alpha k)}{\pi} \int_0^\infty e^{-(rT+iu k)} \times \left(\frac{\varphi_\tau(u - (\alpha + 1)i) (\alpha^2 + \alpha - u^2 - i(2\alpha + 1)u)}{\alpha^4 + 2\alpha^3 + \alpha^2 + (2(\alpha^2 + \alpha) + 1)u^2 + u^4} \right) du + P_t. \quad (4.6.22)$$

In order to extend FFT algorithm to American options computation for the model presented above, with emphasis on economy recession induced uncertainty, we revisit

the definition of Fast Fourier Transform (FFT) in what follows

$$H(k) = \sum_{j=1}^{N-1} e^{-i\frac{2\pi}{N}(j-1)(k-1)} y_j, \quad 1 \leq k \leq N. \quad (4.6.23)$$

Applying FFT algorithm to (4.6.22) yields:

$$A_\tau(k_u) \approx \frac{\exp(-\alpha k)}{\pi} \sum_{j=1}^N e^{-iu_j(-\varpi + \zeta(u-1))} \psi_T(u_j)\eta + P_t. \quad 1 \leq u \leq N, \quad (4.6.24)$$

where $1 \leq u \leq N$, $k_u = -\varpi + \zeta(u-1)$ and $2\varpi = \zeta N$.

ζ represents the consistent spacing size in N values of the logarithm strikes K . By setting $u_j = (j-1)\eta$, and substituting in equation (4.6.24), we have

$$A_\tau(k_u) \approx \frac{\exp(-\alpha k)}{\pi} \sum_{j=1}^N e^{-iu_j\zeta\eta(j-1)(u-1)} e^{i\varpi u_j} \psi_T(u_j)\eta + P_t. \quad 1 \leq u \leq N. \quad (4.6.25)$$

The consistent spacing size, ζ , in N -values of k is related as shown below

$$\zeta = \frac{2\pi}{\eta N} \iff \zeta\eta = \frac{2\pi}{N}. \quad (4.6.26)$$

It is easy to observe such relation if one compares the equations (4.6.23) and (4.6.25). Smaller values assigned to η improves the fineness of the integration grid. The converse is that the larger the values of η , the worse the integration grid becomes.

4.7 STUDY FOUR

4.7.1 Numerical Experiment

We present simulation results based on the first formulation in the following.

Let S be an American-style tradeable stock with initial price $S_0 = 100$, the strike price $K = 80$, the risk-neutral interest rate, $r = 0.04$, the dividend rate $q = 0.002$, the time to expiration $T = 1\text{year}$, Volatilities $\sigma^* = 0.1$, $\sigma^{rec} = \{0.00, 0.025\}$, the integrability parameter $\alpha = 0.25$, and the fineness of integration grid set to $N = 2^{12}$. The value of the call option on the chosen underlying American-style tradeable stock is presented in the table below.

Table 4.1: The Options value comparison via FFT method versus BSM & American option Pricing solver

Volatility $\{\sigma^*, \sigma^{rec}\}$	Dividend (q)	BSM Price	American Option Pricing Solver	FFT Price	Exercising Time (yr.)
0.1, 0.000	0.002	20.249557	20.249556	20.398278	$\frac{1}{12}$
0.1, 0.025	0.002	20.249557	20.249556	20.398278	$\frac{1}{12}$
0.1, 0.000	0.002	20.746027	20.746026	20.894006	0.25
0.1, 0.025	0.002	20.746157	20.746127	20.894135	0.25
0.1, 0.000	0.002	21.484649	21.484550	21.631524	0.5
0.1, 0.025	0.002	21.491432	21.490722	21.638307	0.5
0.1, 0.000	0.002	22.949394	22.948914	23.094093	1
0.1, 0.025	0.002	23.009897	23.009970	23.154597	1

Source: Author's simulation result.

The table 4.1 shows the options prices comparison among FFT-method, Black-Scholes-Merton prices and American pricing solver App. Considering four (4) panels of results with respect to economy recession volatility uncertainty values incorporated, we compared the option's returns for the economic states. The output is invariant in price with a very small fraction of maturity time of $\frac{1}{12}$ for the two states of the economy in panel 1. In the second panel where the exercising time was 0.25year (i.e 3 months), the option's returns varies at the two economy states, as the recession volatility causes price inflation which was not different from the experience of Nigeria recession of 2016. Many investors/traders took advantage of recession to inflate the price of their goods and services. Similar situation was observed in the last two panels when the exercising time was carried out at 0.5year and 1year respectively. The recession volatility impacted the option's prices, being a call-option type, the payoffs increases a little bit than when the economy was to be in a recessed-free state. Graphical illustration are given as follows.

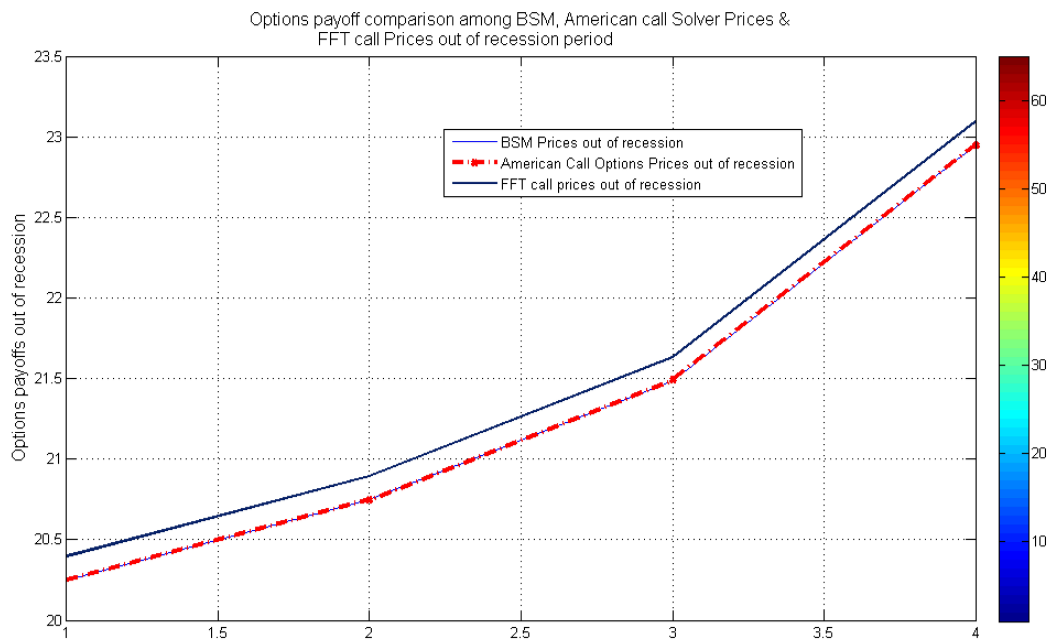


Figure 4.1: The Call options values from FFT versus BSM & American-style option pricing Solver in recession-free state.

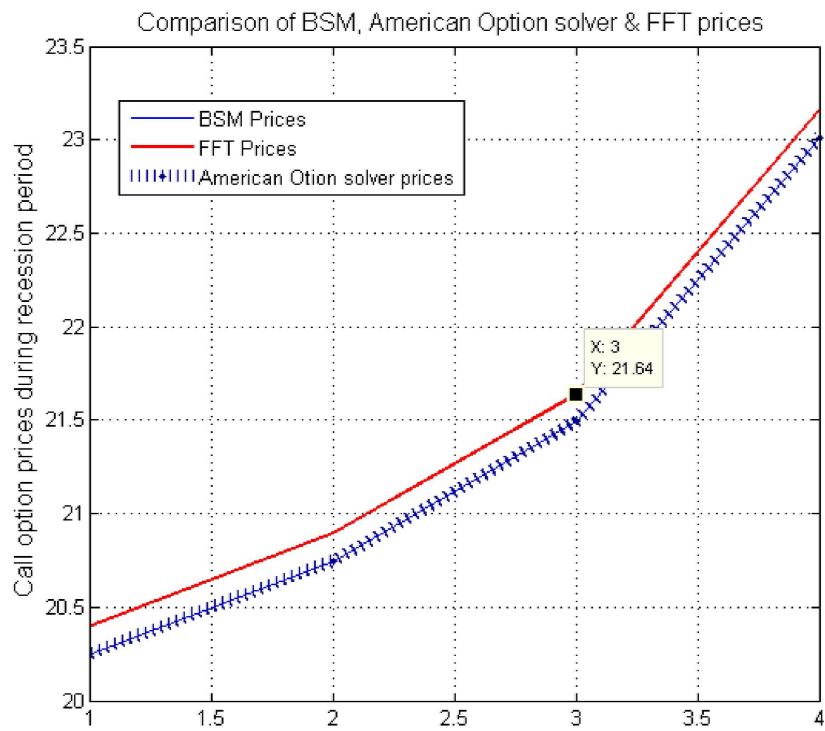


Figure 4.2: The call options output of FFT versus BSM & American-style option pricing solver under recession induced volatility change.

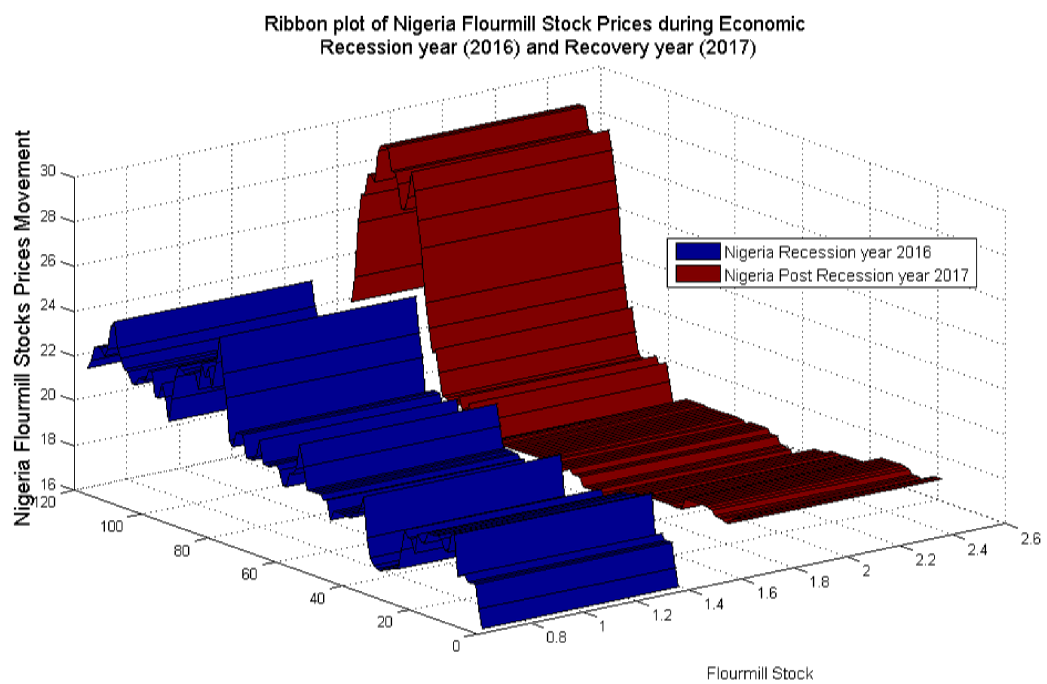
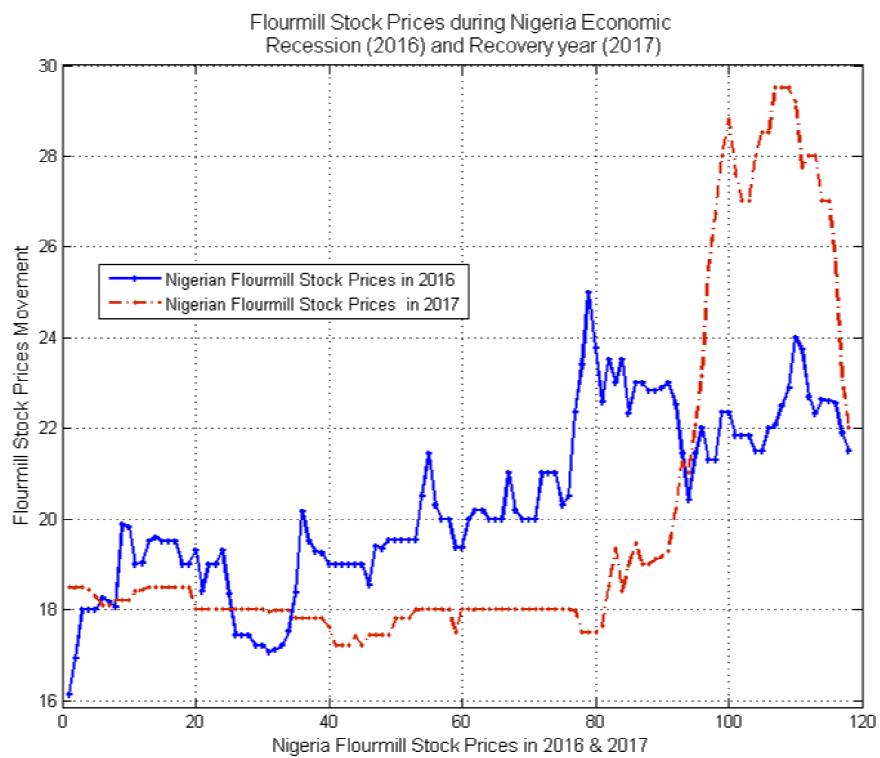


Figure 4.3: The Nigerian Flourmill stock price dynamics under economy recession outbreak in 2016 and the Recovery year 2017

Figure 4.1 shows the graphical representation of the options prices comparison among Black-Sholes-Merton (BSM), American option solver App. & Fast-Fourier Transform (FFT) in recession-free state. The graph shows that the FFT-prices outperformed the other two approaches. No significant variation in options returns obtained via the BSM & American option solver App. Knowing fully that every ‘kobo’ (Nigerian infinitesimal monetary value) gained or lost in investment counts a lot and every investor will always wish to guard against losing any amount no matter how infinitesimal the loss may be. It means that the FFT-price returned on investment as obtained in the above table will be preferable to investors under normal circumstances.

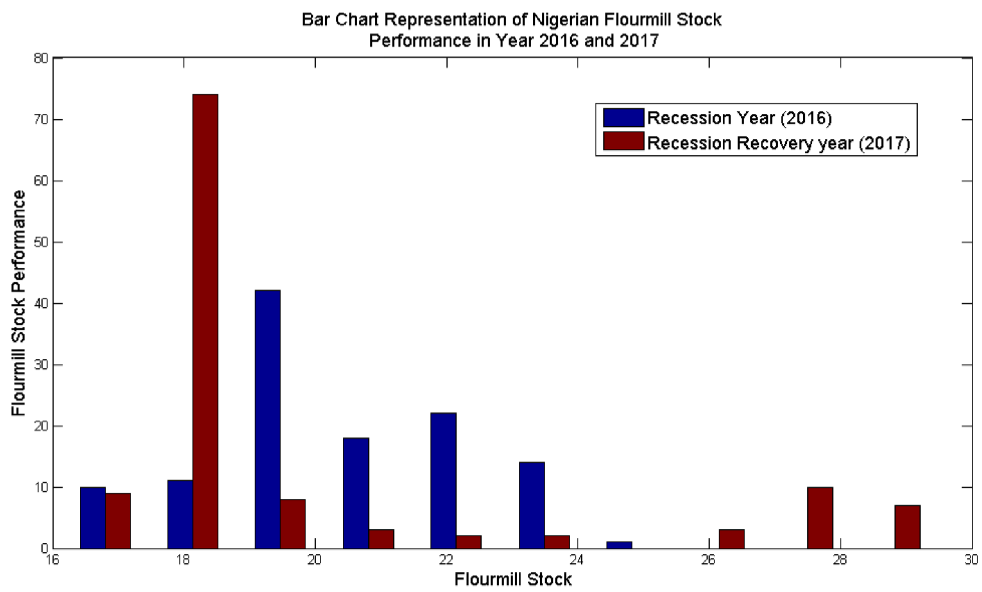
Figure 4.2 shows the graphical representation of the options prices comparison among Black-Sholes-Merton (BSM), American option solver App. & Fast-Fourier Transform (FFT) during recession state of the economy. Figure 4.2, the FFT-prices was still seen to have performed better in comparison with the other two approaches. Significant price variation was observed during the recession state.

Figure 4.3 is a ribbon plot for Nigerian Flourmill stock prices. Two panels of stock prices of Nigerian Flourmill were collected. The first panel consists of the Nigerian Flourmill stock prices during the period of economy recession 2016 while the second panel consists of the Nigerian Flourmill stock prices during the recovery year 2017. Figure 4.3, the blue surface shows the stock performance as well as the variance in the prices within the range of time while the wine colour surface generated was for the Nigerian Flourmill stock prices in the economy recovery year 2017. It was observed that after some time steps, the Flourmill Stock performance was better during recovery year compared to when the economy was in recession state. The implication is that recession has a negative effect on the performance of the stock price.



Source: Author's plotted graph using Flourmill data from Nigerian Stock Exchange website.

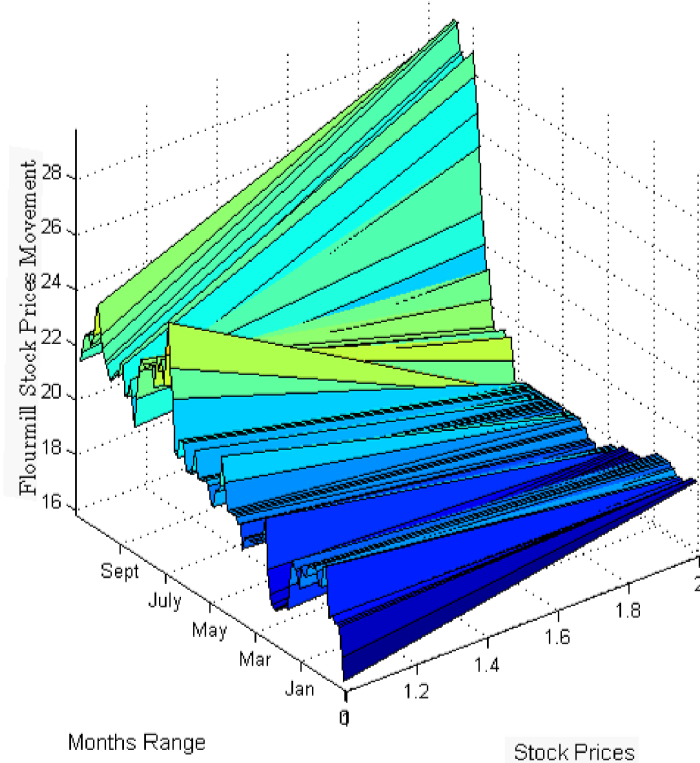
Figure 4.4: The Stock price performance in the time of Nigeria Economy Recession 2016 & Recovery year 2017 of Flourmill stock.



Source: Author's plotted graph using Flourmill data from Nigerian Stock Exchange website.

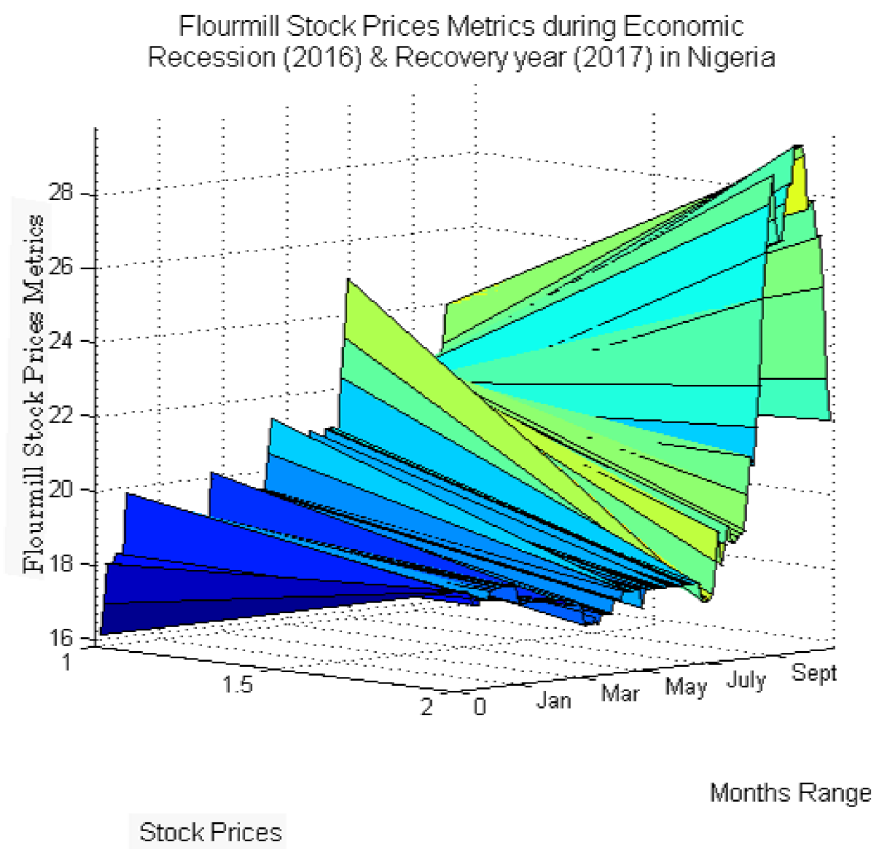
Figure 4.5: The Bar charts presentation of Nigerian Flourmill stock price performance during economy recession in 2016 & economy recovery in 2017

Flourmill Stock Prices during Economic Recession (2016) & Recovery year (2017) in Nigeria



Source: Author's generated graph left view for Flourmill data during years 2016 & 2017

Figure 4.6: Nigerian Flourmill stock prices performance in the period of Economy Recession 2016 & Recovery year 2017



Source: Author's generated graph right view for Flourmill data during years 2016 & 2017

Figure 4.7: Surface plot of Flourmill stock data during Nigerian 2016 recession.

4.8 Discussion of Result 1

The options values obtained in the table (4.1) shows the effectiveness of the model formulated. The options prices obtained during recession period very different from that of the recession-free state indicating recession effect on the stock return. We also noticed that the options prices obtained via FFT method outperformed those of the BSM prices and American option pricing Solver software. The figure 4.1 shows the graphical representation of the options prices comparison among Black-Sholes-Merton (BSM), American option solver App. & Fast-Fourier Transform (FFT) in recession-free state. The graph shows that the FFT-prices outperformed the other two approaches. No significant variation in options returns obtained via the BSM & American option solver App. Knowing fully that every ‘kobo’ (Nigerian infinitesimal monetary value) gained or lost in investment counts a lot and every investor will always wish to guard against losing any amount no matter how infinitesimal the loss may be, this is significant.

Figure 4.2 is a graphical representation of the options prices comparison among Black-Sholes-Merton (BSM), American option solver App. & Fast-Fourier Transform (FFT) during recession state of the economy. In figure 4.2, the FFT-prices performed better in comparison with the other two approaches. Significant price variation was observed during the recession state.

Figure 4.3 is a ribbon plot for Nigerian Flourmill stock prices. Two panels of stock prices of Nigerian Flourmill were collected. The first panel consists of the Nigerian Flourmill stock prices during the period of economy recession 2016 while the second panel consists of the Nigerian Flourmill stock prices during the recovery year 2017. In Figure 4.3, the blue surface shows the stocks performance as well as the variance in the prices within the range of time while the wine colour surface generated was for the Nigerian Flourmill stock prices in economy recovery year 2017. It was observed that after some time steps, the Flourmill Stock performance was better during recovery year compared to when the economy was in recession state. The implication is that

recession has negative effect on the performance of the stock price.

4.9 Conclusion

We introduced the concept of economy recession here under the Result 1 in this thesis. The effect of economy recession on volatility with respect to options payoff under some given assumptions was part of our investigation. The characteristic function of the proposed model UAEM was derived in a closed form and the model fast Fourier transform was implemented. A numerical based *fast Fourier transform*, a variant of Carr & Madan (1999) FFT algorithm was applied to compute the European call Fourier prices. Under additional assumption suitable for American-type option valuation, we extended the FFT algorithm to American-type call options computation by summing up the premium price and the European-type call options prices.

As part of our findings, we further reported the Nigerian Flourmill stock performance during recession state and economy recovery year in the study under the same “Result 1”. This was done to have more insight to the stocks performance in addition to the assumptions made in our model. The volatility has been seen as the key parameter for measuring the uncertainty on the stocks output (returns). In other words, the volatility level determines the magnitude of uncertainties on the stocks’ returns. The stocks volatility rate becomes higher in the state of recession than recession-free state. It is worth noting that volatility in real life, financial stock market situation is never constant. The Nigerian Flourmill stock price data was used for calibration purpose to show that the stocks became more volatile during the Nigerian recession of 2016 compared to one other period when the economy is free from recession. Based on the “Assumption 1” under Result 1, Historical data before recession is hereby suggested to determine the magnitude of economic recession uncertainty posed on stock’s return.

RESULT 2

FFT Computation of a class of Multi-assets Options with Economy Recession Induced Uncertainties

4.10 STUDY FIVE

4.10.1 An overview of the Result 2

The FFT method for a class of correlated Multi-Assets option valuation with respect to economic recession induced volatility uncertainties is presented under the Result 2. We applied the FFT algorithm of Carr & Madan to compute the option on multi-assets with emphasis on multi-dimension. Our presentation harnesses the concept of economy recession induced stochastic volatility uncertainties which is one of the major foci of this thesis. We present numerical results considering assets in 3-dimensions for the purpose of an illustration. The major importance of this *Result 2* revealed options valuation in both lower and higher dimensions with respect to FFT algorithm.

4.10.2 Introduction

Generally, multi-assets options are seen as options set in which payoffs are governed by either double or multi-underlying assets. There are several types of multi-assets options. A basket of options simply called “Basket Option” is a distinctive class (i.e example) of Multi-assets option. It is a type of options which operates on the existence of more than one underlying assets. The underlying assets ranges from two and above. There exists European type basket option which could be a call or put option. Moreover, the general value of a basket of assets play significant role for option on the underlying assets. Without loss of generalities, there exists a form of American basket option based on the principle of early exercising permissibility up to the maturity date. Other categories of multi-assets options in existence involve: Rainbow options, Exchange options, spread option, quanto options etc. Based on payoff function, several types of multi-assets options are describable.

Some researchers have worked on multi options pricing (Kwok, Wu, & Yu, 2011; Yijuan, & Xiuchuan, 2019). The authors Kwok, Yue and Wu, Lixin and Yu, Hong, (2011) gave an approach for Multi-Asset Options valuation taking into consideration an external barrier. In a more recent year 2019, Yijuan and Xiuchuan, presents “Variance and dimension reduction which follows Monte Carlo technique for European-type multi-asset options valuation with stochastic volatilities”. Carol Alexander et al, (2009) also present “analytic form of approximations for multi-assets option price valuation”. Nevertheless, the approach used in this part of the thesis is quite different from that of the above authors but have correlation with some of the word registers used in options pricing and practices in fast Fourier transform technique. Such correlation could vividly be seen in Carr & Madan, (1999) method of using fast Fourier transform algorithm for pricing a single factor European style options. In recent time, Ulrich and Xiaonyu, (2018) presents “an existence of solutions for a class of stochastic control problem in multi-dimension with a singular state constraint”.

However, most researchers focused on two-dimensional multi-asset options valuation. The formulation given by some authors in their studies was in terms of BS-PDE and further extended considered numerical method to obtain the options prices. The reader can see study carried out by Yuwei, (2017). In this part of this study, an attention is given to multi-assets options computation in the presence of economy recession volatility effect and issue of multi-dimension problem in the valuation process using the FFT methodology of Carr & Madan, (1999). We present a more general framework for multi-asset options computation in multi-dimensions.

With reference to Yuwei, (2017), “most multi-asset European-type options as well as the American-type options has no analytical formula for direct computation of their prices. Hence, numerical methods are pragmatically applied to obtain numerical approximations of the prices”. An economy instability effects pose challenges of uncertainty on assets payoffs especially risky assets such as stock assets. The acute

economy factor considered in this formulation is recession. As a result of economy recession, volatility variation is imposed on the term structure of the options pricing during economy recession state (period) referred to as “economy recession induced volatility” adding to the usual volatility uncertainty in the financial market which impacts the price changes.

We applied FFT algorithm in the solution of our formulated pricing model. Many authors had carried out useful studies on Fourier transform in options valuation. For instance, see the studies by: Carr & Madan (1999), Oleksandr (2010), Jiexiang, Wenli, and Xinfeng (2014) among others.

In what follows, we consider options payoff uncertainty posed by economic recession felt in the volatility parameter of the option prices.

Assumption: Suppose there exists bi-volatility source on the assets classified into “economic recession induced volatility”, v^{rec} , and the “volatility from other sources”, v^* , which evolves stochastically in nature. Then the option’s total volatility is defined as:

$$V(t) = \begin{cases} v^{rec} + v^*, & \text{if the economy is in recession;} \\ v^*, & \text{if economy is recession free.} \end{cases} \quad (4.10.1)$$

where v^{rec} denotes the economy recession induced stochastic volatility of the stocks in the market attributable to the filtration (that is, the flow of information) from a recessed economy, and v^* is taking to be the volatility already available in the market emanating from other sources.

Under this Result 2, we achieved our stated objective of study (iii). Our major contribution could be felt in a class of multi-assets options computation based on multi-dimension with respect to economy recession. The remaining part of the “Result 2” is organised in the following sections. Preliminaries on Fast Fourier Transform, Computational Approach, consisting of the sections: Fast Fourier Transform of a

class of correlated multi-assets in finite dimensions, Application on three correlated stock assets, Numerical result presentation in 3-dimensions and conclusion.

4.10.3 The Fast Fourier Transform (FFT) Algorithm

The Fast Fourier Transform (FFT) algorithm is shortly highlighted below.

1. First determine the characteristic function for the asset distribution if not already known.
2. Derive an analytic representation using Fourier Transform technique for the modified options price with respect to the characteristic function (ch.f).
3. Find the inverse Fourier transform of the pricing function (p.f).
4. Do the Discrete Fourier Transform (DFT) in the above steps and use Trapezoidal rule.
5. Take uniform grid size for the FFT computation in step 4 above.
6. Assigning values to the computational parameters such as the grid size N , fineness of integration parameter and the decaying term (α) for optimality, the risk-neutral interest rates and other parameters in the model required for the computation.

4.10.4 Fast Fourier Transform of a class of correlated multi-assets in finite dimension

Suppose there are an n -factor underlying assets $S_j, j = 1, 2, \dots, n$. Define the options payoff function $H(S, K)$ at exercising time (maturity time) τ on the chosen underlying multi-assets by:

$$H(S, K) = \prod_{j=1}^n \left(c(S_j - K_j)^+ \right). \quad (4.10.2)$$

The options' payoff function is further written as:

$$H(S, K) = \left(c(S_1 - K_1)^+ \cdot c(S_2 - K_2)^+ \cdot c(S_3 - K_3)^+ \cdots c(S_n - K_n)^+ \right) \quad (4.10.3)$$

where the S_j and K_j represent the assets and strike prices respectively. The

$$(S_j - K_j)^+ = \left(\max(S_j - K_j, 0), \quad \text{for each } j = 1, 2, \dots, n \right).$$

In order to maintain transition from call to put option prices, a control switch parameter c is introduced. Taking the c - value as defined in (4.10.2) and (4.10.3) to be -1 , then put option will be formed and suppose $c = +1$, then there exists a call option.

Suppose further that we consider $k_j, s_j | j = 1, 2, \dots, n$ as logarithm of the strikes K_j and take assets S_j prices one after the other. Then, the option values in n-dimension is given by:

$$V_T(k_1, k_2, \dots, k_n) = \mathbb{E}^{\mathcal{Q}} \left(e^{-rT} (S_1(T) - K_1(T))^+ \cdot (S_2(T) - K_2(T))^+ \cdots (S_n(T) - K_n(T))^+ \right) \quad (4.10.4)$$

where \mathcal{Q} is taken to be an equivalent Martingale measure (risk neutral measure) while the joint density function is given as q_T for each $s_j(T), j = 1, 2, \dots, n$.

The integral representation of the above equation (4.10.4) is given as:

$$V_T(k_1, k_2, \dots, k_n) = \int_{k_1}^{\infty} \int_{k_2}^{\infty} \cdots \int_{k_n}^{\infty} e^{-rT} (e^{s_1} - e^{k_1})(e^{s_2} - e^{k_2}) \cdots (e^{s_n} - e^{k_n}) \times q_T(s_1, s_2, \dots, s_n) ds_n, \dots ds_2 ds_1. \quad (4.10.5)$$

Let the characteristic function which corresponds to the joint density be expressed as:

$$\varphi(u_1, u_2, \dots, u_n) = \mathbb{E}^{\mathcal{Q}} \left(e^{\sum i u_j s_j(T)} \right) \quad (4.10.6)$$

$$\varphi(u_1, u_2, \dots, u_n) = \int_{-\infty}^{\infty} e^{i u_1 s_1 + i u_2 s_2 + \cdots + i u_n s_n} q_T(s_1, s_2, \dots, s_n) ds_n \cdots ds_2 ds_1. \quad (4.10.7)$$

Ensuring the right hand side (RHS) of equation (4.10.5) is square integrability demands taking the product of the decaying term α over k_j .

This is given by:

$$c_T(k_1, k_2, \dots, k_n) = e^{\alpha_1 k_1 + \alpha_2 k_2 + \dots + \alpha_n k_n} \times V_T(k_1, k_2, \dots, k_n), \quad (4.10.8)$$

where $\alpha_1, \alpha_2, \dots, \alpha_n > 0$.

The Fourier transform (FT) of the modified call option prices is expressed as:

$$\psi_T(u_1, u_2, \dots, u_n) = \int_{-\infty}^{\infty} \int_{-\infty}^{\infty} \dots \int_{-\infty}^{\infty} e^{i(u_1 k_1 + u_2 k_2 + \dots + u_n k_n)} c_T(k_1, k_2, \dots, k_n) dk_n \dots dk_2 dk_1 \quad (4.10.9)$$

$$\begin{aligned} \psi_T(u_1, u_2, \dots, u_n) &= \int \dots \int_{\mathbb{R}^n} e^{(\alpha_1 + iu_1)k_1 + (\alpha_2 + iu_2)k_2 + \dots + (\alpha_n + iu_n)k_n} \times \\ &\times \int_{k_n}^{+\infty} \dots \int_{k_2}^{+\infty} \int_{k_1}^{+\infty} e^{-rT} \left((e^{s_1} - e^{k_1})(e^{s_2} - e^{k_2}) \dots (e^{s_n} - e^{k_n}) \right) \\ &\times q_T(s_1, s_2, \dots, s_n) dk_n \dots dk_2 dk_1 ds_n \dots ds_2 ds_1 \end{aligned} \quad (4.10.10)$$

Further simplification is done as follows:

$$\begin{aligned} \psi_T(u_1, u_2, \dots, u_n) &= \int \dots \int_{\mathbb{R}^n} e^{-rT} q_T(s_1, s_2, \dots, s_n) \\ &\times \int_{-\infty}^{s^n} \dots \int_{-\infty}^{s^2} \int_{-\infty}^{s^1} e^{-rT} \left((e^{s_1} - e^{k_1})(e^{s_2} - e^{k_2}) \dots (e^{s_n} - e^{k_n}) \right) \\ &e^{(\alpha_1 + iu_1)k_1 + (\alpha_2 + iu_2)k_2 + \dots + (\alpha_n + iu_n)k_n} \times dk_n \dots dk_2 dk_1 ds_n \dots ds_2 ds_1 \end{aligned} \quad (4.10.11)$$

which leads to:

$$\psi_T(u_1, u_2, \dots, u_n) = \int \cdots \int_{\mathbb{R}^n} e^{-rT} q_T(s_1, s_2, \dots, s_n) \times \left(\frac{e^{(1+\alpha_1+iu_1)s_1+(1+\alpha_2+iu_2)s_2+\cdots+(1+\alpha_n+iu_n)s_n}}{(\alpha_1+iu_1)(1+\alpha_1+iu_1)(\alpha_2+iu_2)(1+\alpha_2+iu_2)\cdots(\alpha_n+iu_n)(1+\alpha_n+iu_n)} \right) ds_n \cdots ds_2 ds_1 \quad (4.10.12)$$

For a calculated affine characteristic function φ_T or a known characteristic function of a random process, the derivation of an analytic closed form formula for $\Psi_T(u_1, u_2, \dots, u_n)$ is possible. By definition, the inverse Fourier transform of (4.10.4) through (4.10.11 - 4.10.12) is given as:

$$V_T(\mathbf{k}) = \frac{e^{-(\alpha_1 k_1 + \alpha_2 k_2 + \dots + \alpha_n k_n)}}{(2\pi)^n} \int \cdots \int_{\mathbb{R}^n} e^{-i(u_1 k_1 + u_2 k_2 + \dots + u_n k_n)} \psi_T(u_1, u_2, \dots, u_n) du_k \cdots du_2 du_1 \quad (4.10.13)$$

where $\mathbf{k} = k_1, k_2, \dots, k_n$.

In series form, the integrals could be rewritten by using trapezoidal rule such that the equation (4.10.13) is transformed to the form:

$$V_T(\mathbf{k}) = \frac{e^{-(\alpha_1 k_1 + \alpha_2 k_2 + \dots + \alpha_n k_n)}}{(2\pi)^n} \underbrace{\sum_{m_1=1}^{N_1} \sum_{m_2=1}^{N_2} \cdots \sum_{m_n=1}^{N_n}}_{n\text{-tuple}} e^{-i(u_{1,m_1} k_1 + u_{2,m_2} k_2)} \psi_T(u_{1,m_1}, u_{2,m_2}, \dots, u_{n,m_n}) \prod_{j=1}^n h_j \underbrace{\hspace{10em}}_{\Omega(k_1, k_2, \dots, k_n)} \quad (4.10.14)$$

where

$$\mathbf{k} = k_1, k_2, \dots, k_n; \quad \prod_{j=1}^n h_j = h_1 h_2 \cdots h_n, \quad \text{and } h_j, \quad j = 1, 2, \dots, n \text{ denotes integration steps here.}$$

If one considers a single asset for instance, see the FFT equation expressed in (4.6.23) above. Hence, not deviating from the pattern of equation (4.6.23), an n -dimension version

of y_j , $j = 1, 2, \dots, n$, is given in a manner that captures the imaginary part obtainable in the complex form of y_j , which is all encompassing in Fourier transform. We thus have:

$$\xi_j | j = 1, 2, \dots, n := \sum_{m_1=1}^{N_1-1} \sum_{m_2=1}^{N_1-1} \dots \sum_{m_n=1}^{N_1-1} e^{-i\left(\frac{2\pi}{N_1}j_1m_1 + \frac{2\pi}{N_2}j_2m_2 + \dots + \frac{2\pi}{N_n}j_nm_n\right)} y_j, j = 1, 2, \dots, n. \quad (4.10.15)$$

where $m_1 = 1, 2, \dots, N_1 - 1, m_2 = 1, 2, \dots, N_2 - 1$ respectively.

The steps of integration h_j , $j = 1, 2, \dots, n$, in (4.10.14) is chosen uniformly such that

$$h_1 = \frac{u_{1,m_1}}{\left(m_1 - \frac{N}{2}\right)}, \quad h_2 = \frac{u_{2,m_2}}{\left(m_2 - \frac{N}{2}\right)}, \dots, h_n = \frac{u_{n,m_n}}{\left(m_n - \frac{N}{2}\right)}$$

To this end, consider a uniform grid size of $N \times N$ array.

The uniform spacing size ζ between the N values of vector \mathbf{k} with respect to integration steps h_j , $j = 1, 2, \dots, n$ and equation (4.10.15) are related as follows.

$$\zeta_1 h_1 = \zeta_2 h_2 = \dots = \zeta_n h_n = \frac{2\pi}{N} \quad (4.10.16)$$

The prices of the options V_T over logarithm strikes from equation (4.10.14) is thus given by:

$$V_T(k_{1,p_1}, k_{2,p_2}, \dots, k_{n,p_n}) \approx \frac{e^{-(\alpha_1 k_{1,p_1} + \alpha_2 k_{2,p_2} + \dots + \alpha_n k_{n,p_n})}}{(2\pi)^n} \Omega(k_{1,p_1}, k_{2,p_2}, \dots, k_{n,p_n}) \prod_{j=1}^n h_j, \quad (4.10.17)$$

where $0 \leq p_1, p_2, \dots, p_n \leq N - 1$ and

$$\begin{aligned} \Omega(k_{1,p_1}, k_{2,p_2}, \dots, k_{n,p_n}) &= \sum_{m_1=1}^{N_1-1} \sum_{m_2=1}^{N_1-1} \dots \sum_{m_n=1}^{N_1-1} e^{-\frac{2\pi}{N}\left((m_1 - \frac{N}{2})(p_1 - \frac{N}{2}) + (m_2 - \frac{N}{2})(p_2 - \frac{N}{2}) + \dots + (m_n - \frac{N}{2})(p_n - \frac{N}{2})\right)} \\ &\times \psi_T(u_1, u_2, \dots, u_n) \end{aligned}$$

Remark 4.10.1. (i) Our result given in equation (4.10.17) above is hereby referred

to as fast Fourier transform formula for computing the price of European call options on finite n -dimensional underlying multi-assets.

(ii) The European put options value could also be obtained setting the control parameter $c = -1$ in equations (4.10.2) - (4.10.3) implies that negative sign is attached to the logarithm strikes and logarithm assets variation in equation (4.10.4), and the similar technique is followed throughout to attain at (4.10.17). Alternatively, applying the principle of put-call parity, the put options values could be obtained.

(iii) Our result here is the extension of Carr & Madan type FFT in \mathbb{R} -domain to \mathbb{R}^n . In otherwords, we have been able to extend options valuation on a single underlying asset to that of options on n -dimensions valuation of European type with Carr & Madan FFT technique.

4.10.5 Application on three correlated stocks Assets.

Considering asset in 3-dimensions (or three assets). Let $S_j | j = 1, 2, 3$ be three underlying assets and strike prices $K_j | j = 1, 2, 3$ respectively. *The payoff function is defined following the equation (4.10.3) as:*

$$H(S, K) = \left(c(S_1 - K_1)^+ \cdot c(S_2 - K_2)^+ \cdot c(S_3 - K_3)^+ \right), \quad c = +1 \text{ for call option.} \quad (4.10.18)$$

where the S_j and K_j are asset and strike prices respectively.

The option values computational equation in 3-dimension is given as:

$$V_T(k_1, k_2, k_3) = \mathbb{E}^{\mathcal{Q}} \left(e^{-rT} (S_1(T) - K_1(T))^+ \cdot (S_2(T) - K_2(T))^+ \cdot (S_3(T) - K_3(T))^+ \right) \quad (4.10.19)$$

where \mathcal{Q} is an equivalent Martingale Measure (i.e. risk neutral measure) and q_T is taking to be the joint density function of each $s_j(T), j = 1, 2, 3$.

The integral representation of equation (4.10.19) is given by:

$$V_T(k_1, k_2, k_3) = \int_{k_1}^{\infty} \int_{k_2}^{\infty} \int_{k_3}^{\infty} e^{-rT} (e^{s_1} - e^{k_1})(e^{s_2} - e^{k_2})(e^{s_3} - e^{k_3}) q_T(s_1, s_2, s_3) ds_3 ds_2 ds_1. \quad (4.10.20)$$

The characteristic function equivalent to the joint density is explicitly expressed as:

$$\varphi(u_1, u_2, u_3) = \mathbb{E}^{\mathcal{Q}}(e^{\sum iu_j s_j(T)}), \quad j = 1, 2, 3. \quad (4.10.21)$$

$$\varphi(u_1, u_2, u_3) = \int_{-\infty}^{\infty} e^{iu_1 s_1 + iu_2 s_2 + iu_3 s_3} q_T(s_1, s_2, s_3) ds_3 ds_2 ds_1. \quad (4.10.22)$$

Multiply the right hand side of equation (4.10.20) and the decaying term, α , over k_1, k_2, k_3 for square integrable purpose, the result is thus expressed as:

$$c_T(k_1, k_2, k_3) = e^{\alpha_1 k_1 + \alpha_2 k_2 + \alpha_3 k_3} \times V_T(k_1, k_2, k_3), \quad \alpha_1, \alpha_2, \alpha_3 > 0. \quad (4.10.23)$$

The modified call option prices Fourier transform is given by:

$$\psi_T(u_1, u_2, u_3) = \int_{-\infty}^{\infty} \int_{-\infty}^{\infty} \int_{-\infty}^{\infty} e^{i(u_1 k_1 + u_2 k_2 + u_3 k_3)} c_T(k_1, k_2, k_3) dk_3 dk_2 dk_1 \quad (4.10.24)$$

$$\begin{aligned} \psi_T(u_1, u_2, u_3) &= \int_{\mathbb{R}^3} e^{(\alpha_1 + iu_1)k_1 + (\alpha_2 + iu_2)k_2 + (\alpha_3 + iu_3)k_3} \times \\ &\times \int_{k_3}^{+\infty} \int_{k_2}^{+\infty} \int_{k_1}^{+\infty} e^{-rT} \left((e^{s_1} - e^{k_1})(e^{s_2} - e^{k_2})(e^{s_3} - e^{k_3}) \right) \\ &\times q_T(s_1, s_2, s_3) dk_3 dk_2 dk_1 ds_3 ds_2 ds_1 \end{aligned} \quad (4.10.25)$$

Further simplification leads to:

$$\begin{aligned}\psi_T(u_1, u_2, u_3) &= \int_{\mathbb{R}^3} e^{-rT} q_T(s_1, s_2, s_3) \\ &\times \int_{-\infty}^{s_3} \int_{-\infty}^{s_2} \int_{-\infty}^{s_1} e^{-rT} \left((e^{s_1} - e^{k_1})(e^{s_2} - e^{k_2})(e^{s_3} - e^{k_3}) \right) \\ &\times e^{(\alpha_1 + iu_1)k_1 + (\alpha_2 + iu_2)k_2 + (\alpha_3 + iu_3)k_3} dk_3 dk_2 dk_1 ds_3 ds_2 ds_1\end{aligned}\quad (4.10.26)$$

which reduces to:

$$\begin{aligned}\psi_T(u_1, u_2, u_3) &= \int_{\mathbb{R}^3} e^{-rT} q_T(s_1, s_2, s_3) \\ &\times \left[\frac{e^{(1+\alpha_1+iu_1)s_1 + (1+\alpha_2+iu_2)s_2 + (1+\alpha_3+iu_3)s_3}}{(\alpha_1 + iu_1)(1 + \alpha_1 + iu_1)(\alpha_2 + iu_2)(1 + \alpha_2 + iu_2)(\alpha_3 + iu_3)(1 + \alpha_3 + iu_3)} \right] ds_3 ds_2 ds_1\end{aligned}\quad (4.10.27)$$

For a known characteristic function φ_T of the given distribution, a close form formula for $\Psi_T(u_1, u_2, u_3)$ analytically corresponding to the inverse Fourier transform (IFT) of the chosen 3-dimensional underlying multi-assets is expressed as:

$$V_T(k_1, k_2, k_3) = \frac{e^{-(\alpha_1 k_1 + \alpha_2 k_2 + \alpha_3 k_3)}}{(2\pi)^3} \int_{-\infty}^{\infty} \int_{-\infty}^{\infty} \int_{-\infty}^{\infty} e^{-i(u_1 k_1 + u_2 k_2 + u_3 k_3)} \psi_T(u_1, u_2, u_3) du_3 du_2 du_1. \quad (4.10.28)$$

The integrals is rewritten in series form and by trapezoidal rule, (4.10.28) is hence expressed as:

$$V_T(k_1, k_2, k_3) = \frac{e^{-(\alpha_1 k_1 + \alpha_2 k_2 + \alpha_3 k_3)}}{(2\pi)^3} \underbrace{\sum_{m_1=1}^{N_1} \sum_{m_2=1}^{N_2} \sum_{m_3=1}^{N_3} e^{-i(u_{1,m_1} k_1 + u_{2,m_2} k_2)} \psi_T(u_{1,m_1}, u_{2,m_2}, u_{3,m_3})}_{\Omega(k_1, k_2, k_3)} h_3 h_2 h_1 \quad (4.10.29)$$

where $h_1 h_2 h_3$, is the product of the integration steps.

Recalling that the general equation for FFT is usually expressed in the form:

$$H(k) = \sum_{j=1}^{N-1} e^{-i\frac{2\pi}{N}(j-1)(k-1)} y_j, \quad 1 \leq k \leq N. \quad (4.10.30)$$

for a single underlying asset. Therefore, the 3–dimensional version of y_j , $j = 1, 2, 3$, in (4.10.30) having it in mind to capture imaginary part of the complex form of y_j , is expressed as:

$$\xi_j | j = 1, 2, 3 := \sum_{m_1=1}^{N_1-1} \sum_{m_2=1}^{N_1-1} \sum_{m_3=1}^{N_1-1} e^{-i\left(\frac{2\pi}{N_1}j_1m_1 + \frac{2\pi}{N_2}j_2m_2 + \frac{2\pi}{N_3}j_3m_3\right)} y_j, \quad j = 1, 2, 3. \quad (4.10.31)$$

where $m_1 = 1, 2, \dots, N_1 - 1, m_2 = 1, 2, \dots, N_2 - 1, m_3 = 1, 2, \dots, N_2 - 1$ respectively.

The integration steps h_j , $j = 1, 2, 3$, in (4.10.29) is uniformly chosen in the sense that

$$h_1 = \frac{u_{1,m_1}}{\left(m_1 - \frac{N}{2}\right)}, \quad h_2 = \frac{u_{2,m_2}}{\left(m_2 - \frac{N}{2}\right)}, \quad h_3 = \frac{u_{3,m_3}}{\left(m_3 - \frac{N}{2}\right)}$$

Consider a uniform grid size $N \times N$ array. Setting the uniform spacing parameter ζ size between N values of the vector \mathbf{k} , with regards to the integration steps $h_j, j = 1, 2, 3$ and equation (4.10.31), the following relation hold

$$\zeta_1 h_1 = \zeta_2 h_2 = \zeta_3 h_3 = \frac{2\pi}{N} \quad (4.10.32)$$

The options prices V_T over logarithm strikes in equation (4.10.29) is expressed as:

$$V_T(k_{1,p_1}, k_{2,p_2}, k_{3,p_3}) \approx \frac{e^{-(\alpha_1 k_{1,p_1} + \alpha_2 k_{2,p_2} + \alpha_3 k_{3,p_3})}}{(2\pi)^3} \Omega(k_{1,p_1}, k_{2,p_2}, k_{3,p_3}) h_1 h_2 h_3, \quad (4.10.33)$$

where $0 \leq p_1, p_2, p_3 \leq N - 1$, and

$$\begin{aligned} \Omega(k_{1,p_1}, k_{2,p_2}, k_{3,p_3}) &= \sum_{m_1=1}^{N_1-1} \sum_{m_2=1}^{N_1-1} \sum_{m_3=1}^{N_1-1} e^{-\frac{2\pi}{N} \left((m_1 - \frac{N}{2})(p_1 - \frac{N}{2}) + (m_2 - \frac{N}{2})(p_2 - \frac{N}{2}) + (m_3 - \frac{N}{2})(p_3 - \frac{N}{2}) \right)} \\ &\times \psi_T(u_1, u_2, u_3) \end{aligned}$$

Remark 4.10.2. The next section shows options value using the above method on three underlying assets or a single asset consisting of three sub-assets.

4.11 STUDY SIX

4.11.1 Application of the method to three correlated stocks assets.

Consider European call option on vector of underlying assets with Strikes prices expressed as:

$$\mathbf{S} := \begin{cases} S_1 = 100; \\ S_2 = 105; \\ S_3 = 110. \end{cases} \quad (4.11.1)$$

$$\mathbf{K} := \begin{cases} K_1 = 80; \\ K_2 = 85; \\ K_3 = 90. \end{cases} \quad (4.11.2)$$

respectively.

Specifying the following parameters: risk neutral interest rate $r = 0.04$, the dividend rate $d = 0.015$, and the exercising time $T = \{0.5, 1\}$ for all the assets.

Using the FFT-algorithm, and simulation via maplesoft, the results generated were presented in the following tables. Taking the value of fineness of integration grid $N = 2^{12}$ and using the same value for integrability parameter $\alpha := \{\alpha_1 = \alpha_2 = \alpha_3\} = 0.25$. Suppose the volatilities evolves stochastically in away that one can apply the $\text{randn}(\cdot, \cdot)$ function to generate three (3) array of real numbers within the

open interval $(-2, 2)$ for volatilities from the two sources defined in equation (4.10.1) in each case. The following results were gotten and documented in the tables below.

4.11.2 Tables of Result 2

Table 4.2: A dividend compensating (paying) multi-assets European-type call options returns under double source of volatility

Three underlying Assets prices, \mathbf{S}	Strike prices \mathbf{K}	Volatility $\{\sigma^*, \sigma^{rec}\}$	Exercising Time (year)	Call Options Prices (FFT)
$S_1 = 100$	80	0.93001, 0.074916	0.5	36.50909180
$S_2 = 105$	85	-1.85574, -0.098738	0.5	58.48441338
$S_3 = 110$	90	0.89337, 1.139327	0.5	62.35039645
$S_1 = 100$	80	0.31079, -0.052239	1	21.65478068
$S_2 = 105$	85	-1.38470, 1.571944	1	21.08179072
$S_3 = 110$	90	0.71091, -0.912938	1	21.13924135

Source: Author's model simulation result analysis

Table 4.2 shows Call option prices obtained on three underlying assets under the bi-volatility sources presented above. The Other non-specified parameters values used are fineness of integration grid point, $N = 2^{12}$, integrability parameter $\alpha := \{\alpha_1 = \alpha_2 = \alpha_3\} = 0.25$, risk-neutral interest rate, $r = 0.04$, the dividend rate, $q = 0.015$, and exercising time, $T := \{0.5, 1\}$ for all the assets. However, in the market, we assumed that recession volatility may be measured based on the market price index with respect to timely recession filtration data. It could also be determined from Historical volatility of the options which is economy state dependent.

Table 4.3: Non-dividend paying multi-assets European call options returns under double source of volatility

Three underlying Assets prices, \mathbf{S}	Strike prices \mathbf{K}	Volatility $\{\sigma^*, \sigma^{rec}\}$	Exercising Time (year)	The Call Options Prices (FFT)
$S_1 = 100$	80	0.93001, 0.074916	0.5	37.073957451
$S_2 = 105$	85	-1.85574, -0.098738	0.5	59.106692530
$S_3 = 110$	90	0.89337, 1.139327	0.5	63.001682466
$S_1 = 100$	80	0.31079, -0.052239	1	25.097452976
$S_2 = 105$	85	-1.38470, 1.571944	1	24.001337261
$S_3 = 110$	90	0.71091, -0.912938	1	24.407361676

Source: Author's model simulation result analysis

Considering the similar data used for the parameters specified in Table 4.2 but the dividend parameter $q = 0$ being a non-dividend paying type. The result obtained is presented in the Table 4.3 for European call option prices obtained via FFT-method on three underlying assets under the bi-volatility sources defined in equation 4.10.1. The other non-specified parameters values used are fineness of integration grid point, $N = 2^{12}$, integrability parameter $\alpha := \{\alpha_1 = \alpha_2 = \alpha_3\} = 0.25$, risk-neutral interest rate $r = 0.04$ and the exercising time, $T := \{0.5, 1\}$. It is observed that the FFT-call options payoff in the table 4.3 outperformed the option prices in the Table 4.2 because 4.3 is a non-dividend paying type. However, the recession volatility has contributed to the options price variation.

4.12 Conclusion

Fast Fourier Transform algorithm to compute options price on an underlying multi-assets with rigorous mathematical computation procedures were fully documented under the “Result 2”. The highlights of the result presented incorporated the concept of economic recession induced volatility. The Carr & Madan (1999) - type algorithm of FFT in European-type call options computation proposed for a single underlying asset is extended to a class of correlated multi-assets with finite-dimension. For illustration purpose, numerical values for the approach discussed here were experimented using maple software. The major importance of the ‘Result 2’ presented here among others are: Rigorous mathematical computational procedure via fast Fourier transform algorithm, extension of Fast Fourier Transform to a class of multi-assets options valuation, multi-dimensional study, and economic recession induced volatility concept introduced.

RESULT 3

Accuracy of Fast Fourier Transform Method with Control Fineness of Integration grid for Valuation of American Option

4.13 An overview of Result 3

We present Fast Fourier Transform method with control fineness of integration grid for the valuation of a non-dividend and dividend compensating American options. Fourier Transform technique was used in deriving an integral representations for an American-type options price as well as its moving (free) boundary conditions. The results was further extended to arrive at a fundamental analytical valuation formula for computing an American call and put options price. Numerical experiments were presented to show the importance of controlling the fineness of integration grid parameter. In general, the Fast Fourier Transform method has speed advantage, flexible to implement, and produces accurate prices for an optimal exercise boundary of the American call option over a wide range of parameters. Without Loss of generalities, the findings showed that when the integration grid parameter value becomes minimal, the payoff of the option prices via FFT diverges beyond normal compared to the payoff obtained through analytical solution via Black Scholes model. Accurate result of the option prices are then obtained when we control the fineness of integration grid parameter to take values from 2^3 and above in comparison with analytical option prices produced by Black Scholes model. Hence, the Fast Fourier Transform method with control fineness of integration grid is reliable and in agreement with the option values obtained through the analytical valuation formula of Black- Scholes model.

4.13.1 Introduction

In this Result 3, we achieved our stated objective of study (iv), (v) and (vi). An American options computation problem is very domineering in mathematical theory applicable in the field of modern finance. This task involves finding a rational price satisfying the no-arbitrage principle of the option as well as an optimal stopping time τ at which the option is to be exercised. Most of the standard options pricing found in practice are American style in nature due to the early exercise privilege prior and up to the expiry date. The typical difference between an American option and European options is in terms of the exercising time. European option is only exercisable if the maturity date (expiry date) is reached while the American option is allowed to be exercised by its holder at any time $t \leq T$ up to the expiry date T . Whence, American option is more supple (flexible) and eye-catching (attention grabbing) for investors. Also, the American options owner has more exercise chances than the owner of the corresponding European options. This makes American options more expensive than the equivalent European options. An exact solution for European style options are readily available unlike American style options. It is very essential to use Numerical experiments while determining the value of an American style options and for many exotic options. It is common to use uniform spacing while pricing options via Fast Fourier Transform technique. We wish to investigate the control fineness of integration grid effect on options computation while using this technique of fast Fourier transform among other findings under the heading “Result 3”.

There are scenarios whereby one comes across computation of integral(s) in financial computation or quantitative analysis of finance. At times the integrals can be computed analytically but in some cases, the integrals can be computed through partial differential equation, or transformed to numerical integration form before computation is carried out. In the next study, we gave Factorial function Black-Scholes PDE.

4.14 STUDY SEVEN

4.14.1 Factorial function Black - Scholes PDE formulation for Option Pricing

Definition 4.14.1. Let $n \in \mathbb{N}$ be set of natural numbers. The factorial function denoted by $n!$ is the function that computes the product of the first n natural numbers defined by:

$$n! = n(n - 1) \cdots 3 \cdot 2 \cdot 1. \quad (4.14.1)$$

For large values of n , $n! \sim n^n e^{-n}$, equation (4.14.1) is equivalent to the restriction of the gamma function to positive integers. The restriction $f_E(x)$ of a function $f(x)$ to a given non-empty set E is the set of pairs $\langle x, y \rangle$ such that $y = f(x)$ and $x \in E$. For integral n , the factorial function

$$n! = \Gamma(n + 1) \quad (4.14.2)$$

Definition 4.14.2. A Gamma function is one of the special functions with the property that

$$\Gamma(z + 1) = \int_0^{\infty} x^z e^{-x} dx = z \Gamma(z) \quad (4.14.3)$$

with the real part of z denoted $\Re(z) > -1$. Factorial function, which it thus extends to all real or complex z . The definition in (4.14.3) is due to Euler. Another standard definition given due to Gauss with z being a non-negative integer is given as:

$$\Gamma(z + 1) = \lim_{n \rightarrow \infty} \left(\frac{n! n^z}{(z + 1)(z + 2) \dots (z + n)} \right). \quad (4.14.4)$$

Proposition 4.14.1. Consider a filtered probability space $(\Omega, \mathcal{F}, \mathbb{P}, \mathbb{F}(\mathcal{F}))$ and $X = \{X_t : t \geq 0\}$ an adapted stochastic process satisfying the *Stochastic Differential Equation*

$$dX(t) = n! \left(\alpha X(t) dt + \sigma X(t) dW(t) \right), \quad X(t_0) = x_0 \quad (4.14.5)$$

where $W = \{W(t) : t \in [t \geq 0]\}$ is a Brownian motion, $\alpha \in \mathbb{R}$ and $\sigma > 0$. Then, the stochastic process $X = \{X_t : t \geq 0\}$ known as a *geometric or exponential Brownian motion* has an explicit solution given by:

$$X(t) = x_0 \exp \left\{ n! \left(\alpha - \frac{\sigma^2}{2} \right) (t - t_0) + n! \sigma \left(W(t) - W(t_0) \right) \right\} \quad (4.14.6)$$

Theorem 4.14.1. Let $S(t)$ be the price of underlying asset, σ the volatility, r the risk interest rate and $W(t)$, the Wiener process. Suppose further that the underlying price of the asset $S(t)$ satisfies a random process in the Stochastic Differential Equation (SDE) given below

$$dS(t) = \left(n! r + \frac{1}{2} n! (n - 1) \sigma^2 \right) S(t) dt + n! \sigma S(t) dW_t \quad (4.14.7)$$

An explicit solution of the underlying asset price is given as

$$S(T) = S(t_0) \exp \left[n! \left(r + \frac{1}{2} (n-1) \sigma^2 \right) (T - t_0) + n! \sigma (W(T) - W(t_0)) \right] \quad (4.14.8)$$

Proof. Let

$$u(S(t), t) = \ln S(t) \quad (4.14.9)$$

By differentiating equation (4.14.9) partially with respect to $S(t)$ and t , we have:

$$\frac{\partial u}{\partial t} = 0, \quad \frac{\partial u}{\partial S(t)} = \frac{1}{S(t)}, \quad \frac{\partial^2 u}{\partial S^2(t)} = \frac{-1}{S^2(t)} \quad (4.14.10)$$

On application of Itô's lemma, with respect to equation (4.14.7), we have:

$$du(S(t), t) = \left(\frac{\partial u}{\partial t} + f \frac{\partial u}{\partial S(t)} + \frac{1}{2} g^2 \frac{\partial^2 u}{\partial S^2(t)} \right) dt + g \frac{\partial u}{\partial S(t)} dW(t) \quad (4.14.11)$$

The corresponding values for the functions f and g from the equation (4.14.7) are given as:

$$\begin{cases} f = (n! r + \frac{1}{2} n! (n-1) \sigma^2) S(t) \\ g = n! \sigma S(t) \end{cases} \quad (4.14.12)$$

By substituting equation (4.14.9), (4.14.10) and (4.14.12) into (4.14.11), we have:

$$\begin{aligned} d \ln S(t) = & \left[\left(0 + n! r + \frac{1}{2} n! (n-1) \sigma^2 \right) S(t) \cdot \frac{1}{S(t)} \right] dt \\ & + \left[\left(\frac{n! \sigma S(t)}{2} \right)^2 \cdot \frac{1}{S^2(t)} \right] dt + \left(n! \sigma S(t) \cdot \frac{1}{S(t)} \right) dW_t \end{aligned} \quad (4.14.13)$$

$$d \ln S(t) = \left[n! r + \frac{1}{2} n! (n-1) \sigma^2 - \frac{(n! \sigma)^2}{2} \right] dt + n! \sigma dW(t) \quad (4.14.14)$$

The log asset price in (4.14.14) above is seen to be Brownian motion in nature with

drift and variance parameters $n!(r + \frac{1}{2}(n-1)\sigma^2) - \frac{n!^2\sigma^2}{2}$ and $n!\sigma$ respectively.

Integrating the sides of (4.14.14) from t_0 to T gives the following equations.

$$\int_{t_0}^T d \ln S(t) = \int_{t_0}^T \left[n! \left(r + \frac{1}{2}(n-1)\sigma^2 \right) - \frac{n!^2\sigma^2}{2} \right] dt + n! \sigma dW(t), \quad n \in [0, 1). \quad (4.14.15)$$

$$\ln S(T) - \ln S(t_0) = \int_{t_0}^T \left[n! \left(r + \frac{1}{2}(n-1)\sigma^2 \right) - \frac{n!^2\sigma^2}{2} \right] dt + n! \sigma dW(t), \quad n \in [0, 1). \quad (4.14.16)$$

$$\ln \left(\frac{S(T)}{S(t_0)} \right) = \int_{t_0}^T n! \left(r + \frac{1}{2}(n-1)\sigma^2 \right) dt + n! \int_{t_0}^T \sigma dW(t), \quad n \in [0, 1). \quad (4.14.17)$$

$$\ln \left(\frac{S(T)}{S(t_0)} \right) = n! \left(r + \frac{1}{2}(n-1)\sigma^2 \right) \Big|_{t_0}^T + n! \sigma W(t) \Big|_{t_0}^T, \quad n \in [0, 1). \quad (4.14.18)$$

$$\ln \left(\frac{S(T)}{S(t_0)} \right) = n! \left(r + \frac{1}{2}(n-1)\sigma^2 \right) (T - t_0) + n! \sigma (W(T) - W(t_0)), \quad S(t_0) \neq 0. \quad (4.14.19)$$

Taking the exponential of the entire sides yields:

$$\frac{S(T)}{S(t_0)} = \exp \left[n! \left(r + \frac{1}{2}(n-1)\sigma^2 \right) (T - t_0) + n! \sigma (W(T) - W(t_0)) \right], \quad S(t_0) \neq 0. \quad (4.14.20)$$

Equivalent result to equation (4.14.20) is:

$$S(T) = S(t_0) \exp \left[n! \left(r + \frac{1}{2}(n-1)\sigma^2 \right) (T - t_0) + n! \sigma (W(T) - W(t_0)) \right], \quad S(t_0) \neq 0. \quad (4.14.21)$$

□

Remark 4.14.1.

(i) Setting $n = 0$, $t_0 = 0$, we know zero factorial is one, then we obtained

$$S(T) = S(0) \exp \left[\left(r - \frac{1}{2}\sigma^2 \right) (T) + \sigma W(T) \right], \quad S(0) \neq 0. \quad (4.14.22)$$

(ii) Suppose we set $W(T) = Z\sqrt{T}$.

Then we have

$$S(T) = S(0) \exp \left[\left(r - \frac{1}{2}\sigma^2 \right) (T) + \sigma Z\sqrt{T} \right], S(0) \neq 0. \quad (4.14.23)$$

(iii) The equation (4.14.23) is a log-normal distribution of the underlying stock.

Equivalently, one will say that plain vanilla option is log-normally distributed.

To this end, we wish to give an explicit formula for an arbitrary financial derivative written on Stock $S(t)$ in the form of partial differential equation in (4.14.24) based on our formulation in the following sense:

Let $h \in C^n$, $n \geq 2 \in \mathbb{Z}$, be an arbitrary at least twice continuously differentiable function written on $S(t)$.

The partial differential equation for h is written as:

$$\frac{\partial h}{\partial t} + n! \left(r + \frac{1}{2}(n-1)\sigma^2 \right) S(t) \frac{\partial h}{\partial S(t)} + \frac{1}{2} \left(n! \sigma S(t) \right)^2 \frac{\partial^2 h}{\partial (S(t))^2} - rh = 0 \quad (4.14.24)$$

The popular Black - Scholes PDE can be obtained from equation (4.14.24) above by setting $n = 1$ as $1! = 1$.

Hence (4.14.24) reduces to:

$$\frac{\partial h}{\partial t} + rS(t) \frac{\partial h}{\partial S(t)} + \frac{1}{2} \sigma^2 S^2(t) \frac{\partial^2 h}{\partial S^2(t)} = rh \quad (4.14.25)$$

which is Black and Scholes pde.

Without loss of generality, many standard options may be written in the form of (4.14.24) with their respective boundary conditions.

For example, consider a non dividend paying European style option $E(S(t), t = T)$.

For European call and put option on $S(t)$, setting $h = E^{call}(S(t), T) \equiv E^{call}$ and

$E^{put}(S(t), T) = E^{put}$ respectively, we have:

$$\frac{\partial E^{call}}{\partial t} + n! \left(r + \frac{1}{2}(n-1)\sigma^2 \right) S(t) \frac{\partial E^{call}}{\partial S(t)} + \frac{1}{2} (n! \sigma S(t))^2 \frac{\partial^2 E^{call}}{\partial S^2(t)} - r E^{call} = 0 \quad (4.14.26)$$

subject to boundary conditions:

$$\lim_{S(t) \rightarrow \infty} E^{call}(S(t), T) = \infty \text{ on } [0, T], S > 0. \quad (4.14.27)$$

$$E^{call}(S(t), T) = \phi(S(t)) = (S(t) - K)^+ \text{ on } [0, T] \quad (4.14.28)$$

$$E^{call}(0, T) = 0 \text{ on } [0, T]. \quad (4.14.29)$$

Similarly, for put, we have:

$$\frac{\partial E^{put}}{\partial t} + n! \left(r + \frac{1}{2}(n-1)\sigma^2 \right) S(t) \frac{\partial E^{put}}{\partial S(t)} + \frac{1}{2} (n! \sigma S(t))^2 \frac{\partial^2 E^{put}}{\partial S^2(t)} - r E^{put} = 0 \quad (4.14.30)$$

subject to boundary conditions:

$$\lim_{S(t) \rightarrow \infty} E^{put}(S(t), T) = 0 \text{ on } [0, T], S(t) > 0. \quad (4.14.31)$$

$$E^{put}(S(t), T) = \phi(S(t)) = (K - S(t))^+ \text{ on } [0, T] \quad (4.14.32)$$

$$E^{put}(0, T) = K e^{-r(T-t)} \text{ on } [0, T]. \quad (4.14.33)$$

The equations (4.14.26) and (4.14.30) are the generalisation of the popular Black and Scholes PDE for European options with specified values for $n \in \mathbb{Z}$. The solution are easy to be obtained following the same procedure for solving Black and Scholes PDE.

Remark 4.14.2. For American-style options, we use moving boundary conditions (free boundary conditions) as shown in what follows.

4.14.2 Moving Boundary for American Options

A striking difference in European and American style options with respect to the equations (4.14.26) to (4.14.30) is that we must formulate American style options in subject to moving (free) boundary problems. The task is to determine the appropriate exercise time for the option knowing fully that American options can be exercised at any time up to expiry date.

4.14.3 Determination of Optimal Exercise Boundaries for American Put Options

Suppose $A^{put}(S(t), T)$ is the value of an American put option at a given time, t , on an asset $S(t) = S$. Then we have the expression below that:

$$A^{put}(S(t), T) \geq \max(K - S(t), 0). \quad (4.14.34)$$

This is necessary to prevent an arbitrage opportunity.

Naturally, one will exercise the American put option $A^{put}(S(t), T)$ when $S(t) = S$, becomes very negligible. In this case, it is expedient to have an *optimal exercise*

boundary given by $S^* = S^*(t)$. Whenever $S^* \leq S^*(t)$ at a time, t , the put option must be exercised but if $S > S^*(t)$, then it is not optimal to exercise the option at the time, $t < T$.

Hence, for $S > S^*(t)$, the American put option:

$$A^{put}(S, T) > \max(K - S(t), t). \quad (4.14.35)$$

In a continuation region defined by

$$\mathcal{C} := \left\{ (S, t) \mid S > S^*(t) \right\}, \quad (4.14.36)$$

the price of the option satisfy the classical Black – Scholes pde by setting $n = 0$ in equation (4.14.24) which we write as:

$$\frac{\partial A^{put}}{\partial t}(S(t), T) + \frac{1}{2}\sigma^2 S^2 \frac{\partial^2 A^{put}}{\partial S^2(t)}(S(t), T) + rS \frac{\partial A^{put}(S(t), T)}{\partial S(t)} = rA^{put}(S(t), T) \quad (4.14.37)$$

subject to, $S > S^*(t)$, $t < T$.

We need some other additional conditions that must be satisfied in order to have a suitable explicit formula for the American put option, this we discuss in what follows.

If $S = S^*(t)$, one can exercise the option and then its payoff will be exactly its *exercise value* leading to the boundary condition given by:

$$A^{put}(S(t), t) = \max(K - S^*(t), 0) = K - S^*(t). \quad (4.14.38)$$

The condition given in equation (4.14.38) above is for equation (4.14.37).

Another boundary condition which we impose on the pricing problem of American put option is given by:

$$A^{put}(S(t), T) = \max(K - S, 0), \quad (4.14.39)$$

which implies that the option must be exercised at the maturity date, T , if we have not exercised the option at time, $t < T$.

The final condition to *uniquely* solve the problem is the *smooth pasting condition* which we defined by:

$$\frac{\partial A^{put}}{\partial S}(S(t), t) = \frac{\partial}{\partial S}(K - S^*(t)) = -1. \quad (4.14.40)$$

The equations (4.14.37)-(4.14.40) form the anticipated moving (free) boundary problem for the American put option.

4.15 STUDY EIGHT

4.15.1 Fourier transform Solution steps of the Factorial function Black-Scholes pde formulation for American Options

In attempt to solve the pde representation of the American Option depicted in equation (4.14.37) subject to the moving boundary conditions in equation (4.14.38, 4.14.39, 4.14.40) respectively highlighted earlier, we adopted Fourier transform approach using some properties of Fourier transform and change of variables technique. Suppose the stochastic variation of an American Stock, S , is driven by the Stochastic

Differential Equation

$$dS(t) = \left(n!r + \frac{1}{2}n!(n-1)\sigma^2 - q \right)_{x_t} S(t)dt + n!\sigma_{x_t} S(t)dW_t \quad (4.15.1)$$

whose pde representation is given as:

$$\frac{\partial A^{put}}{\partial t}(S(t), T) + \frac{1}{2}\sigma^2 S^2 \frac{\partial^2 A^{put}}{\partial S^2(t)}(S(t), T) + rS \frac{\partial A^{put}(S(t), T)}{\partial S(t)} = rA^{put}(S(t), T). \quad (4.15.2)$$

The following change of variables were made at constant interest rate r , and volatility σ .

Let $\tau : t \mapsto T - t$ such that $\frac{\partial A}{\partial t} \mapsto -\frac{\partial A}{\partial \tau}$. The pde (4.15.2) in backward time becomes:

$$-\frac{\partial A^{put}}{\partial \tau}(S(t), T) + \frac{1}{2}\sigma^2 S^2 \frac{\partial^2 A^{put}}{\partial S^2(t)}(S(t), T) + rS \frac{\partial A^{put}(S(t), T)}{\partial S(t)} - rA^{put}(S(t), T) = 0. \quad (4.15.3)$$

Equivalently given as:

$$\frac{\partial A^{put}}{\partial \tau}(S(t), T) = \frac{1}{2}\sigma^2 S^2 \frac{\partial^2 A^{put}}{\partial S^2(t)}(S(t), T) + rS \frac{\partial A^{put}(S(t), T)}{\partial S(t)} - rA^{put}(S(t), T) \quad (4.15.4)$$

By considering the logarithm of the American stock defined by $y := \ln(S(t))$ as $S(t) \mapsto \ln S(t)$ whose options value is denoted by $A(S, t)$ in the pde at a time t base on the new variables. The derivatives are now transformed as follows.

$$\frac{\partial A(S, t)}{\partial S(t)} = \frac{\partial A(S, t)}{\partial y} \cdot \frac{\partial y}{\partial S(t)} = \frac{\partial A(S, t)}{\partial y} \cdot \frac{\partial \ln S(t)}{\partial S(t)} \quad (4.15.5)$$

which reduces to:

$$\frac{\partial A(S, t)}{\partial S(t)} = \frac{1}{S(t)} \frac{\partial A(S, t)}{\partial y}. \quad (4.15.6)$$

Similarly,

$$\frac{\partial^2 A(S, t)}{\partial S^2(t)} = \frac{\partial}{\partial S(t)} \cdot \frac{\partial A(S, t)}{\partial S(t)} = \frac{\partial}{\partial S(t)} \left(\frac{1}{S(t)} \frac{\partial A(S, t)}{\partial y} \right) \quad (4.15.7)$$

$$\frac{\partial^2 A(S, t)}{\partial S^2(t)} = \frac{1}{S(t)} \frac{\partial}{\partial S(t)} \frac{\partial A(S, t)}{\partial y} + - \frac{1}{S^2(t)} \frac{\partial A(S, t)}{\partial y} \quad (4.15.8)$$

$$\frac{\partial^2 A(S, t)}{\partial S^2(t)} = \frac{1}{S(t)} \left(\frac{\partial y}{\partial S(t)} \cdot \frac{\partial}{\partial y} \right) \frac{\partial A(S, t)}{\partial y} - \frac{1}{S^2(t)} \frac{\partial A(S, t)}{\partial y} \quad (4.15.9)$$

Substituting for $\frac{\partial y}{\partial S(t)} = \frac{1}{S(t)}$ yields the following

$$\frac{\partial^2 A(S, t)}{\partial S^2(t)} = \frac{1}{S(t)} \left(\frac{1}{S(t)} \right) \cdot \frac{\partial}{\partial y} \frac{\partial A(S, t)}{\partial y} - \frac{1}{S^2(t)} \frac{\partial A(S, t)}{\partial y} \quad (4.15.10)$$

$$\frac{\partial^2 A(S, t)}{\partial S^2(t)} = \frac{1}{S^2(t)} \cdot \frac{\partial^2 A(S, t)}{\partial y^2} - \frac{1}{S^2(t)} \frac{\partial A(S, t)}{\partial y} \quad (4.15.11)$$

Factorising $\frac{1}{S^2(t)}$, we obtained

$$\frac{\partial^2 A(S, t)}{\partial S^2(t)} = \frac{1}{S^2(t)} \left(\frac{\partial^2 A(S, t)}{\partial y^2} - \frac{\partial A(S, t)}{\partial y} \right). \quad (4.15.12)$$

Next, we substitute equation (4.15.6) and (4.15.12) in the pde representation given in (4.15.4) as follow.

$$\frac{\partial A^{put}}{\partial \tau}(S(t), T) = \frac{1}{2} \sigma^2 S^2 \frac{\partial^2 A^{put}}{\partial S^2(t)}(S(t), T) + rS \frac{\partial A^{put}(S(t), T)}{\partial S(t)} - rA^{put}(S(t), T) \quad (4.15.13)$$

Based on the initial dynamics of the stock given as:

$$dS(t) = \left(n!r + \frac{1}{2}n!(n-1)\sigma^2 - q \right)_{x_t} S(t)dt + n!\sigma_{x_t} S(t)dW_t \quad (4.15.14)$$

We first revert the pde (4.15.13) to the form:

$$\frac{\partial A^{put}}{\partial \tau}(S(t), T) = \frac{1}{2}(n!)^2 \sigma^2 S^2 \frac{\partial^2 A^{put}}{\partial S^2(t)}(S(t), T) + n! \left(r - \frac{1}{2}(n-1)\sigma^2 \right) S(t) \frac{\partial A^{put}}{\partial S(t)}(S(t), T) - r A^{put}(S(t), T) \quad (4.15.15)$$

and then make the substitution for the derivatives so that we have the following equations.

$$\frac{\partial A}{\partial \tau}(S_t, T) = \frac{1}{2}(n!)^2 \sigma^2 S_t^2 \frac{1}{S_t^2} \left(\frac{\partial^2 A(S, t)}{\partial y^2} - \frac{\partial A(S, t)}{\partial y} \right) + n! \left(r - \frac{1}{2}(n-1)\sigma^2 \right) S_t \frac{1}{S_t} \frac{\partial A(S, t)}{\partial y} - r A(S_t, T) \quad (4.15.16)$$

which reduces to:

$$\frac{\partial A}{\partial \tau}(S_t, T) = \frac{1}{2}(n!)^2 \sigma^2 \left(\frac{\partial^2 A(S, t)}{\partial y^2} - \frac{\partial A(S, t)}{\partial y} \right) + n! \left(r - \frac{1}{2}(n-1)\sigma^2 \right) \frac{\partial A(S, t)}{\partial y} - r A(S_t, T). \quad (4.15.17)$$

$$\frac{\partial A}{\partial \tau}(S_t, T) = \frac{1}{2}(n!)^2 \sigma^2 \frac{\partial^2 A(S, t)}{\partial y^2} + n! \left(-\frac{n!\sigma^2}{2} + \left(r - \frac{(n-1)\sigma^2}{2} \right) \right) \frac{\partial A(S, t)}{\partial y} - r A(S_t, T) \quad (4.15.18)$$

We are now set to take the Fourier transform of the derivatives with respect to the independent variable $y := \ln S(t)$ as follows:

$$\mathcal{F}\left(\frac{\partial A}{\partial \tau}(S_t, T)\right) = \frac{(n!)^2 \sigma^2}{2} \mathcal{F}\left(\frac{\partial^2 A(S, t)}{\partial y^2}\right) + n! \left(-\frac{n!\sigma^2}{2} + \left(r - \frac{(n-1)\sigma^2}{2} \right) \right) \mathcal{F}\left(\frac{\partial A(S, t)}{\partial y}\right) - \mathcal{F}(r A(S_t, T)). \quad (4.15.19)$$

The above transformation results to an ordinary differential equation of the form:

$$\frac{\partial \hat{A}}{\partial \tau}(S_t, T) = -\frac{1}{2}(n!)^2 \sigma^2 \omega^2 \hat{A}(S_t, T) + n! \left(-\frac{n!\sigma^2}{2} + \left(r - \frac{(n-1)\sigma^2}{2} \right) \right) i\omega \hat{A} - r \hat{A}(S_t, T) \quad (4.15.20)$$

Solving the above equation yields:

$$\hat{A} = \hat{A}_0 e^{-r\tau} \exp \left[-\frac{1}{2}(n!)^2 \sigma^2 \omega^2 \tau + i\omega n! \left(-\frac{n!\sigma^2}{2} + \left(r - \frac{(n-1)\sigma^2}{2} \right) \right) \tau \right], \hat{A}_0 \neq 0, n \in \mathbb{Z}^+ \quad (4.15.21)$$

With different values of $n \in \mathbb{Z}^+$, various solution will emanate from the generalized solution (4.15.21). For an illustration, setting $n = 0$ with $0! = 1$, we have a solution

of the form:

$$\widehat{A} = \widehat{A}_0 e^{-r\tau} \exp \left[-\frac{\sigma^2}{2} \omega^2 \tau + i\omega \left(r + \frac{\sigma^2}{2} \right) \tau \right] \quad (4.15.22)$$

For $n = 1$, $1! = 1$, the solution in equation (4.15.21) reduces to the form:

$$\widehat{A} = \widehat{A}_0 e^{-r\tau} \exp \left[-\frac{\sigma^2}{2} \omega^2 \tau + i\omega \left(r - \frac{\sigma^2}{2} \right) \tau \right] \quad (4.15.23)$$

Next by considering Fourier transform such that we set say $\mu = \left(\frac{\sigma^2}{2} - r \right) \tau$ and $s = \sigma \sqrt{\tau}$. The term:

$$e^{-r\tau} \exp \left(-\frac{\sigma^2}{2} \omega^2 \tau + i\omega \left(r - \frac{\sigma^2}{2} \right) \tau \right) = \mathcal{F} \left[\frac{1}{\sigma \sqrt{2\pi\tau}} \exp \left(-\frac{1}{2} \left(\frac{y - \left(\frac{\sigma^2}{2} - r \right) \tau}{\sigma \sqrt{\tau}} \right)^2 \right) \right] \quad (4.15.24)$$

Choosing the solution in equation (4.15.23) with respect to (4.15.24) yields:

$$\widehat{A}(y, \tau) = \widehat{A}_0 \frac{1}{\sigma \sqrt{2\pi\tau}} e^{-r\tau} \mathcal{F} \left[A_0 \cdot \exp \left(-\frac{1}{2} \left(\frac{y - \left(\frac{\sigma^2}{2} - r \right) \tau}{\sigma \sqrt{\tau}} \right)^2 \right) \right] \quad (4.15.25)$$

In the next step of solution, we take the *inverse Fourier transform* in order to revert to the normal form as follows.

$$A(y, \tau) = \frac{1}{\sigma \sqrt{2\pi\tau}} e^{-r\tau} \int_{-\infty}^{\infty} A_0(z) \exp \left(-\frac{1}{2} \left(\frac{y - z - \left(\frac{\sigma^2}{2} - r \right) \tau}{\sigma \sqrt{\tau}} \right)^2 \right) dz \quad (4.15.26)$$

Equivalently stated as:

$$A(y, \tau) = \frac{1}{\sigma \sqrt{2\pi\tau}} e^{-r\tau} \int_{-\infty}^{\infty} A_0(z) \exp \left(-\frac{1}{2} \left(\frac{z - \left(y + \left(r - \frac{\sigma^2}{2} \right) \tau \right)}{\sigma \sqrt{\tau}} \right)^2 \right) dz \quad (4.15.27)$$

The final step of solution which entails switching back to the original variables suitable for the initial setting such that logarithm of the initial American stock price is defined by $y := \ln S(t_0)$ and $S(t) \mapsto \ln S(t)$ whose options value was initially

denoted by $A(S, t)$. It remains to change the variable z back such that the American stock price $S_\tau = e^z$ implies $z := \ln S_{\tau \leq T}$ and the known initial American stock price at time $t_0 = 0$ is S_0 . With the possible change of variables highlighted, we have an analytic formula for the American stock of the form:

$$A(S, \tau) = \frac{1}{\sigma\sqrt{2\pi\tau}} e^{-r\tau} \int_0^\infty A_0(S_T) \frac{1}{S_T} \exp\left(-\frac{1}{2}\left(\frac{\ln S_T - \left(\ln S_0 + \left(r - \frac{\sigma^2}{2}\right)\tau\right)}{\sigma\sqrt{\tau}}\right)^2\right) dS_T. \quad (4.15.28)$$

Equivalently stated as:

$$A(S, \tau) = \frac{1}{\sigma\sqrt{2\pi\tau}} e^{-r\tau} \int_0^\infty A_0(S_T) \frac{1}{S_T} \exp\left(-\frac{1}{2}\left(\frac{\ln\left(\frac{S_T}{S_0}\right) - \left(r - \frac{\sigma^2}{2}\right)\tau\right)}{\sigma\sqrt{\tau}}\right)^2\right) dS_T. \quad (4.15.29)$$

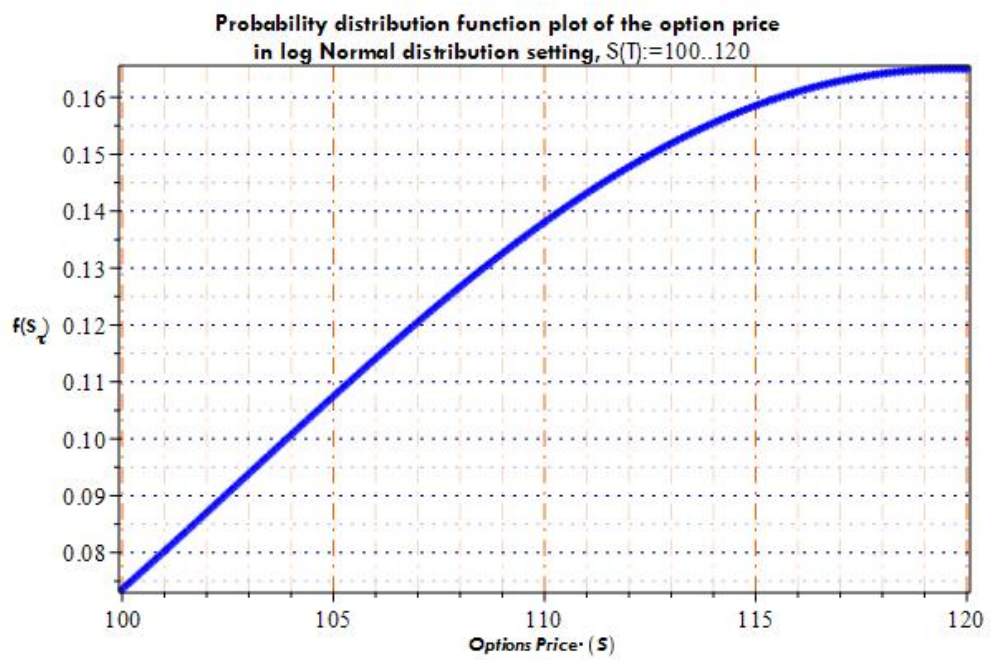
Remark 4.15.1.

(i) *The analytical formula for the American option given above demands that the time τ is the optimal exercising time for the option satisfying $\tau \leq T$ where T is the maturity time for the option. In other words, the optimal time τ is an early exercising time which American options allow before expiration of options' time life.*

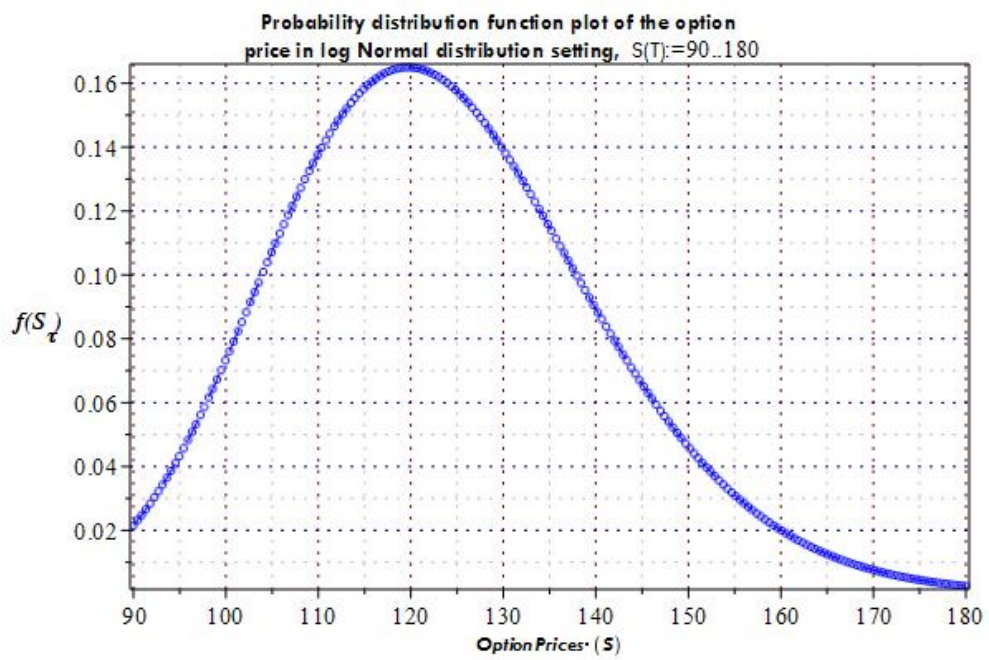
(ii) In a setting of log normal distribution, the probability density function (pdf) for the option's price is given as:

$$f(S_\tau) = \frac{1}{S_T\sigma\sqrt{2\pi\tau}} \exp\left(-\frac{1}{2}\left(\frac{\ln\left(\frac{S_T}{S_0}\right) - \left(r - \frac{\sigma^2}{2}\right)\tau\right)}{\sigma\sqrt{\tau}}\right)^2\right). \quad (4.15.30)$$

Setting parameters, interest rate $r = 0.2$, $\sigma = 0.02$, $S_0 = 100$, and Time, $T = 1$ year, the following figures for the probability density function were obtained for range of values of the Option prices $S(\tau)$.



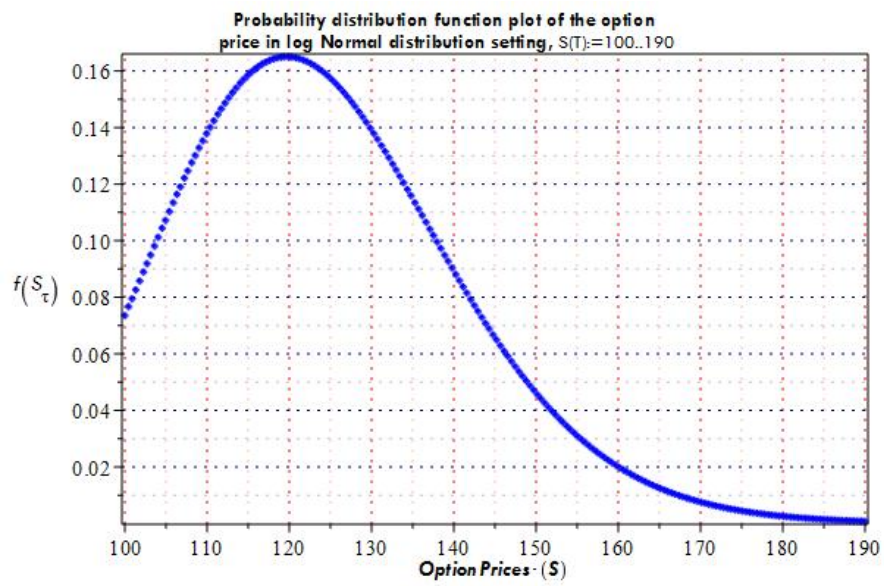
Source: Author's generated graph for pdf result analysis of equation 4.15.30.
 Figure 4.8: Plots of Probability density function $f(S_\tau)$ for a shorter range of Options prices.



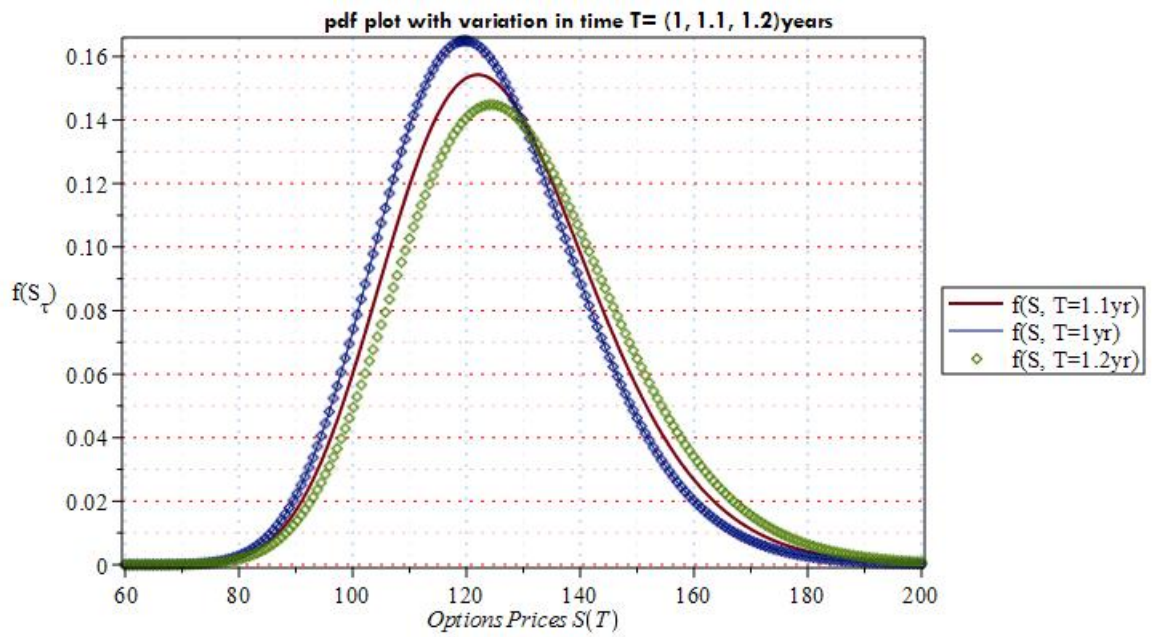
Source: Author's generated graph for pdf result analysis of equation 4.15.30.
 Figure 4.9: Probability density function $f(S_T)$ plots wrt variants of Options prices.

The figure 4.8 is a graph of probability density function in equation 4.15.30 for a range of values for S_t from 100 to 120. The parameters used for the simulation are declared as: interest rate, $r = 0.2$, constant volatility rate, $\sigma = 0.02$, and exercising time, $T = 1$ year, the initial asset price, $S_0 = 100$. The mathematical software used is Maple 2017. The major observation is that the graph begins to curve at $S_T = 110$ up to 120. In order to behold the behaviour of the density function at a wider range of stocks prices, we extended the range of values for S_T and the following graphs provide more information.

The figure 4.9 shows the graph of the equation 4.15.30 which is the density function for the model considered. The plot is for range of values for S_t from 90 to 180. The same set of parameters used in 4.8 was maintained for the simulation of the figure 4.9 except that a wider range of values for S_T was considered. The basic parameters are: interest rate, $r = 0.2$, constant volatility rate, $\sigma = 0.02$, and exercising time, $T = 1$ year, the initial asset price, $S_0 = 100$. It was observed that the graph forms a normal distribution curve although not perfectly visible as normal curve towards the left hand side.



Source: Author's generated graph for pdf result analysis of equation 4.15.30.
 Figure 4.10: Plots of Probability density function $f(S_\tau)$ for range of Options prices.



Source: Author's generated Normal Distribution Curve result analysis from equation 4.15.30.
 Figure 4.11: Plots of Probability density functions $f(S_\tau)$ for range of Option prices with respect to time variation.

The figure 4.10 is a graph of the equation 4.15.30, the density function for the factorial function based BS-model. The pdf $f(S_\tau)$ was graphed for a range of stocks prices, S_T , over a range of values from 100 to 190 subject to the model basic parameters used in the simulation result given in table 4.8. The basic parameters are: interest rate, $r = 0.2$, constant volatility rate, $\sigma = 0.02$, and exercising time, $T = 1$ year, the initial asset price, $S_0 = 100$. The shape of the graph is still a normal distribution but not totally visible for some values at the left hand side.

The figure 4.11 shows the time variation effect on the density function of the equation (4.15.30). In the above graph, we define the probable exercising time of an option price on an underlying stock asset S_τ such that $\tau := \{T_1, T_2, T_3\} = \{1\text{year}, 1.1\text{year}, 1.2\text{year}\}$ respectively. The aforementioned basic parameters in the density function remained valid for the above graph. That is, the risk-neutral interest rate, $r = 0.2$, the constant volatility rate, $\sigma = 0.02$, and the initial stock asset price, $S_0 = 100$. The plot is for a range of values for $S_{T_i}, i = 1, 2, 3$ from 60 to 200. Three normal distribution plots was obtained from the plotting of the derived density function, $f(S_\tau)$ over the specified range for S_τ . From the graph, it was observed that the options' probable exercising time $T_1 = 1$ year would give a shorter range of options prices but the highest amplitude along the vertical axis of the density function $F(S_\tau)$. The highest exercising time $T_3 = 1.2$ years would give the highest range of options prices, i.e the curve in red colour, but has the least amplitude among it's counterpart. The graph is a true representation of an expected probable option's returns in a certain condition, that is, the longer the life span of a traded asset, the better the asset returns (payoff) should be, but the reverse may be the case under uncertainties situation not limited to economy recession alone.

4.16 STUDY NINE

4.16.1 Valuation of a dividend paying American put option under Economy recession induced Volatility uncertainty

Let the stochastic variation of an American Stock, X , be driven by the stochastic Differential Equation:

$$dS(t) = \left(n!r + \frac{1}{2}n!(n-1)\sigma^2 - q \right)_{x_t} S(t)dt + n!\sigma_{x_t}S(t)dW_t \quad (4.16.1)$$

where X is a two-state Markov chain which is free to jump from one state to the other. The parameters in the SDE are interest rate r , volatility σ , dividend rate q , the underlying stock price $S(t)$, Wiener process W_t and factorial function, $n!$, with $n \in \mathbb{Z}^+ \cup \{0\}$. The Wiener process W and the stochastic process X are independent but both the drift term and the volatility are functions of X_t .

Define

$$X_t = \begin{cases} 1, & \text{if the Economy is in Expansion state;} \\ 2, & \text{if the Economy is in Recession state.} \end{cases} \quad (4.16.2)$$

Suppose further that in the stock market, the American style stock X can switch between the two states described above in the (4.16.2) depending on the state of the economy. Song-Ping et al., (2012) stressed that the risk associated with switching from one regime to another is diversifiable and this was in line with the opinion of Naik, (1993) that one only needs to adjust the rate parameters of the transition process accounting for non-diversifiable risk. In this study, we incorporate recession induced volatility uncertainty parameter $\sigma_{x_{t,2}}$ if the economy is in the state 2 (re-

cession state) with the assumption that the volatility rate $\sigma_{x_{t,1}}$ (expansion state) is less than that of recession state, i.e. $\sigma_{x_{t,1}} < \sigma_{x_{t,2}}$.

Let the transition from one state to the other evolve as a *Poisson process* such that:

$$P(\tau_{m,n} > t) = \exp(-\lambda_{mn}t), \quad m, n = 1, 2, \quad m \neq n \quad (4.16.3)$$

where λ_{mn} denotes the transition rate from m - state to an n - state and τ_{mn} is the time spent in m - state before transiting to n - state. Consider the partial differential equation representation for a dividend paying American put option $A^{put}(S(t), t)$ for (4.16.1) in the light of equation (4.14.30) given as:

$$\frac{\partial A^{put}}{\partial t} + n! \left(r + \frac{1}{2}(n-1)\sigma^2 - q \right) S(t) \frac{\partial A^{put}}{\partial S(t)} + \frac{1}{2} (n! \sigma S(t))^2 \frac{\partial^2 A^{put}}{\partial S^2(t)} - r A^{put} = 0 \quad (4.16.4)$$

subject to the boundary conditions highlighted in (4.14.38)-(4.14.40) which is necessary to be satisfied by American options in the context of moving boundary. Upholding the assumption that risk associated with regime switching is diversifiable (Song-Ping et al., 2012; and Naik, 1993), the equation (4.16.4) is re-written as:

$$\frac{\partial A_1^{put}}{\partial t} + n! \left(r + \frac{1}{2}(n-1)\sigma^2 - q \right) S(t) \frac{\partial A_1^{put}}{\partial S(t)} + \frac{1}{2} (n! \sigma S(t))^2 \frac{\partial^2 A_1^{put}}{\partial S^2(t)} - r A_1^{put} = \lambda_{12}(A_1 - A_2) \quad (4.16.5)$$

subject to the boundary conditions:

$$\left\{ \begin{array}{l} S > S^*, t < T, \\ A_1(0, t) = Ke^{-r(T-t)}, \\ A_1(S, t) = \max(K - S^*(t), 0) = K - S^*(t), \text{ if } S = S^*. \\ A_1(S(t), T) = \max(K - S, 0), \text{ for } S = S^* \\ \frac{\partial A_1}{\partial S}(S(t), t) = \frac{\partial}{\partial S}(K - S^*(t)) = -1 \end{array} \right.$$

and when transiting from state 2 back to state 1, we have:

$$\frac{\partial A_2^{put}}{\partial t} + n! \left(r + \frac{1}{2}(n-1)\sigma^2 - q \right) S(t) \frac{\partial A_2^{put}}{\partial S(t)} + \frac{1}{2} (n! \sigma S(t))^2 \frac{\partial^2 A_2^{put}}{\partial S^2(t)} - r A_2^{put} = \lambda_{12}(A_2 - A_1) \quad (4.16.6)$$

subject to the boundary conditions:

$$\left\{ \begin{array}{l} S > S^*, t < T, \\ A_2(0, t) = Ke^{-r(T-t)}, \\ A_2(S, t) = \max(K - S^*(t), 0) = K - S^*(t), \text{ if } S = S^*. \\ A_2(S(t), T) = \max(K - S(T), 0), \text{ for } S = S^* \\ \frac{\partial A_2}{\partial S}(S(t), t) = \frac{\partial}{\partial S}(K - S^*(t)) = -1 \end{array} \right.$$

where t is the current time, S is the underlying American asset value (stock) value, r is the interest rate (which we assume to be constant here), K is the strike price, $A_m(S, T)$ with $m = 1, 2$ is the option's value when in state m of the economy and T is the maturity time of the option if not exercised earlier, at time $t < T$, and S^* remain as the optimal exercise boundary. Since we are dealing with an American option, owing to the fact that an American style option can be exercised at any

time up to the maturity time. An investor may exercise the option at an optimal stopping time, t^* , prior to the time of expiry, T , within the region of the optimal exercise boundary.

Remark 4.16.1. It should be noted that $A_1 \neq A_2$ on the right hand side of the equations (4.16.5) and (4.16.6) owing to the transition between states and the effect of recession factor on the stock while in state 2.

On the application of change of variable technique to ease the process of solving partial differential equation, see (Heston, 1993; Song-Ping et al., 2012), the equations (4.16.5) and (4.16.6) are written such that Fourier transform technique is applicable in sequel.

Setting

$$\begin{aligned}\tau_m &= \frac{\sigma_m^2}{2}(T - t) \\ x &= \log\left(\frac{S}{K}\right) \\ f_m(x, \tau_m) &= \frac{e^x A_m}{K}(S, t \leq T)\end{aligned}$$

$$S \rightarrow x, \quad t \rightarrow \tau, \quad A \rightarrow f$$

for states $m = 1, 2$. The above variables are dimensionless and the equations (4.16.5) - (4.16.6) are transformed to the form:

$$-\frac{\partial f_1}{\partial \tau_1} + \frac{\partial^2 f_1}{\partial x^2} + \left(\frac{2r}{\sigma_1^2} - 3\right)\frac{\partial f_1}{\partial x} - \left(\frac{4r}{\sigma_1^2} + \alpha_{12} - 2\right)f_1 = -\beta_{12}f_2 \quad (4.16.7)$$

subject to the boundary conditions:

$$\left\{ \begin{array}{l} f_1(x, 0) = (e^x(1 - e^x))^+ \equiv (e^x - e^{2x})^+ \\ \lim_{x \rightarrow -\infty} f_1(x, \tau_1) = 0 \\ \lim_{x \rightarrow \infty} f_1(x, \tau_1) = 0 \end{array} \right.$$

and

$$-\frac{\partial f_2}{\partial \tau_2} + \frac{\partial^2 f_2}{\partial x^2} + \left(\frac{2r}{\sigma_1^2} - 3\right) \frac{\partial f_2}{\partial x} - \left(\frac{4r}{\sigma_2^2} + \alpha_{21} - 2\right) f_2 = -\beta_{21} f_1 \quad (4.16.8)$$

subject to the boundary conditions:

$$\left\{ \begin{array}{l} f_2(x, 0) = (e^x(1 - e^x))^+ \equiv (e^x - e^{2x})^+ \\ \lim_{x \rightarrow -\infty} f_2(x, \tau_1) = 0 \\ \lim_{x \rightarrow \infty} f_2(x, \tau_1) = 0 \end{array} \right.$$

such that from $\tau_m = \frac{\sigma_m^2}{2}(T - t)$, we have $T - t = \frac{2\tau_m}{\sigma_m^2}$.

Setting $T - t = \gamma_m \equiv \frac{2}{\sigma_m^2} \underbrace{\tau_m}_r$, this implies that $\gamma_m = \frac{2r}{\sigma_m^2}$

and $\alpha_{mn} \equiv \frac{2\lambda_{mn}}{\sigma_m^2}$, $m, n = 1, 2$, for $m \neq n$.

Remark 4.16.2. All the drift parameters including the interest rate and the dividend have been transformed. We envisage that the volatility in the two states cannot be equal. In accordance with Bankole et al., (2017), volatility tends to increase during economy recession compared to when the economy is in the expansion (growth) state. Hence, there is need to show relativity between the transition rate from one state to the other and the volatility from that state which is the major reason for

writing $\alpha_{mn} = \frac{2\lambda_{mn}}{\sigma_m^2}$.

Before solving the equations (4.16.7) and (4.16.8) using Fourier Transform method, we wish to examine briefly the solution of differential equations by transformation.

4.16.2 Fourier Transform of Ordinary Differential Equations

Example 4.16.1. Consider an Airy equation of the form $g'' - xg = 0$, with the boundary condition $\lim_{|x| \rightarrow \infty} g(x) = 0$.

Solution:

Applying Fourier transform of derivative for both x and ω , we have:

$$\begin{aligned}\mathcal{F}(g'' - xg) &= \mathcal{F}(0) \\ \Rightarrow (i\omega)^2 \tilde{g}(\omega) - i\tilde{g}'(\omega) &= 0\end{aligned}$$

$$-\omega^2 \hat{g}(\omega) - i\hat{g}'(\omega) = 0 \quad (4.16.9)$$

Equation (4.16.9) is still an ODE which can also be solved through separation of variables as follows.

$$i\hat{g}'(\omega) = -\omega^2 \hat{g}(\omega) \quad (4.16.10)$$

$$\hat{g}'(\omega) = \frac{-\omega^2 \hat{g}(\omega)}{i} \quad (4.16.11)$$

$$\frac{\hat{g}'(\omega)}{\hat{g}(\omega)} = -\frac{\omega^2}{i} \quad (4.16.12)$$

Integrating the entire sides:

$$\begin{aligned}\int \frac{\hat{g}'(\omega)}{\hat{g}(\omega)} &= \int \frac{-\omega^2}{i} d\omega \\ \ln \hat{g}(\omega) &= -\frac{\omega^3}{3i} + c \\ \hat{g}(\omega) &= e^{\frac{-\omega^3}{3i}} \cdot e^c \\ \hat{g}(\omega) &= ke^{\frac{-\omega^3}{3i}} \text{ where } k = e^c; \text{ is a constant of integration} \\ \therefore \hat{g}(\omega) &= ke^{\frac{-\omega^3}{3}} \quad \because \frac{-1}{i} \equiv i.\end{aligned}$$

Taking the inverse Fourier transform, one will have:

$$g(w) = \frac{k}{2\pi} \int_{-\infty}^{\infty} e^{i(wx + \frac{w^3}{3})} dw. \quad (4.16.13)$$

Setting $k = 1$ gives the desired *Airy function*:

$$A_i(x) = \frac{1}{2\pi} \int_{-\infty}^{\infty} e^{i(wx + \frac{w^3}{3})} dw \equiv \frac{1}{\pi} \int_0^{\infty} e^{i(wx + \frac{w^3}{3})} dw.$$

4.16.3 Fourier Transform of Partial Differential Equation

Consider PDE in two variables. Transform is done by reducing the number of variables with derivatives to one and then apply ODE method.

Example 4.16.2. Solve the Laplace equation on the half plane:

$$\frac{\partial^2 u}{\partial x^2} + \frac{\partial^2 u}{\partial y^2} = 0 \quad (4.16.14)$$

with boundary conditions

$$-\infty < x < \infty, \quad y > 0, \quad u(x, 0) = g(x), \quad \lim_{y \rightarrow \infty} u(x, y) = 0.$$

Solution:

Transforming in the x - variable, the equation below holds:

$$F(w, y) = \int_{-\infty}^{\infty} e^{-i\omega x} u(x, y) dx. \quad (4.16.15)$$

Since the derivative in y commutes with the Fourier integral in x , denote the transform of u_{yy} as F_{yy} . Therefore the Fourier transform of the equation (4.16.14) became:

$$\mathcal{F}(u_{xx} + u_{yy}) = \mathcal{F}(0) \text{ subject to the boundary conditions in (4.16.14)}$$

$$(i\omega)^2 F + F_{yy} = 0$$

$$-\omega^2 F + F_{yy} = 0$$

$$F(w, 0) = \hat{g}(\omega), \quad \lim_{y \rightarrow \infty} F(w, y) = 0.$$

Solving the set of the ODEs above for w one for each, we obtain:

$$F = k_1 E^{+|w|y + k_2 e^{-|w|y}}, \quad (4.16.16)$$

the constants k_1 and k_2 depends on w . With respect to the boundary conditions, F can only vanish at infinity provided we set the first term to be zero. Hence using $F(w, 0) = \hat{g}(w)$, then

$$F(w, y) = \hat{g}(w) e^{-|w|y}. \quad (4.16.17)$$

The inverse Fourier transform consists of a convolution and exponential in w . Taking the inverse Fourier Transform invF of equation 4.16.17, the following equations holds:

$$\begin{aligned} u(x, y) &= g(x) * \text{invFT}(e^{-|w|y}) \\ &= g(x) * \left(\frac{y}{\pi(x^2 + y^2)} \right) \\ u(x, y) &= \frac{1}{\pi} \int_{-\infty}^{\infty} \frac{yg(x_0)}{(x - x_0)^2 + y^2} dx_0. \end{aligned} \quad (4.16.18)$$

Remark 4.16.3. Following the knowledge of Fourier transform of differential equations presented in the examples above and using the conventional representation given by Song-Ping et al., (2012), we proceed the transformation of the equations (4.16.7) and (4.16.8) in what follows.

$$\mathcal{F}(f_m(x, \tau_m)) = \mathcal{F}\left(\frac{e^x A_m(S, t \leq T)}{K}\right) \quad (4.16.19)$$

$$\mathcal{F}(f_m(x, \tau_m)) = \int_{-\infty}^{\infty} e^{-i\omega x} f_m(x, \tau_m) dx = \hat{f}_m(\omega, \tau_m) \quad (4.16.20)$$

where $i = \sqrt{-1}$.

The following systems of ODE emerged from (4.16.7) and (4.16.8) respectively given by:

$$\left(\frac{d}{d\tau_1} + \alpha_{12}(\omega) \right) \hat{f}_1(\omega, \tau_1) = \beta_{12} \hat{f}_2(\omega, \tau_1) \quad (4.16.21)$$

with the boundary conditions:

$$\begin{cases} \hat{f}_1(x, 0), = \hat{f}_0 = \mathcal{F}(e^x(1 - e^x))^+ = \int_{-\infty}^{\infty} (e^x(1 - e^x))e^{-i\omega x} dx = \frac{1}{(1 - i\omega)(2 - i\omega)} \\ \left. \frac{d\hat{f}_1}{d\tau_1} \right|_{\tau_1=0} + \alpha_{12}(\omega) \hat{f}_0 = \beta_{12} \hat{f}_0 \end{cases}$$

and

$$\left(\left(\frac{\sigma_1}{\sigma_2} \right)^2 \frac{d}{d\tau_1} + \alpha_{21}(\omega) \right) \hat{f}_2(\omega, \tau_1) = \beta_{12} \hat{f}_1(\omega, \tau_1) \quad (4.16.22)$$

with boundary conditions:

$$\begin{cases} \hat{f}_2(x, 0) \equiv \hat{f}_0 = \mathcal{F}(e^x(1 - e^x))^+ = \int_{-\infty}^{\infty} (e^x(1 - e^x))e^{-i\omega x} dx = \frac{1}{(1 - i\omega)(2 - i\omega)}, \\ \left(\frac{\sigma_1}{\sigma_2} \right)^2 \frac{d\hat{f}_2}{d\tau_1} \Big|_{\tau_1=0} + \alpha_{21}(\omega) \hat{f}_0 = \beta_{21} \hat{f}_0 \end{cases}$$

with $\alpha_{mn}(\omega) = \omega^2 - i\omega(\gamma_m - 3) + (2\gamma_m + \beta_{mn} - 2)$, $m, n = 1, 2$, $m \neq n$, $\gamma_m = \frac{2r}{\sigma_m^2}$

and $\beta_{mn} \equiv \frac{2\lambda_{mn}}{\sigma_m^2}$, $m, n = 1, 2$ for $m \neq n$.

The solution of the first-order system of linear ordinary differential equations is given respectively by:

$$\begin{cases} \hat{f}_1(\omega, \tau_1) = \hat{f}_0 \left(\frac{[\beta_{12} - k_2 - \alpha_{12}(\omega)]e^{k_1\tau_1} - [\beta_{12} - k_1 - \alpha_{12}(\omega)]e^{k_2\tau_1}}{k_1 - k_2} \right), & k_1 \neq k_2, \\ \hat{f}_2(\omega, \tau_2) = \hat{f}_0 \left(\frac{[\beta_{21} - \Phi k_2 - \alpha_{21}(\omega)]e^{\Phi k_1\tau_2} - [\beta_{21} - \Phi k_1 - \alpha_{21}(\omega)]e^{\Phi k_2\tau_2}}{(k_1 - k_2)\Phi} \right), & k_1 \neq k_2 \end{cases}$$

where $\Phi = \left(\frac{\sigma_1}{\sigma_2} \right)^2$, and $\hat{f}_0 = \mathcal{F}(e^x(1 - e^x))^+ = \int_{-\infty}^{\infty} (e^x(1 - e^x))e^{-i\omega x} dx = \frac{1}{(1 - i\omega)(2 - i\omega)}$,

$$k_{1,2} = -\frac{\alpha_{12}(\omega)}{2} - \frac{\alpha_{21}(\omega)}{2\Phi} \pm \frac{\sqrt{[\Phi\alpha_{12}(\omega) - \alpha_{21}(\omega)]^2 + 4\Phi\beta_{21}\beta_{12}}}{2\Phi}$$

From equation (4.16.20), using the property of inverse Fourier transformation which is required to recover the options value, we have:

$$f_m(x, \tau_m) = \mathcal{F}^{-1} \left(\mathcal{F}(f_m(x, \tau_m)) \right) = \frac{1}{2\pi} \int_{-\infty}^{\infty} \hat{f}_m(\omega, \tau_m) e^{-i\omega x} d\omega, \quad m = 1, 2 \quad (4.16.23)$$

The equation (4.16.23) is the solution of the transformed ODEs presented for the option prices which incorporated moving boundary condition for American options valuation in this case. The numerical value of the options prices are now computed using FFT algorithm with the focus on determining the appropriate values of grid point for obtaining a better performance of options returns. However, an American options require the determination of the appropriate time to exercise the option. So we invoke optimal stopping problem formulation into FFT algorithm in Carr & Madan, (1999).

Definition 4.16.1. A stopping time, t^* , can be well-thought-out as a function taking value in an interval $[0, T]$ such that the decision to stop at a time t^* is determined based on the information available concerning the asset's price path say S_u , $0 \leq u \leq t^*$.

Remark 4.16.4. It is remarkable to point out here that an analytic solution for European option valuation to a related ODEs problem was presented by Song-Ping et al, (2012). However, we consider more variables in our formulation and the boundary conditions considered are more for American options.

4.17 Numerical Results

This section shows numerical approximations of American call options valued using FFT and compare with analytic Black - Scholes model prices. The analytic Black-Scholes payoffs were taken as the benchmark for comparing the payoffs of the option at various grid points for fast Fourier transform prices (FFT). Considering the flexibility of American style options that permits early exercise, we express the

American Fourier prices as the sum of early exercise premium and European Fourier prices using FFT algorithm of Carr & Madan (1999) to handle the European Fourier prices. Let the value of American option V_{Amer} be expressed as the addition of European option $V_{Eur}(T)$ and the Early exercise premium price $P(t)$. This we give as:

$$V_{Amer} = V_{Eur}(T) + P_t, \quad (4.17.1)$$

where $\lim_{t \rightarrow T} P(t) \rightarrow 0$.

4.17.1 American call Option Payoffs with Dividend

Consider a stock with an initial price $S_0 = 110$, Strike price $K = 100$, Risk-neutral interest rate $r = 0.05$, Dividend rate $q = 0.03$, Time to Maturity, $T = 4$ years, Volatility $\sigma = 0.35$, Integrability Parameter $\alpha = 3$, Fineness of integration grid point $N = 2^n, n = 1, 2, 3, \dots, 15$. *The above specified basic parameters values were used to generate the simulation results in the following tables 4.4 - 4.7 in addition to the specified grid points in each case.*

Table 4.4: A dividend paying American call Option prices under variant Grid points

FFT Grid Points	BSM Price	FFT Price	Metrics BSM-FFT
2^1	33.12906368	59.1502292543738	26.021165574
2^2	33.12906368	35.3173716785242	2.188307999
2^3	33.12906368	33.1303231018313	0.001259422
2^4	33.12906368	33.1253535065033	0.003710173
2^5	33.12906368	33.1253534977647	0.003710182
2^6	33.12906368	33.1253532564758	0.003710424
2^7	33.12906368	33.1303231018313	0.001259422
2^8	33.12906368	33.1253535065033	0.003710173
2^9	33.12906368	33.1253534977647	0.003710182
2^{10}	33.12906368	33.1253532564758	0.00371042
2^{11}	33.12906368	33.1253532564758	0.00371042
2^{12}	33.12906368	33.1303231018313	0.001259428
2^{13}	33.12906368	33.1253535065033	0.003710173
2^{14}	33.12906368	33.1253534977647	0.003710182
2^{15}	33.12906368	33.1253532564758	0.003710424

Source: Author's simulation result analysis 1 via Maple 2017

The table 4.4 shows the simulation results for an American call option price comparison with analytic Black-Scholes model (BSM) and Fast-Fourier-Transform (FFT) method. For the FFT-price, it was observed that the options price at grid point, $N = 2^1, 2^2$ were far huge than the benchmark price set as the BSM analytic method. The metrics BSM-FFT column shows the detail. However, FFT-price for the American option converges to a neighbourhood of the desirable benchmark prices (BSM) from grid points N^3 to N^{16} .

Table 4.5: The Option prices comparison at specified grid points for FFT method with BSM price as the benchmark price.

S_0	Strike Price K	BSM Price	FFT @ $N = 2$	FFT @ $N = 2^3$	FFT @ $N = 2^5$
100	80	26.0367509	21.9482362226	26.0827767722	26.03618568596
100	90	19.89044278	15.9805352839	19.6997354115	19.89002174025
100	100	14.91294422	11.8010959959	14.6431003793	14.91262066770
100	110	11.01054502	8.84160136154	10.7817092149	11.01029009354

Source: Author's simulation result analysis 2 using Maple 2017

The Table 4.5 above shows numerical values of the American call option payoff at various grid points for FFT in comparison with analytic Black - Scholes Model (BSM). For rate of return $r = 0.02$, Volatility rate $\sigma = 0.35$, dividend rate $q = 0.02$, Time $t = 1$ year, Integrability parameter $\alpha = 2.5$. The FFT-prices at grid point, $N = 2$, was far less than the corresponding benchmark prices (BSM). However, for $N = 2^3$, the FFT-prices get better while compared to the analytic Black-Scholes model prices (BSM). The best result was achieved for the FFT method at grid point set to $N = 2^5$ as the prices obtained were almost surely converged to the targeted benchmark prices (BSM).

Table 4.6: The Option prices at various grid points using integrability parameter $\alpha = 4.9$

N	S_0	K	BSM Price	FFT Price	T year(s)
2^6	100	80	22.91724060	22.9172404308017	0.5
2^{10}	100	80	22.91724060	22.9172405529068	0.5
2^{18}	100	80	22.91724060	22.9172404308017	0.5
2^6	100	80	26.03675091	26.0367506722856	1
2^{10}	100	80	26.03675091	26.0367508524346	1
2^{18}	100	80	26.03675091	26.0367506722856	1
2^6	100	80	30.8593226612	30.8593226612457	2
2^{10}	100	80	30.8593226612	30.8593229199321	2
2^{18}	100	80	30.8593226612	30.8593226612457	2

Source: Author's simulation result analysis 3 via Maple 2017

In the Table 4.6 above, we show the payoffs of American call options choosing a higher integrability parameter $\alpha = 4.9$ for the FFT method, initial asset price $S_0 = 100$, Strike price $K = 80$, risk-neutral rate of return $r = 0.05$, the dividend rate $q = 0.02$, volatility rate $\sigma = 0.35$, grid points $N = 2^n$, $n = 6, 10, 18$, exercising time $T = 0.5, 1, 2$ years. At the three specified grid points, the options price obtained via the FFT-method were very close to that of the BSM for each maturity time. The major observation is that the longer the lifespan of options in the market, the better the options returns. This is synonymous to an anticipating returns of lower risk investments with compounding interest strategy. However, for risky assets such as stocks especially under the exposure of uncertainties not exempting recession, the anticipating investment payoff may not be profitable.

Table 4.7: The Option prices at various grid points using integrability parameter $\alpha = 2.5$

N	S_0	K	BSM Price	FFT Price	T year(s)
2^6	100	80	22.91724060	22.9166697933614	0.5
2^{10}	100	80	22.91724060	22.9166697809921	0.5
2^{19}	100	80	22.91724060	22.9166697859229	0.5
2^6	100	80	26.03675091	26.0361856517776	1
2^{10}	100	80	26.03675091	26.0361856791478	1
2^{19}	100	80	26.03675091	26.0361856433266	1
2^6	100	80	30.85932482	30.8587705200271	2
2^{10}	100	80	30.85932482	30.8587705976372	2
2^{19}	100	80	30.85932482	30.8587705100108	2

Source: Author's simulation result analysis 4 via Maple 2017

In the table 4.7 above, we show the payoffs of American call options choosing an integrability parameter $\alpha = 2.5$ for the FFT method subject to the same values of the parameters used in the table 4.6 above. Taking initial asset price $S_0 = 100$, the strike price $K = 80$, the options rate of return $r = 0.05$, dividend rate $q = 0.02$, volatility rate $\sigma = 0.35$, grid points $N = 2^n, n = 6, 10, 18,$ time $t = 0.5, 1, 2$ years.

Remark 4.17.1. We compared the performance of using a higher integrability parameter $\alpha = 4.9$ to $\alpha = 2.5$ for Option prices. The numerical results presented in the tables (4.4) - (4.7) shows that integrability parameter $\alpha = 4.9$ outperformed that of $\alpha = 2.5$ for the FFT method in this study. However, the value assigned to the parameter, *alpha*, usually depends on the nature of the model.

4.17.2 Non-dividend paying American call Option Payoffs

In the Table 4.8 in the following page, we show the payoffs for a non-dividend paying American call options choosing a higher integrability parameter $\alpha = 4.9$ for the FFT method, initial Asset price $S_0 = 100$, the Strike price $K = 80$, options rate of return $r = 0.05$, volatility rate $\sigma = 0.35$, grid points $N = 2^n$, $n = 6, 10, 18$, time $t = 0.5, 1, 2$ years.

Table 4.8: The Option prices at various grid points using integrability parameter $\alpha = 2.5$

N	S_0	K	BSM Price	FFT Price	T year(s)
2^6	100	80	23.77859595	23.778595756644	0.5
2^{10}	100	80	23.77859595	23.7785958869413	0.5
2^{18}	100	80	23.77859595	23.7785957489258	0.5
2^6	100	80	27.66637407	27.6663737994014	1
2^{10}	100	80	27.66637407	27.6663739954822	1
2^{18}	100	80	27.66637407	27.6663737904213	1
2^6	100	80	34.01615097	34.0161469197921	2
2^{10}	100	80	34.01615097	34.0161472109604	2
2^{18}	100	80	34.01615097	34.0161469087509	2

Source: Author's simulation result analysis 5 via Maple 2017

The table 4.8 is a non-dividend paying version of the American call option presented in the table 4.6. The major observation in the two results is that the non-dividend paying option prices were more than that of the dividend-paying version. This result of course is economically feasible as a non-dividend paying investment is more profitable to the holder than dividend paying type. However, in the table 4.8 above, the two methods (that is, BSM and FFT) gave almost surely same options payoffs.

4.18 The Result 3 Analysis

We compared the performance of using a higher integrability parameter $\alpha = 4.9$ to $\alpha = 2.5$ for the Option prices. It is observed that the numerical results presented in the tables (4.4) - (4.7) with integrability parameter $\alpha = 4.9$ outperformed that of $\alpha = 2.5$ for the FFT method in this study. Hence, models performance in the sense of FFT for some models requires a careful selection of the fineness of integrability parameter to achieve better option prices.

4.19 Conclusion

As the fineness of the grid increases, the aliasing error in the return of the option prices decreases. In other words, increase in the fineness of the grid points for FFT enhances the convergence of the prices of the options or the underlying assets prices. From the above table, we obtained more accurate option value at lower grid point of $N = 2^3$ in comparison with Analytical payoff by the BSM. At very lower grid points below 2^3 , the payoff were not comparable with the BSM as the values of the option were so high. Hence, in a market where the BSM is the bench mark for option price evaluation, to alternatively compute option prices via FFT, the fineness of the grid parameter should be controlled to compute option values at grid points greater than or equal to 8. However, it is advisable to consider a grid point value up to $N = 4096$ for an optimal comparable result with other widely used analytical solution via Black - Scholes model. Finally, the fast Fourier transform method has been commended to have the capability of increasing the speed of options' computation as reported in many literature on Fourier transform of options prices in comparison with most other methods.

RESULT 4

A Control Regime - Switching Triple Stochastic Volatility Heston-like model for Options valuation in a Recessed Economy

4.20 An Overview of the Result 4

A control regime-switching triple stochastic volatility Heston-like (TSVH) model is proposed for options valuation in a recessed economy. The model description involves inclusion of an economy recession induced volatility process driven by its own Stochastic Differential Equation (SDE) with respect to Double Heston model. The third volatility process is considered necessary when there is transition of an economy from the state of *normalcy* to *recession* state. Mathematical formulation and rigorous solution of the proposed triple stochastic volatility Heston-like model is presented and solved. Some numerical simulations are carried out to compare volatility smile during recession period and that of Double Heston model during state of normalcy. The triple Stochastic volatility Heston-like model was able to capture volatility smile posed by recession factor on the Double Heston model. A new option pricing model emerged and capable of capturing extra volatility smile during economy recession on Options. Numerical results were presented to compare the effectiveness and reliability of the model to the existing ones. The results confirm that the proposed model is effective and reliable.

4.21 STUDY TEN

The TSVH model

4.21.1 Introduction

The result presented in this part of the thesis shows a new intuition to double Heston model while pricing an options in a recessed economy. The proposed model as we shall see shortly allow an inclusion of a recession induced volatility driven by its own stochastic differential equation to the double Heston model. A binary control parameter was introduced such that one can switch between the original double

Heston model proposed by Christoffersen et al., (2009) and the TSVH- model we proposed here in terms of economy recession induced volatility. However, our stated objectives (vii), (viii) and (ix) in the Chapter 1 of this thesis were achieved under this Result 4 as we shall see in the sequel.

4.21.2 Preliminaries to the model formulation

There are standard options pricing models which are considered better in comparison with the classical Black-Scholes model in terms of generating volatility smile. The reason is that Black - Scholes model lacks some reality structures. Among the well known stochastic models used in finance, Heston model is one used for pricing options. The model can be calibrated utilising the prices of vanilla option and thereafter used in exotic derivatives pricing. Another stochastic volatility model among others considered better, an extension of the univariate version of the Heston stochastic volatility model (Heston, 1993) is *Double Heston model* (Christoffersen et al., 2009). The double Heston model was proposed by Christoffersen et al. in which a second source of variance was introduced to the univariate version of Heston model 1993 driven by its own Stochastic Differential Equation (SDE). The set of the SDEs emerged are given in what follows:

$$\left\{ \begin{array}{l} \frac{dS(t)}{S(t)} = (r - q)dt + \sqrt{v_1(t)}dW_1(t) + \sqrt{v_2(t)}dW_2(t), \quad S(0) = S_0 > 0 \\ \\ dv_1(t) = \kappa_1(\theta_1 - v_1(t))dt + \sigma_1\sqrt{v_1(t)}d\widehat{W}_1(t), \quad v_1(0) = v_{1_0} > 0. \\ \\ dv_2(t) = \kappa_2(\theta_2 - v_2(t))dt + \sigma_2\sqrt{v_2(t)}d\widehat{W}_2(t), \quad v_2(0) = v_{2_0} > 0. \end{array} \right. \quad (4.21.1)$$

subject to the following stochastic correlation structure:

$$\begin{aligned} \text{cor}(dW_1, dW_2)_t &= \text{cor}(dW_1, d\widehat{W}_2)_t = \text{cor}(dW_2, d\widehat{W}_1)_t = \text{cor}(d\widehat{W}_1, d\widehat{W}_2)_t = 0 \\ \text{cor}(dW_1, d\widehat{W}_1)_t &= \rho_1 dt \\ \text{cor}(dW_2, d\widehat{W}_2)_t &= \rho_2 dt. \end{aligned}$$

The parameters in the above model have the following names: r is the *interest rate*, q is the *dividend rate*, $\kappa_j, j = 1, 2$ are the *mean reverting rate*, $\theta_j, j = 1, 2$ are the *volatility of variance (vol of vol) constant*.

4.21.3 The control regime-switching Triple Stochastic Volatility Heston-like (TSVH) model formulation

Consider an unstable economy which could change from one state to the other. Suppose the Economy can only switch between two states: that is, State of *normalcy* and state of *recession*. During recession, the uncertainty level of financial security is inevitable to be on the high side, especially stock assets. Suppose further that economy recession induces another source of volatility uncertainty on a stock market in a recessed economy in addition to two other sources of volatility emphasised in the double Heston model, such that the economy recession induced volatility process is driven by its own Stochastic Differential Equation. One major point to note is that an assumption of constant volatility is not suitable in an ideal real life situation battling with uncertainty. However, the fluctuations in stock prices during recession is on the high side compared to recession-free period. In order to account for stochastic volatility during the period of recession, or applying the double Heston model in the valuation of options in a recessed economy compels us to come up with an intuition for proposing the three stochastic volatility processes here. Consequently, an options pricing in a recessed double Heston world is proposed to be referred to as “ a control regime-switching Triple Stochastic Volatility Heston-like model (TSVH)” in this thesis.

The proposed (TSVH) model is presented as:

$$\left\{ \begin{array}{l} \frac{dS(t)}{S(t)} = (r - q)dt + \sqrt{v_1(t)}dW_1(t) + \sqrt{v_2(t)}dW_2(t) + \alpha(\sqrt{v_3(t)}dW_3(t)), \quad S(0) = S_0 > 0 \\ \\ dv_1(t) = \kappa_1(\theta_1 - v_1(t))dt + \sigma_1\sqrt{v_1(t)}d\widehat{W}_1(t), \quad v_1(0) = v_{10} > 0. \\ \\ dv_2(t) = \kappa_2(\theta_2 - v_2(t))dt + \sigma_2\sqrt{v_2(t)}d\widehat{W}_2(t), \quad v_2(0) = v_{20} > 0. \\ \\ dv_3(t) = \alpha\left(\kappa_3(\theta_3 - v_3(t))dt + \sigma_3\sqrt{v_3(t)}d\widehat{W}_3(t)\right)_{recession}, \quad v_3(0) = v_{30} > 0 \end{array} \right. \quad (4.21.2)$$

where α is a binary control parameter defined as:

$$\alpha := \begin{cases} 0, & \text{if the economy is not in recession;} \\ 1, & \text{if the economy is in recession.} \end{cases}$$

used to switch between the double Heston and the proposed Triple Stochastic Volatility (TSVH) model depending on the state of the Economy. This is so in order to ensure the model is applicable in any state of the economy.

The control parameter is considered useful as it ensures that the TSVH - model will still be relevant to options valuation when the economy recession vanishes by setting the control parameter to zero (0). If this happens, then we have the double Heston model presented in (4.21.1).

$S(t)$ is the underlying asset at time t , r is the interest rate, dividend rate, q , the first two volatilities, v_1, v_2 have their bearing from the double Heston model while v_3 emerged from economy recession induced volatility process, $\kappa_1, \kappa_2, \kappa_3$ are mean reverting rates for the three volatility processes respectively, $\theta_1, \theta_2, \theta_3$ are long term volatility constants and $\sigma_1, \sigma_2, \sigma_3$ are *volatility of variance (vol of vol)* constants

which are all positive. The constant θ_3 is assumed to be less than θ_1 , and θ_2 since there is possibility of an economy taking a shorter period to recover from recession. The Wiener process, W_3 , describes the Brownian movement in the stock prices emanating during the period of recession while W_1 and W_2 originated from the Double Heston model. The remaining Wiener processes $\widehat{W}_j, j = 1, 2, 3$, shows the stochastic movement of the stock volatilities from the three sources.

The model is subjected to the following stochastic correlation structure:

$$\left\{ \begin{array}{l} \text{cor}(dW_1, dW_2)_t = \text{cor}(dW_1, dW_3)_t = \text{cor}(dW_2, dW_3)_t = 0 \\ \text{cor}(dW_1, d\widehat{W}_2)_t = \text{cor}(dW_2, d\widehat{W}_1)_t = \text{cor}(d\widehat{W}_1, d\widehat{W}_2)_t = 0 \\ \text{cor}(dW_1, d\widehat{W}_3)_t = \text{cor}(dW_2, d\widehat{W}_3)_t = \text{cor}(d\widehat{W}_1, d\widehat{W}_3)_t = \text{cor}(d\widehat{W}_2, d\widehat{W}_3)_t = 0 \\ \text{cor}(dW_1, d\widehat{W}_1)_t = \rho_1 dt \\ \text{cor}(dW_2, d\widehat{W}_2)_t = \rho_2 dt \\ \text{cor}(dW_3, d\widehat{W}_3)_t = \rho_3 dt. \end{array} \right. \quad (4.21.3)$$

Remark 4.21.1. The inclusion of the third volatility process emanated from economy recession factor which results in three different correlations as given in the above model.

4.22 Options computation in the control regime-switching Triple Stochastic Volatility Heston-like model (TSVH)

It is possible to derive the partial differential equation (PDE) form of the proposed Triple Stochastic Volatility (TSVH) model. In order to do this, we consider the application of Ito's lemma to the logarithm stock price say $y_t = \log S_t$.

Hence, the model presented in equation (4.21.2) is therefore restated as:

$$\left\{ \begin{array}{l} dy_t = (r - q)dt + \sqrt{v_1(t)}dW_1(t) + \sqrt{v_2(t)}dW_2(t) + \alpha(\sqrt{v_3(t)}dW_3(t)), \quad S(0) = S_0 > 0 \\ dv_1(t) = \kappa_1(\theta_1 - v_1(t))dt + \sigma_1\sqrt{v_1(t)}d\widehat{W}_1(t), \quad v_1(0) = v_{1_0} > 0. \\ dv_2(t) = \kappa_2(\theta_2 - v_2(t))dt + \sigma_2\sqrt{v_2(t)}d\widehat{W}_2(t), \quad v_2(0) = v_{2_0} > 0. \\ dv_3(t) = \alpha\left(\kappa_3(\theta_3 - v_3(t))dt + \sigma_3\sqrt{v_3(t)}d\widehat{W}_3(t)\right), \quad v_3(0) = v_{3_0} > 0 \end{array} \right. \quad (4.22.1)$$

Following Rouah (2013) and Zhao (2016) in the Double Heston model, we made the following parametrization for the Wiener processes in our TSVH model.

Letting

$$\left\{ \begin{array}{l} W_1 = Z_1 \\ W_2 = Z_2 \\ W_3 = Z_3 \\ W_1 = \rho_1\widehat{W}_1(t) + \sqrt{1 - \rho_1^2}Z_1(t) \\ W_2 = \rho_2\widehat{W}_2(t) + \sqrt{1 - \rho_2^2}Z_2(t) \\ W_3 = \rho_3\widehat{W}_3(t) + \sqrt{1 - \rho_3^2}Z_3(t) \end{array} \right. \quad (4.22.2)$$

where each $\widehat{W}_j, j = 1, 2, 3$ and each $Z_j, j = 1, 2, 3$ are Brownian motions which evolve independently. We wish to write the system of SDEs for the process $y_t = (y, v_1, v_2, v_3)$ in the model (4.22.1).

Suppose the process y_t is an n -dimensional stochastic process written in the form:

$$dy_t = \mu(y_t, t) + \sigma(y_t, t)dZ_t \quad (4.22.3)$$

where Z_t is a Q - Brownian motion of dimension m , y_t and $\mu(y_t, t)$ are taken to be n -dimensional vectors respectively and $\sigma(y_t, t)$ is a volatility matrix of size $n \times m$.

Then, we write equation (4.22.3) in the form:

$$\begin{bmatrix} dy_1(t) \\ \vdots \\ dy_n(t) \end{bmatrix} = \begin{bmatrix} \mu_1(y_1, t) \\ \vdots \\ \mu(y_n, t) \end{bmatrix} dt + \begin{bmatrix} \sigma_{11}(y_t, t) & \dots & \sigma_{1m}(y_t, t) \\ \vdots & \ddots & \vdots \\ \sigma_{n1}(y_t, t) & \dots & \sigma_{nm}(y_t, t) \end{bmatrix} \begin{bmatrix} dZ_1(t) \\ \vdots \\ dZ_m(t) \end{bmatrix} \quad (4.22.4)$$

In an attempt to solve the TSVH-model presented in equation (4.22.1), we first give the matrix representation of the drift and volatility terms in sequel.

The drift term is given as:

$$\mu = \begin{pmatrix} r - q - \frac{1}{2}(v_1 + v_2 + v_3) \\ \kappa_1(\theta_1 - v_1) \\ \kappa_2(\theta_2 - v_2) \\ \alpha\kappa_3(\theta_3 - v_3) \end{pmatrix} \quad (4.22.5)$$

and the volatility,

$$\sigma(y_t, t) = \begin{pmatrix} \sqrt{v_1} & \sqrt{v_2} & \sqrt{v_3} & 0 & 0 & 0 \\ \sigma_1\sqrt{v_1}\rho_1 & 0 & 0 & \sigma_1\sqrt{v_1(1-\rho_1^2)} & 0 & 0 \\ 0 & \sigma_2\sqrt{v_2}\rho_1 & 0 & 0 & \sigma_2\sqrt{v_2(1-\rho_2^2)} & 0 \\ 0 & 0 & \alpha\sigma_3\sqrt{v_3}\rho_3 & 0 & 0 & \alpha\sigma_3\sqrt{v_3(1-\rho_3^2)} \end{pmatrix} \quad (4.22.6)$$

The transpose matrix σ^T of the above volatility processes is given as:

$$\sigma^T(y_t, t) = \begin{pmatrix} \sqrt{v_1} & \sigma_1 \sqrt{v_1} \rho_1 & 0 & 0 \\ \sqrt{v_2} & 0 & \sigma_2 \sqrt{v_2} \rho_1 & 0 \\ \sqrt{v_3} & 0 & 0 & \sigma_3 \sqrt{v_3} \rho_3 \\ 0 & \sigma_1 \sqrt{v_1(1 - \rho_1^2)} & 0 & 0 \\ 0 & 0 & \sigma_2 \sqrt{v_2(1 - \rho_2^2)} & 0 \\ 0 & 0 & 0 & \alpha \sigma_3 \sqrt{v_3(1 - \rho_3^2)} \end{pmatrix} \quad (4.22.7)$$

The product of the volatility matrices in equations (4.22.6) and (4.22.7) gives the volatility matrix below:

$$\sigma \sigma^T = \begin{pmatrix} v_1 + v_2 + v_3 & \sigma_1 v_1 \rho_1 & \sigma_2 v_2 \rho_2 & \sigma_3 v_3 \rho_3 \\ \sigma_1 v_1 \rho_1 & \sigma_1^2 v_1 & 0 & 0 \\ \sigma_2 v_2 \rho_2 & 0 & \sigma_2^2 v_2 & 0 \\ \alpha^2 \sigma_3 v_3 \rho_3 & 0 & 0 & \alpha^2 \sigma_3^2 v_3 \end{pmatrix} \quad (4.22.8)$$

The volatility matrix (4.23.1) makes the coefficients of terms associated with a partial differential equation formulation for the Triple stochastic volatility Heston-like (TSVH) model easy to see. This we shall see in the next section.

4.23 A control regime-switching Triple Stochastic Volatility Heston-like model (TSVH) PDE form

Let $f(y_t, v_1, v_2, v_3)$ be a twice continuously differentiable function with respect to Itô's Calculus. Assume further that the $f(y_t, v_1, v_2, v_3)$ satisfies the TSVH model in equation (4.22.1), then the partial differential equation PDE representation is given as:

$$\begin{aligned} \frac{\partial f}{\partial t} = & \frac{1}{2}(v_1 + v_2 + v_3) \frac{\partial^2 f}{\partial y^2} + \left(r - q - \frac{1}{2}(v_1 + v_2 + v_3) \frac{\partial f}{\partial y} \right) + \frac{1}{2} \sigma_1^2 v_1 \frac{\partial^2 f}{\partial v_1^2} \\ & + \frac{1}{2} \sigma_2^2 v_2 \frac{\partial^2 f}{\partial v_2^2} + \frac{1}{2} \sigma_3^2 v_3 \frac{\partial^2 f}{\partial v_3^2} + \rho_1 \sigma_1 v_1 \frac{\partial^2 f}{\partial y \partial v_1} + \rho_2 \sigma_2 v_2 \frac{\partial^2 f}{\partial y \partial v_2} + \rho_3 \sigma_3 v_3 \frac{\partial^2 f}{\partial y \partial v_3} \\ & + \kappa_1(\theta_1 - v_1) \frac{\partial f}{\partial v_1} + \kappa_2(\theta_2 - v_2) \frac{\partial f}{\partial v_2} + \kappa_3(\theta_3 - v_3) \frac{\partial f}{\partial v_3} \end{aligned} \quad (4.23.1)$$

From equations (4.16.15)-(4.16.21), we restated Feynman-Kac formula for TSVH-model as follow.

Theorem 4.23.1. (*Feynman-Kac formula*)

Let $f(y, t)$ be C^2 - differentiable function with respect to some Itô diffusion processes. Then the partial differential equation of $f(y, t)$ is given by:

$$\frac{\partial f}{\partial t} + \mathcal{G}f(y, t) - r(y, t) = 0 \quad (4.23.2)$$

subject to the boundary condition (f_τ, τ) . The solution is given in the form:

$$f(y_t, t) = \mathbb{E}_Q \left[\exp \left(\int_t^\tau r(y_u, u) du \right) f(y_\tau, \tau) \middle| \mathcal{F}_t \right]$$

where \mathcal{F}_t is the filtration up to time t .

\mathcal{G} is an *infinitesimal generator* of the TSVH-model partial differential equation form defined by:

$$\mathcal{G} := \sum_{i=1}^n \mu_i \frac{\partial}{\partial y_i} + \frac{1}{2} \sum_{i=1}^n \sum_{j=1}^n (\sigma \sigma^T)_{ij} \frac{\partial^2}{\partial y_i \partial y_j} \quad (4.23.3)$$

with $y = \ln S(t)$, μ and $(\sigma \sigma^T)$ remains as defined in equations (4.22.5) and (4.23.1) above.

This implies that \mathcal{G} could generate the right hand side of the TSVH pde and thus, equation (4.23.1) is equivalently stated as:

$$\frac{\partial f}{\partial t} = \mathcal{G}_{y_t, v_1(t), v_2(t), v_3(t)} f \quad (4.23.4)$$

subject to terminal condition, $f(\omega, 0, y) = \exp(i\omega y)$

with

$$\begin{aligned} \mathcal{G}_{y_t, v_1(t), v_2(t), v_3(t)} f = & \frac{1}{2}(v_1 + v_2 + v_3) \frac{\partial^2 f}{\partial y^2} + \left(r - q - \frac{1}{2}(v_1 + v_2 + v_3) \frac{\partial f}{\partial y} \right) + \frac{1}{2} \sigma_1^2 v_1 \frac{\partial^2 f}{\partial v_1^2} \\ & + \frac{1}{2} \sigma_2^2 v_2 \frac{\partial^2 f}{\partial v_2^2} + \frac{1}{2} \sigma_3^2 v_3 \frac{\partial^2 f}{\partial v_3^2} + \rho_1 \sigma_1 v_1 \frac{\partial^2 f}{\partial y \partial v_1} + \rho_2 \sigma_2 v_2 \frac{\partial^2 f}{\partial y \partial v_2} + \rho_3 \sigma_3 v_3 \frac{\partial^2 f}{\partial y \partial v_3} \\ & + \kappa_1 (\theta_1 - v_1) \frac{\partial f}{\partial v_1} + \kappa_2 (\theta_2 - v_2) \frac{\partial f}{\partial v_2} + \kappa_3 (\theta_3 - v_3) \frac{\partial f}{\partial v_3} \end{aligned} \quad (4.23.5)$$

4.24 Characteristic function derivation for the TSVH model

The TSVH-model is affine in nature. On the application of Duffie et al., (2000) result, we gave the characteristic function $f(\omega_0, \omega_1, \omega_2, \omega_3; y_t, v_1(t), v_2(t), v_3(t))$ for

$(y_T, v_1(T), v_2(T), v_3(T))$ in log linear form as:

$$\begin{aligned} f(\omega_0, \omega_1, \omega_2, \omega_3; y_t, v_1(t), v_2(t), v_3(t)) &= \mathbb{E} \left(e^{i\omega_0 y_t + i\omega_1 v_1(t) + i\omega_2 v_2(t) + i\omega_3 v_3(t)} \right) \\ &= e^{(A(\tau, \omega) + B_0(\tau, \omega) y_t + B_1(\tau, \omega) v_1(t) + B_2(\tau, \omega) v_2(t) + B_3(\tau, \omega) v_3(t))} \end{aligned} \quad (4.24.1)$$

where $A, B_0, B_1, B_2,$ and B_3 are coefficients terms of the stochastic processes;

$y_t, v_1(t), v_2(t), v_3(t)$ which depends on the time to expiry $\tau = T - t$ and each $\omega_i, i = 0, 1, \dots, 3$.

Duffie et al., (2000) has also established the fact that characteristic function could be given as a system of Ricatti equations which many authors such as: Rouah (2013) and Zhao, (2016); to mention but few, used in the recent time in their research studies.

Thus, the system of Ricatti equations (differential) for our TSVH model is given as:

$$\left\{ \begin{array}{l} \frac{\partial B_0}{\partial t} = -\mathbf{J}_1^T \beta - \frac{1}{2} \beta^T \mathbf{H}_1 \beta \\ \frac{\partial B_1}{\partial t} = -\mathbf{J}_2^T \beta - \frac{1}{2} \beta^T \mathbf{H}_2 \beta \\ \frac{\partial B_2}{\partial t} = -\mathbf{J}_3^T \beta - \frac{1}{2} \beta^T \mathbf{H}_3 \beta \\ \frac{\partial B_3}{\partial t} = -\mathbf{J}_4^T \beta - \frac{1}{2} \beta^T \mathbf{H}_4 \beta \\ \frac{\partial A}{\partial t} = -\mathbf{J}_0^T \beta - \frac{1}{2} \beta^T \mathbf{H}_0 \beta \end{array} \right. \quad (4.24.2)$$

where $\beta^T := (B_0, B_1, B_2, B_3)$ and the boundary conditions to the above Ricatti

equations are given as:

$$\left\{ \begin{array}{l} B_0(0) = i\omega_0 \\ B_1(0) = i\omega_1 \\ B_2(0) = i\omega_2 \\ B_3(0) = i\omega_3 \\ A(0) = 0 \end{array} \right. \quad (4.24.3)$$

The coefficient matrices terms \mathbf{J}_i , \mathbf{H}_i , $i = 1, 2, \dots, 4$ emanated from the drift term $\mu(y_t)$ and σ^T in equations (4.22.5) and (4.23.1) respectively.

The values are given as:

$$\mathbf{J}_0 = \begin{pmatrix} r - q \\ \kappa_1\theta_1 \\ \kappa_2\theta_2 \\ \kappa_3\theta_3 \end{pmatrix}, \quad \mathbf{J}_1 = \begin{pmatrix} 0 \\ 0 \\ 0 \\ 0 \end{pmatrix}, \quad \mathbf{J}_2 = \begin{pmatrix} -\frac{1}{2} \\ -\kappa_1 \\ 0 \\ 0 \end{pmatrix}, \quad \mathbf{J}_3 = \begin{pmatrix} -\frac{1}{2} \\ 0 \\ -\kappa_2 \\ 0 \end{pmatrix}, \quad \mathbf{J}_4 = \begin{pmatrix} -\frac{1}{2} \\ 0 \\ 0 \\ -\kappa_3 \end{pmatrix}$$

satisfying

$$\mu = \mathbf{J}_0 + \mathbf{J}_1 y + \mathbf{J}_2 v_1 + \mathbf{J}_3 v_2 + \mathbf{J}_4 v_3 \quad (4.24.4)$$

while

$$\mathbf{H}_0 = \mathbf{H}_1 = \begin{pmatrix} 0 & 0 & 0 & 0 \\ 0 & 0 & 0 & 0 \\ 0 & 0 & 0 & 0 \\ 0 & 0 & 0 & 0 \end{pmatrix}, \quad \mathbf{H}_2 = \begin{pmatrix} 1 & \sigma_1\rho_1 & 0 & 0 \\ \sigma_1\rho_1 & \sigma_1^2 & 0 & 0 \\ 0 & 0 & 0 & 0 \\ 0 & 0 & 0 & 0 \end{pmatrix},$$

$$\mathbf{H}_3 = \begin{pmatrix} 1 & 0 & \sigma_2 \rho_2 & 0 \\ 0 & 0 & 0 & 0 \\ \sigma_2 \rho_2 & 0 & \sigma_2^2 & 0 \\ 0 & 0 & 0 & 0 \end{pmatrix}, \quad \text{and} \quad \mathbf{H}_4 = \begin{pmatrix} 1 & 0 & 0 & \sigma_3 \rho_3 \\ 0 & 0 & 0 & 0 \\ 0 & 0 & 0 & 0 \\ \sigma_3 \rho_3 & 0 & 0 & \sigma_3^3 \end{pmatrix}$$

such that

$$\sigma \sigma^T = \mathbf{H}_0 + \mathbf{H}_1 y + \mathbf{H}_2 v_1 + \mathbf{H}_3 v_2 + \mathbf{H}_4 v_3. \quad (4.24.5)$$

Next, upon the use of the boundary conditions highlighted in equation (4.24.3), the first Ricatti differential equation in (4.24.2) with respect to its own boundary condition yields a solution $B_0(\tau) = i\omega_0$.

The Ricatti differential equations in (4.24.2) are further transformed upon substituting the boundary condition for other terms and reversing the sign so as to get derivatives in form of time - to - maturity τ leads to:

$$\left\{ \begin{array}{l} \frac{\partial B_1}{\partial \tau} = \frac{1}{2} \sigma_1^2 B_1^2 - (\kappa_1 - i\omega_0 \rho_1 \sigma_1) B_1 - \frac{1}{2} \omega_0 (\omega_0 + i) \\ \frac{\partial B_2}{\partial \tau} = \frac{1}{2} \sigma_2^2 B_2^2 - (\kappa_2 - i\omega_0 \rho_2 \sigma_2) B_2 - \frac{1}{2} \omega_0 (\omega_0 + i) \\ \frac{\partial B_3}{\partial \tau} = \frac{1}{2} \sigma_3^2 B_3^2 - (\kappa_3 - i\omega_0 \rho_3 \sigma_3) B_3 - \frac{1}{2} \omega_0 (\omega_0 + i) \\ \frac{\partial A}{\partial \tau} = \kappa_1 \theta_1 B_1 + \kappa_2 \theta_2 B_2 + \kappa_3 \theta_3 B_3. \end{array} \right. \quad (4.24.6)$$

The fourth equation in the above set of transformed Ricatti differential equations only requires a straightforward integration while the first three equations are just

1-dimensional Ricatti equations. The initial conditions for (4.24.6) reduces to $B_1(0) = B_2(0) = B_3(0) = 0$ but $B_0(0) = i\omega$ as obtained earlier while $A(0) = 0$ so that we can set $\omega = \omega_0$. The decision is based on the fact that the characteristic function for the log stock price $y_T = \ln S_T$ is of paramount interest to us rather than joint characteristic function for the stochastic processes $(y_T, v_1(T), v_2(T), v_3(T))$. The solution for $B_1(\tau), B_2(\tau)$ and $B_3(\tau)$ follows the pattern of univariate and bivariate counterparts. Hence, we gave the solution of the Ricatti equations (4.24.6) for the TSVH model as:

$$\left\{ \begin{array}{l}
 A(\omega, \tau) = (r - q)\omega_1(\tau) + \frac{\kappa_1\theta_1}{\sigma_1^2} \left[(\kappa_1 - \rho_1\sigma_1\omega_1i + d_1)\tau - 2 \ln \left(\frac{1-g_1e^{d_1\tau}}{1-g_1} \right) \right] \\
 \quad + (r - q)\omega_2(\tau) + \frac{\kappa_2\theta_2}{\sigma_2^2} \left[(\kappa_2 - \rho_2\sigma_2\omega_2i + d_2)\tau - 2 \ln \left(\frac{1-g_2e^{d_2\tau}}{1-g_2} \right) \right] \\
 \quad + (r - q)\omega_3(\tau) + \frac{\kappa_3\theta_3}{\sigma_3^2} \left[(\kappa_3 - \rho_3\sigma_3\omega_3i + d_3)\tau - 2 \ln \left(\frac{1-g_3e^{d_3\tau}}{1-g_3} \right) \right] \\
 B_1(\omega, \tau) = \frac{1}{\sigma_1^2} (\kappa_1 - \rho_1\sigma_1\omega i + d_1) \left[\frac{1-g_1e^{d_1\tau}}{1-g_1} \right] \\
 B_2(\omega, \tau) = \frac{1}{\sigma_2^2} (\kappa_2 - \rho_2\sigma_2\omega i + d_2) \left[\frac{1-g_2e^{d_2\tau}}{1-g_2} \right] \\
 B_3(\omega, \tau) = \frac{1}{\sigma_3^2} (\kappa_3 - \rho_3\sigma_3\omega i + d_3) \left[\frac{1-g_3e^{d_3\tau}}{1-g_3} \right]
 \end{array} \right. \tag{4.24.7}$$

where

$$\left\{ \begin{array}{l} d_1 = \sqrt{(\kappa_1 - \rho_1 \sigma_1 \omega i)^2 + \sigma_1^2 \omega (\omega + i)} \\ d_2 = \sqrt{(\kappa_2 - \rho_2 \sigma_2 \omega i)^2 + \sigma_2^2 \omega (\omega + i)} \\ d_3 = \sqrt{(\kappa_3 - \rho_3 \sigma_3 \omega i)^2 + \sigma_3^2 \omega (\omega + i)} \\ g_1 = \frac{\kappa_1 - \rho_1 \sigma_1 \omega i - d_1}{\kappa_1 - \rho_1 \sigma_1 \omega i + d_1} \\ g_2 = \frac{\kappa_2 - \rho_2 \sigma_2 \omega i - d_2}{\kappa_2 - \rho_2 \sigma_2 \omega i + d_2} \\ g_3 = \frac{\kappa_3 - \rho_3 \sigma_3 \omega i - d_3}{\kappa_3 - \rho_3 \sigma_3 \omega i + d_3} \end{array} \right.$$

Remark 4.24.1. There is an alternate representation for the solution presented above following the suggestion of Albrecher et al., (2007) popularly known as “The Little Heston Trap” which was formulated for univariate version of Heston model. This involves replacing the positive sign attached to the term $d_j, j = 1, \dots, 3$ by negative sign. In our own case, we set $c_j = \frac{1}{g_j}$. A comparison can be made between the two approaches (Albrecher, 2007; Gauthier, and Possamaÿ, 2010).

Thus, ensuring that one has a well-behaved integrand for the proposed TSVH model demands setting $c_j = \frac{1}{g_j}$.

This gives:

$$\left\{ \begin{array}{l}
 A(\omega, \tau) = (r - q)\omega_1(\tau) + \frac{\kappa_1 \theta_1}{\sigma_1^2} \left[(\kappa_1 - \rho_1 \sigma_1 \omega_1 i - d_1)\tau - 2 \ln \left(\frac{1 - c_1 e^{-d_1 \tau}}{1 - c_1} \right) \right] \\
 \quad + (r - q)\omega_2(\tau) + \frac{\kappa_2 \theta_2}{\sigma_2^2} \left[(\kappa_2 - \rho_2 \sigma_2 \omega_2 i - d_2)\tau - 2 \ln \left(\frac{1 - c_2 e^{-d_2 \tau}}{1 - c_2} \right) \right] \\
 \quad + (r - q)\omega_3(\tau) + \frac{\kappa_3 \theta_3}{\sigma_3^2} \left[(\kappa_3 - \rho_3 \sigma_3 \omega_3 i - d_3)\tau - 2 \ln \left(\frac{1 - c_3 e^{-d_3 \tau}}{1 - c_3} \right) \right] \\
 B_1(\omega, \tau) = \frac{1}{\sigma_1^2} (\kappa_1 - \rho_1 \sigma_1 \omega_1 i + d_1) \left[\frac{1 - c_1 e^{-d_1 \tau}}{1 - c_1} \right] \\
 B_2(\omega, \tau) = \frac{1}{\sigma_2^2} (\kappa_2 - \rho_2 \sigma_2 \omega_2 i + d_2) \left[\frac{1 - c_2 e^{-d_2 \tau}}{1 - c_2} \right] \\
 B_3(\omega, \tau) = \frac{1}{\sigma_3^2} (\kappa_3 - \rho_3 \sigma_3 \omega_3 i + d_3) \left[\frac{1 - c_3 e^{-d_3 \tau}}{1 - c_3} \right]
 \end{array} \right. \tag{4.24.8}$$

where

$$\left\{ \begin{array}{l} d_1 = \sqrt{(\kappa_1 - \rho_1 \sigma_1 \omega i)^2 + \sigma_1^2 \omega (\omega + i)} \\ d_2 = \sqrt{(\kappa_2 - \rho_2 \sigma_2 \omega i)^2 + \sigma_2^2 \omega (\omega + i)} \\ d_3 = \sqrt{(\kappa_3 - \rho_3 \sigma_3 \omega i)^2 + \sigma_3^2 \omega (\omega + i)} \\ c_1 = \frac{\kappa_1 - \rho_1 \sigma_1 \omega i - d_1}{\kappa_1 - \rho_1 \sigma_1 \omega i + d_1} \\ c_2 = \frac{\kappa_2 - \rho_2 \sigma_2 \omega i - d_2}{\kappa_2 - \rho_2 \sigma_2 \omega i + d_2} \\ c_3 = \frac{\kappa_3 - \rho_3 \sigma_3 \omega i - d_3}{\kappa_3 - \rho_3 \sigma_3 \omega i + d_3} \end{array} \right.$$

The call price could be obtained once we determine the characteristic function

$$\begin{aligned} f(\omega_0, \omega_1, \omega_2, \omega_3; y_t, v_1(t), v_2(t), v_3(t)) &= \mathbb{E} \left(e^{i\omega_0 y_t + i\omega_1 v_1(t) + i\omega_2 v_2(t) + i\omega_3 v_3(t)} \right) \\ &= e^{(A(\tau, \omega) + B_0(\tau, \omega) y_t + B_1(\tau, \omega) v_1(t) + B_2(\tau, \omega) v_2(t) + B_3(\tau, \omega) v_3(t))} \end{aligned} \quad (4.24.9)$$

with respect to the information provided in equation (4.24.1).

In a similar fashion to the double Heston-model but different in terms of an additional volatility imposed due to recession, the call pricing formula is then given as:

$$C(K) = S_t e^{-q\tau} P_1 - K e^{-r\tau} P_2 \quad (4.24.10)$$

such that

$$P_1 = \frac{1}{2} + \frac{1}{\pi} \int_0^\infty \Re \left[\frac{\exp(-i\omega \ln K) f(\omega - i; y_t, v_1(t), v_2(t), v_3(t))}{i\omega S_t e^{(r-q)\tau}} \right] d\omega \quad (4.24.11)$$

$$P_2 = \frac{1}{2} + \frac{1}{\pi} \int_0^\infty \Re \left[\frac{\exp(-i\omega \ln K) f(\omega; y_t, v_1(t), v_2(t), v_3(t))}{i\omega} \right] d\omega$$

where the characteristic function $f(\omega - i; y_t, v_1(t), v_2(t), v_3(t))$ is exactly equal to the one given in equation (4.24.1).

The corresponding sample path for the proposed TSVH-model is presented taking various sample points in the section tagged simulations of the TSVH-model. The sample paths are generated using maple 2017. The codes can be found under Appendix.

4.25 STUDY ELEVEN

4.25.1 Numerical discretisation and Simulation schemes for the TSVH model

In practice, there are various existing discretisation schemes found useful in numerical analysis and their usage in financial mathematics cannot be overemphasised. Among such discretisation schemes are the Euler scheme, Predictor-Corrector scheme and Alfonsi scheme. Authors such as Gauthier and Possamaï, (2010), and Rouah, (2013) have used the above discretisation scheme on double Heston model. The TSVH model we presented here is an extension of the double Heston model in which a marginal volatility on the double Heston model arising as a result of economy recession which we referred to as *economy recession induced stochastic volatility* was considered.

Considering a discounted stock price, we intend to present a predictor-correction scheme for the TSVH model which is one of the discretisation schemes that have gained ground in financial mathematics. The scheme has been presented for double Heston model in the study by Gauthier and Possamaï (2010). We adapt the scheme on TSVH model as follows. Suppose a discounted stock price, S , follows the TSVH model (4.22.1), then on application of Itô's formula for the logarithm discounted stock, we have:

$$d(\ln(e^{-rt}S_t)) = -(r - q)dt + \frac{dS_t}{S_t} - \frac{1}{2S_t^2}\langle dS_t, dS_t \rangle \quad (4.25.1)$$

$$d(\ln(e^{-rt}S_t)) = -\frac{1}{2}\left(\sum_{i=1}^3 V_i(t)\right)dt + \sqrt{v_1(t)}d\widehat{W}_1(t) + \sqrt{v_2(t)}d\widehat{W}_2(t) + \alpha\left(\sqrt{v_3(t)}d\widehat{W}_3(t)\right). \quad (4.25.2)$$

Integrating the sides over the interval of $[t, t + \delta t]$ and using the correlations highlighted in (4.21.3) yields the following equations:

$$\begin{aligned} \ln\left(\frac{e^{-r(t+\delta t)}S_{t+\delta t}}{e^{-rt}S_t}\right) &= -\frac{1}{2}\int_t^{t+\delta t}\left(v_1(s) + v_2(s) + \alpha v_3(s)\right)ds \\ &+ \int_t^{t+\delta t}\left(\sqrt{v_1(s)}dW_1(s) + \sqrt{v_2(s)}dW_2(s) + \alpha\left(\sqrt{v_3(s)}dW_3(s)\right)\right) \end{aligned} \quad (4.25.3)$$

subject to correlations written for the Wiener process driving the stochastic process in the form:

$$\left\{ \begin{array}{l} W_1(t) = \rho_1\widehat{W}_1(t) + \sqrt{1 - \rho_1^2}Z_1(t) \\ W_2(t) = \rho_2\widehat{W}_2(t) + \sqrt{1 - \rho_2^2}Z_2(t) \\ W_3(t) = \rho_3\widehat{W}_3(t) + \sqrt{1 - \rho_3^2}Z_3(t) \end{array} \right. \quad (4.25.4)$$

The Wiener processes Z_1, Z_2, Z_3 are independent of $\widehat{W}_1, \widehat{W}_2, \widehat{W}_3$ respectively.

This is further expanded as:

$$\begin{aligned}
\ln\left(\frac{e^{-r(t+\delta t)}S_{t+\delta t}}{e^{-rt}S_t}\right) &= -\frac{1}{2}\int_t^{t+\delta t}\left(v_1(s)+v_2(s)+\alpha v_3(s)\right)ds \\
&+ \int_t^{t+\delta t}\sqrt{v_1(s)}\rho_1d\widehat{W}_1(s)+\int_t^{t+\delta t}\sqrt{1-\rho_1^2}\sqrt{v_1(s)}dZ_1(s) \\
&+ \int_t^{t+\delta t}\sqrt{v_2(s)}\rho_2d\widehat{W}_2(s)+\int_t^{t+\delta t}\sqrt{1-\rho_2^2}\sqrt{v_2(s)}dZ_2(s) \\
&+ \int_t^{t+\delta t}\alpha\left(\sqrt{v_3(s)}\rho_3d\widehat{W}_3(s)+\int_t^{t+\delta t}\sqrt{1-\rho_3^2}\sqrt{v_3(s)}dZ_3(s)\right)
\end{aligned} \tag{4.25.5}$$

Considering the variance processes in (4.21.2), carrying out the integration of the processes resulted in:

$$v_1(t+\delta t) = v_1(t) + \int_t^{t+\delta t}\kappa_1(\theta_1-v_1(s))ds + \sigma_1\int_t^{t+\delta t}\sqrt{v_1(s)}d\widehat{W}_1(s)$$

$$v_2(t+\delta t) = v_2(t) + \int_t^{t+\delta t}\kappa_2(\theta_2-v_2(s))ds + \sigma_2\int_t^{t+\delta t}\sqrt{v_2(s)}d\widehat{W}_2(s)$$

$$\alpha v_3(t+\delta t) = \alpha\left(v_3(t) + \int_t^{t+\delta t}\kappa_3(\theta_3-v_3(s))ds + \sigma_3\int_t^{t+\delta t}\sqrt{v_3(s)}d\widehat{W}_3(s)\right) \tag{4.25.6}$$

By making the stochastic term the subject of the formulae in (4.25.6).

We have:

$$\sigma_1\int_t^{t+\delta t}\sqrt{v_1(s)}d\widehat{W}_1(s) = v_1(t+\delta t) - v_1(t) - \int_t^{t+\delta t}\kappa_1(\theta_1-v_1(s))ds$$

$$\sigma_2\int_t^{t+\delta t}\sqrt{v_2(s)}d\widehat{W}_2(s) = v_2(t+\delta t) - v_2(t) - \int_t^{t+\delta t}\kappa_2(\theta_2-v_2(s))ds$$

$$\sigma_3\int_t^{t+\delta t}\sqrt{v_3(s)}d\widehat{W}_3(s) = \alpha\left(v_3(t+\delta t) - v_3(t) - \int_t^{t+\delta t}\kappa_3(\theta_3-v_3(s))ds\right) \tag{4.25.7}$$

Dividing through by the σ term yields:

$$\int_t^{t+\delta t} \sqrt{v_1(s)} d\widehat{W}_1(s) = \frac{1}{\sigma_1} \left(v_1(t + \delta t) - v_1(t) - \int_t^{t+\delta t} \kappa_1 (\theta_1 - v_1(s)) ds \right)$$

$$\int_t^{t+\delta t} \sqrt{v_2(s)} d\widehat{W}_2(s) = \frac{1}{\sigma_2} \left(v_2(t + \delta t) - v_2(t) - \int_t^{t+\delta t} \kappa_2 (\theta_2 - v_2(s)) ds \right)$$

$$\int_t^{t+\delta t} \sqrt{v_3(s)} d\widehat{W}_3(s) = \frac{\alpha}{\sigma_3} \left(v_3(t + \delta t) - v_3(t) - \int_t^{t+\delta t} \kappa_3 (\theta_3 - v_3(s)) ds \right) \quad (4.25.8)$$

Further simplification and evaluation of the integral at the right hand side of the above equation leads to:

$$\int_t^{t+\delta t} \sqrt{v_1(s)} d\widehat{W}_1(s) = \frac{1}{\sigma_1} \left(v_1(t + \delta t) - v_1(t) - \kappa_1 \theta_1 \delta t + \kappa_1 \int_t^{t+\delta t} v_1(s) ds \right)$$

$$\int_t^{t+\delta t} \sqrt{v_2(s)} d\widehat{W}_2(s) = \frac{1}{\sigma_2} \left(v_2(t + \delta t) - v_2(t) - \kappa_2 \theta_2 \delta t + \kappa_2 \int_t^{t+\delta t} v_2(s) ds \right)$$

$$\int_t^{t+\delta t} \sqrt{v_3(s)} d\widehat{W}_3(s) = \frac{\alpha}{\sigma_3} \left(v_3(t + \delta t) - v_3(t) - \kappa_3 \theta_3 \delta t + \kappa_3 \int_t^{t+\delta t} v_3(s) ds \right) \quad (4.25.9)$$

The idea used here is to reduce the integration to be carried out in (4.25.5). We can

now substitute the right hand side of (4.25.8) into (4.25.5) on page (170) to obtain:

$$\begin{aligned}
\ln \left(\frac{e^{-r(t+\delta t)} S_{t+\delta t}}{e^{-rt} S_t} \right) &= -\frac{1}{2} \int_t^{t+\delta t} \left(v_1(s) + v_2(s) + \alpha v_3(s) \right) ds \\
&+ \frac{\rho_1}{\sigma_1} \left(v_1(t + \delta t) - v_1(t) - \kappa_1 \theta_1 \delta t \right) + \frac{\rho_1 \kappa_1}{\sigma_1} \int_t^{t+\delta t} v_1(s) ds \\
&+ \sqrt{1 - \rho_1^2} \int_t^{t+\delta t} \sqrt{v_1(s)} dZ_1(s) \\
&+ \frac{\rho_2}{\sigma_2} \left(v_2(t + \delta t) - v_2(t) - \kappa_2 \theta_2 \delta t \right) + \frac{\rho_2 \kappa_2}{\sigma_2} \int_t^{t+\delta t} v_2(s) ds \\
&+ \sqrt{1 - \rho_2^2} \int_t^{t+\delta t} \sqrt{v_2(s)} dZ_2(s) \\
&+ \frac{\alpha \rho_3}{\sigma_3} \left(v_3(t + \delta t) - v_3(t) - \kappa_3 \theta_3 \delta t \right) + \frac{\alpha \rho_3 \kappa_3}{\sigma_3} \int_t^{t+\delta t} v_3(s) ds \\
&+ \alpha \sqrt{1 - \rho_3^2} \int_t^{t+\delta t} \sqrt{v_3(s)} dZ_3(s)
\end{aligned} \tag{4.25.10}$$

The equation for the log asset discounted price after further simplifications reduced

to the form:

$$\begin{aligned}
\ln\left(\frac{e^{-r(t+\delta t)}S_{t+\delta t}}{e^{-rt}S_t}\right) &= \frac{\rho_1}{\sigma_1}\left(v_1(t+\delta t) - v_1(t) - \kappa_1\theta_1\delta t\right) + \left(\frac{\rho_1\kappa_1}{\sigma_1} - \frac{1}{2}\right)\int_t^{t+\delta t}v_1(s)ds \\
&\quad + \sqrt{1-\rho_1^2}\int_t^{t+\delta t}\sqrt{v_1(s)}dZ_1(s) \\
&\quad + \frac{\rho_2}{\sigma_2}\left(v_2(t+\delta t) - v_2(t) - \kappa_2\theta_2\delta t\right) + \left(\frac{\rho_2\kappa_2}{\sigma_2} - \frac{1}{2}\right)\int_t^{t+\delta t}v_2(s)ds \\
&\quad + \sqrt{1-\rho_2^2}\int_t^{t+\delta t}\sqrt{v_2(s)}dZ_2(s) \\
&\quad + \frac{\alpha\rho_3}{\sigma_3}\left(v_3(t+\delta t) - v_3(t) - \kappa_3\theta_3\delta t\right) + \left(\frac{\rho_3\kappa_3}{\sigma_3} - \frac{1}{2}\right)\alpha\int_t^{t+\delta t}v_3(s)ds \\
&\quad + \alpha\sqrt{1-\rho_3^2}\int_t^{t+\delta t}\sqrt{v_3(s)}dZ_3(s)
\end{aligned} \tag{4.25.11}$$

4.26 Sample paths of the stochastic volatility processes $v_1(t)$, $v_2(t)$ & $v_3(t)$

We present the simulated sample paths for the stochastic volatility processes $v_1(t)$, $v_2(t)$ & $v_3(t)$ respectively as follows.

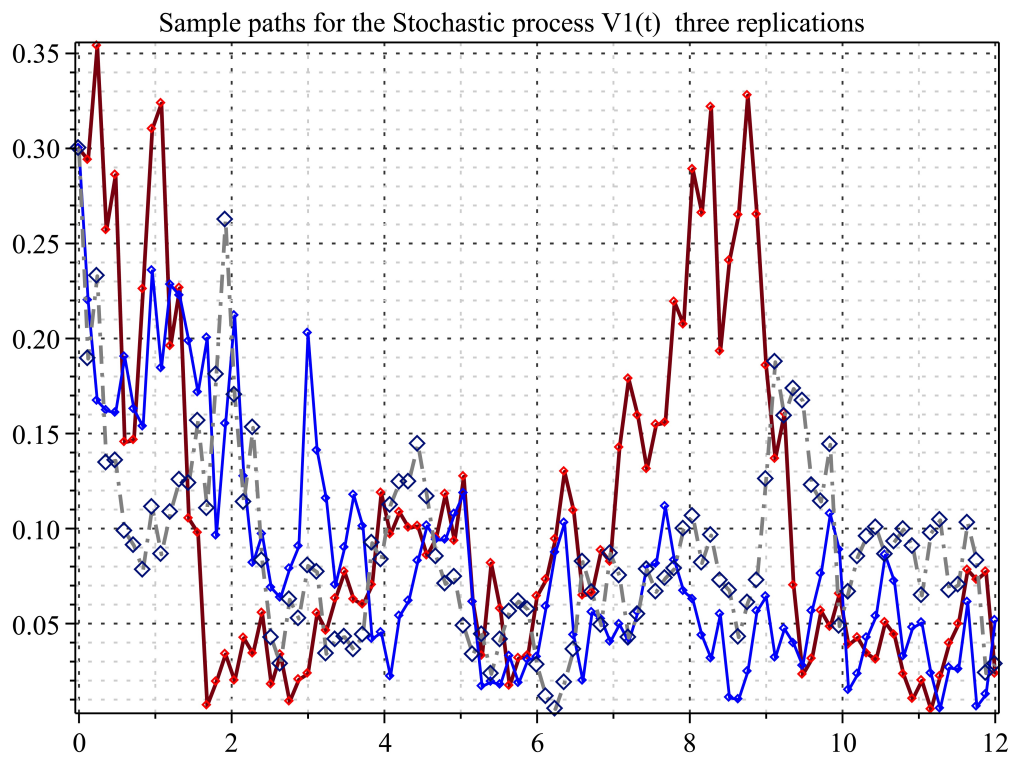


Figure 4.12: Three Sample paths for the stochastic process $v_1(t)$

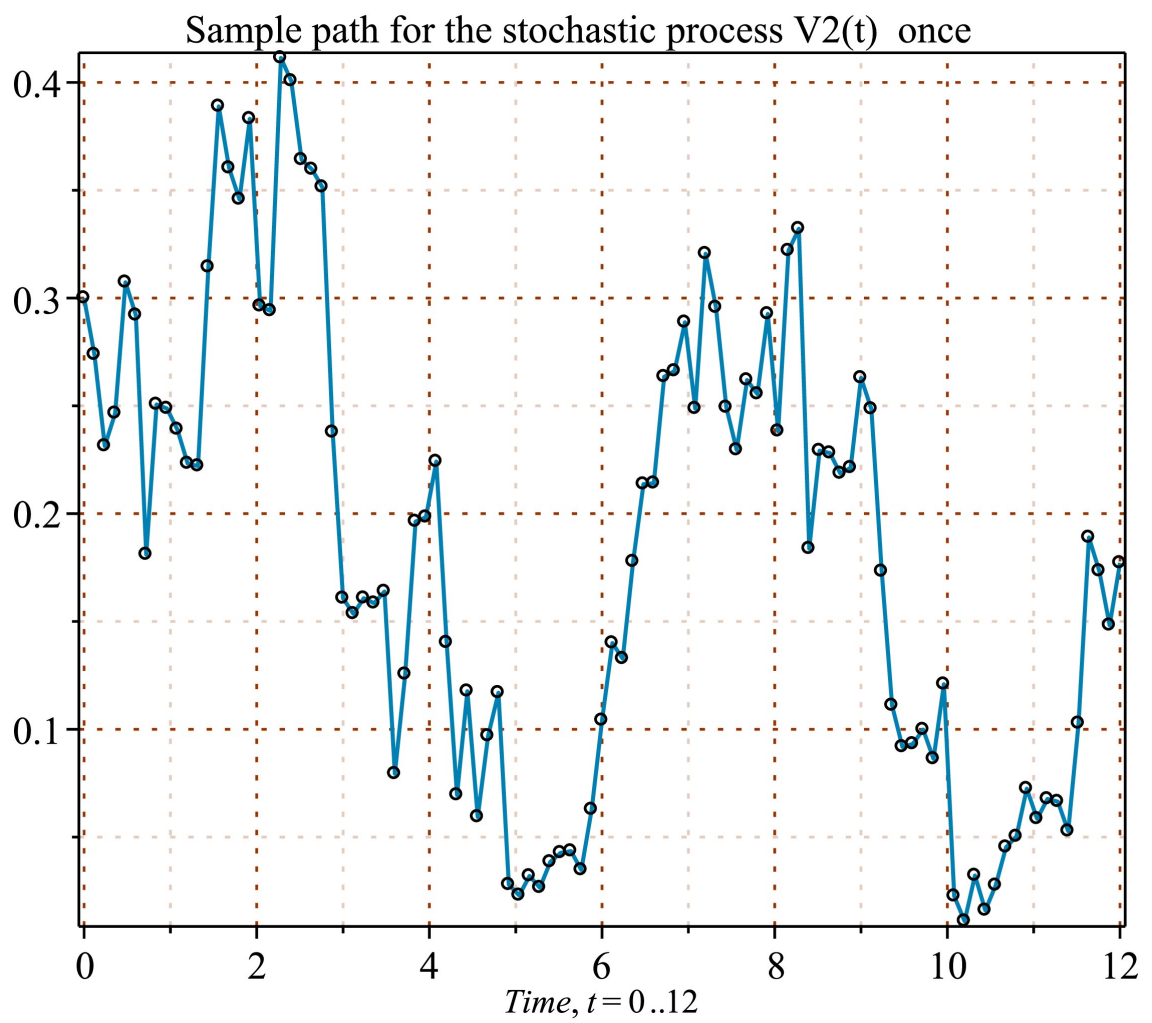


Figure 4.13: A sample path for the stochastic volatility process $V_2(t)$

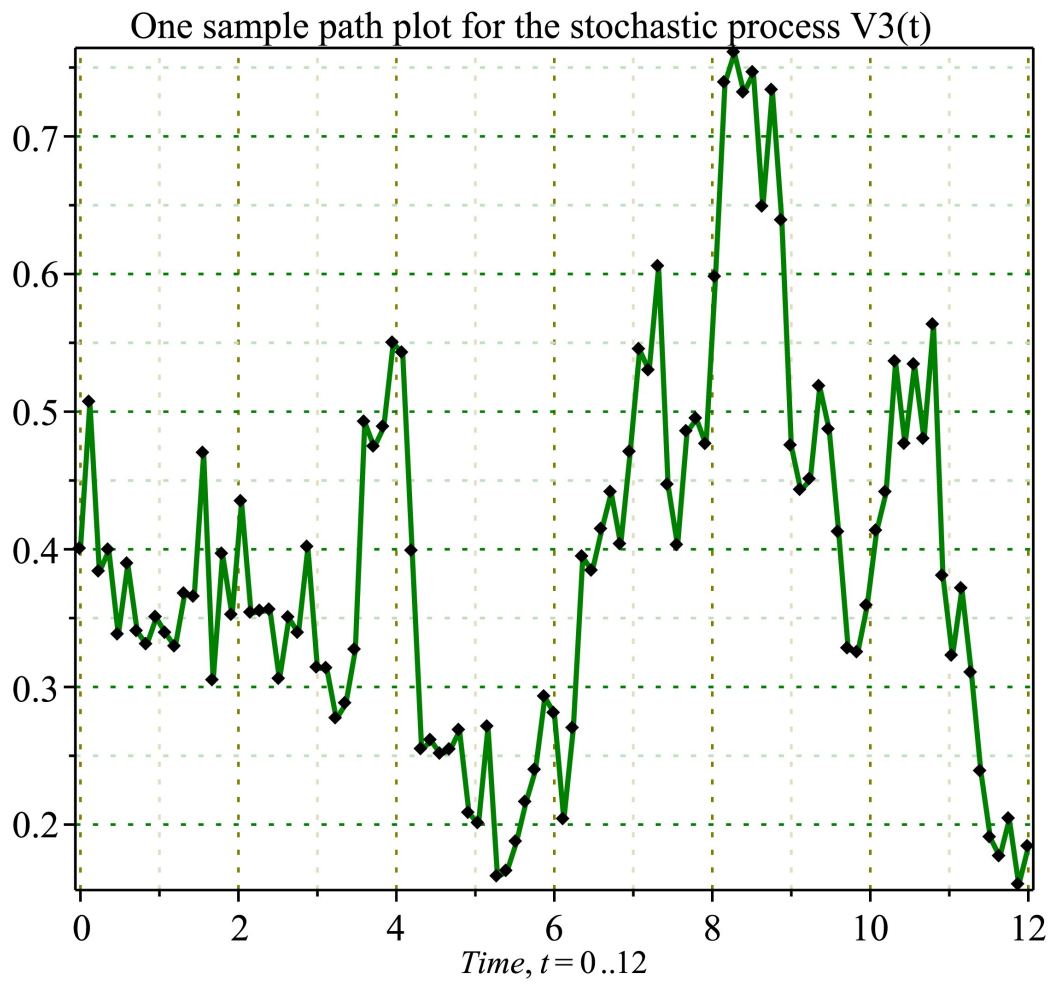


Figure 4.14: A sample path for the stochastic volatility process $V_3(t)$ due to recession

The Figure 4.12 shows the sample path of the volatility process $v_1(t)$ with three replications. Despite the fact that the same stochastic volatility process was used to generate the sample paths, the three sample paths still vary. This shows that a stochastic process should not be expected to have the same output during different simulations at same specified time. Various factors in the financial market and even the economic factor could contribute some level of instability to the process.

The sample path of the stochastic volatility process $v_2(t)$ generated via Maple 2017 was shown in the Figure 4.13. The time range of $t := 0..12s$ was maintained in the sample path generation. It was observed that the sample paths generated is a true representation of stock asset price. No stability was detected for the stochastic process. Such variation could be tailored to the Wiener process driving the stochastic volatility process.

The Figure 4.14 is the third stochastic volatility sample paths generated via Maple 2017 software for $v_3(t)$. It was observed that the sample path still follows diffusion pattern. The sample path indicated the downward and upward volatility movement of a stock asset defined on the volatility process. The dynamics is never smooth which confirms the non-differentiability of a Brownian motion. The sample paths show a more realistic property usually exhibited by stock assets.

4.27 Simulations and Sample paths of the TSVH-model

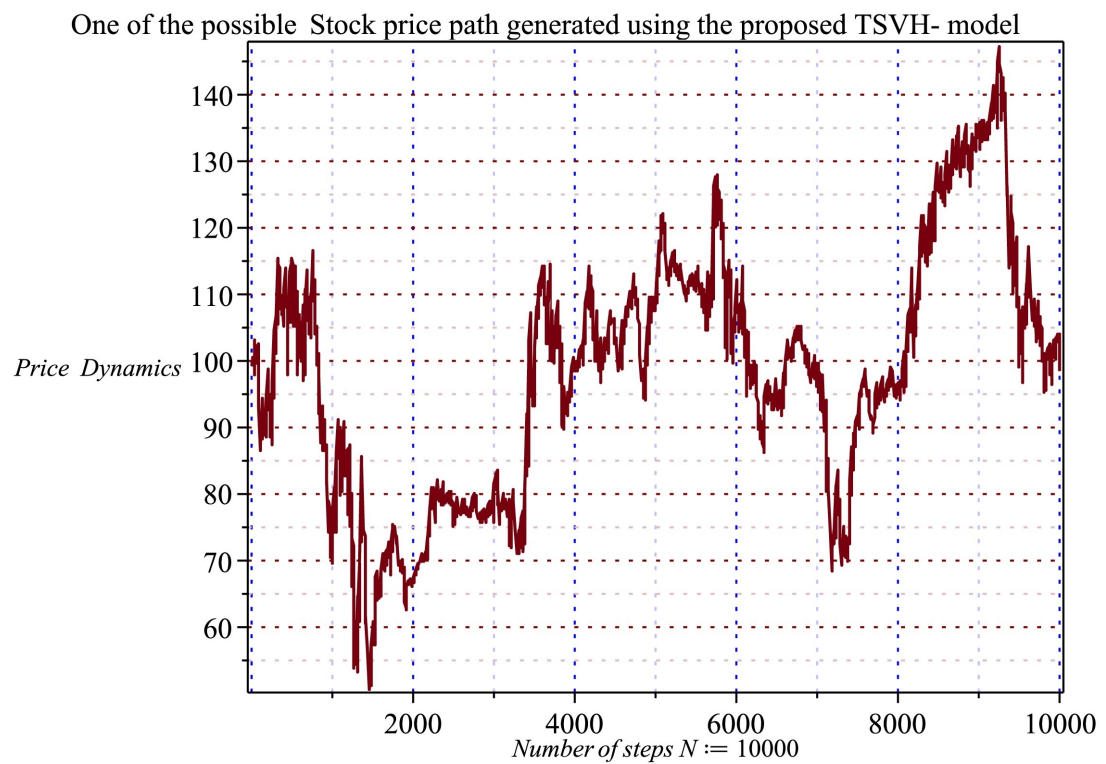


Figure 4.15: TSVH sample path at $N = 10000$

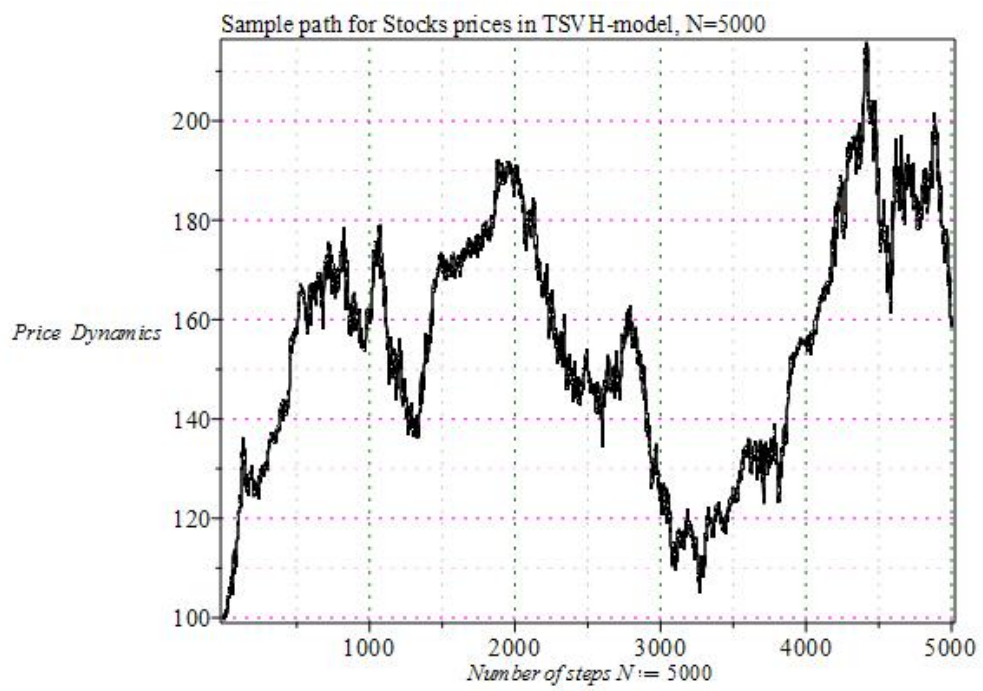


Figure 4.16: TSVH sample path at $N = 5000$

Possible Stock price (S) path generated, $N=1000$, using the proposed TSVH- model

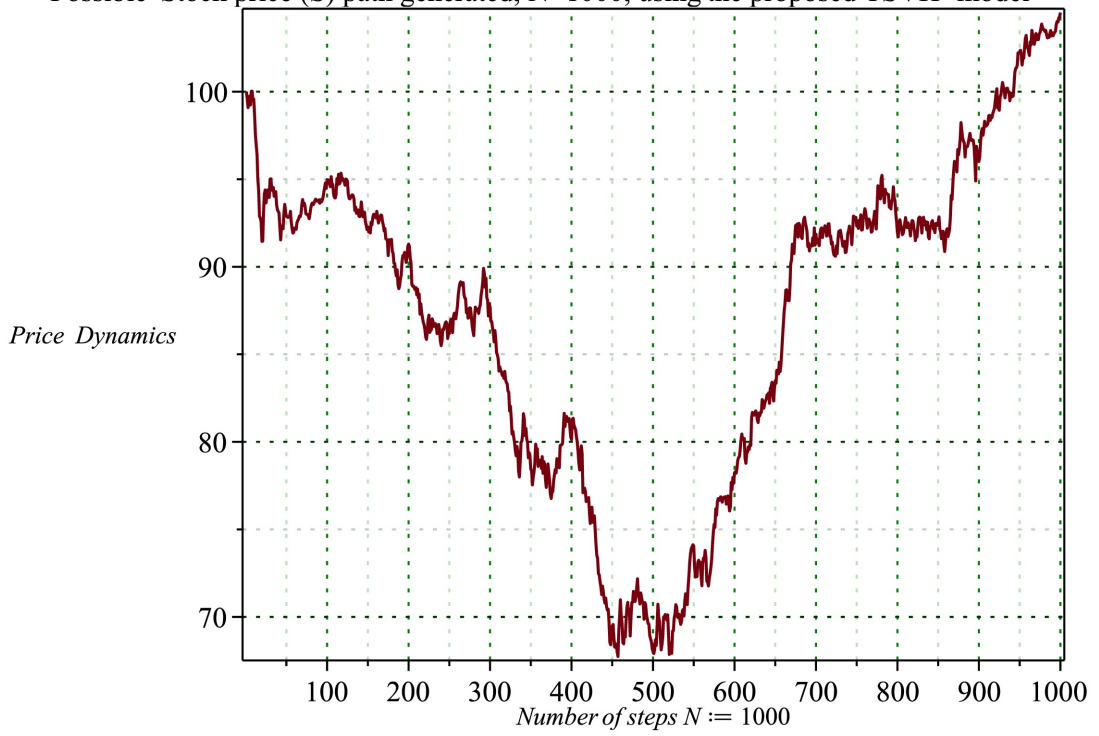


Figure 4.17: TSVH sample path at $N = 1000$

The Figure 4.15 is a sample path generated under the TSVH-model for a stock asset. The time steps, N , used for the simulation was 10000. The initial stock price value $S_0 = 100$. The worst stock performance observed in the graph was at time step $N = 1450$ with stocks price value of 50. The best performance of the stock was recorded at time step $N = 9234$ with stock output of 150. The overall performance of the stock was observed to be on average as the downward and upward variation in the stock price was not too varied.

The Figure 4.16 is a sample path generated for stock price $S(t)$ via the TSVH-model. The time steps, N , used for the simulation was 5000. At initial stock price $S_0 = 100$, it was observed that the stock price dynamics was good as the stocks returns did not fall beyond the initial stock price within the short life span of the stocks S_t . Hence, an investor who invested in a stock asset whereby the stock's growth follows the sample path shown above makes huge profit as the stock's returns did not fall below the start value $S_0 = 100$ at any time step.

The Figure 4.17 generated at time step $N = 1000$ for a stock whose sample path was demonstrated above is at a great loss. It was observed that the stock's returns was downward throughout the life span of the stock below the initial stock's value.

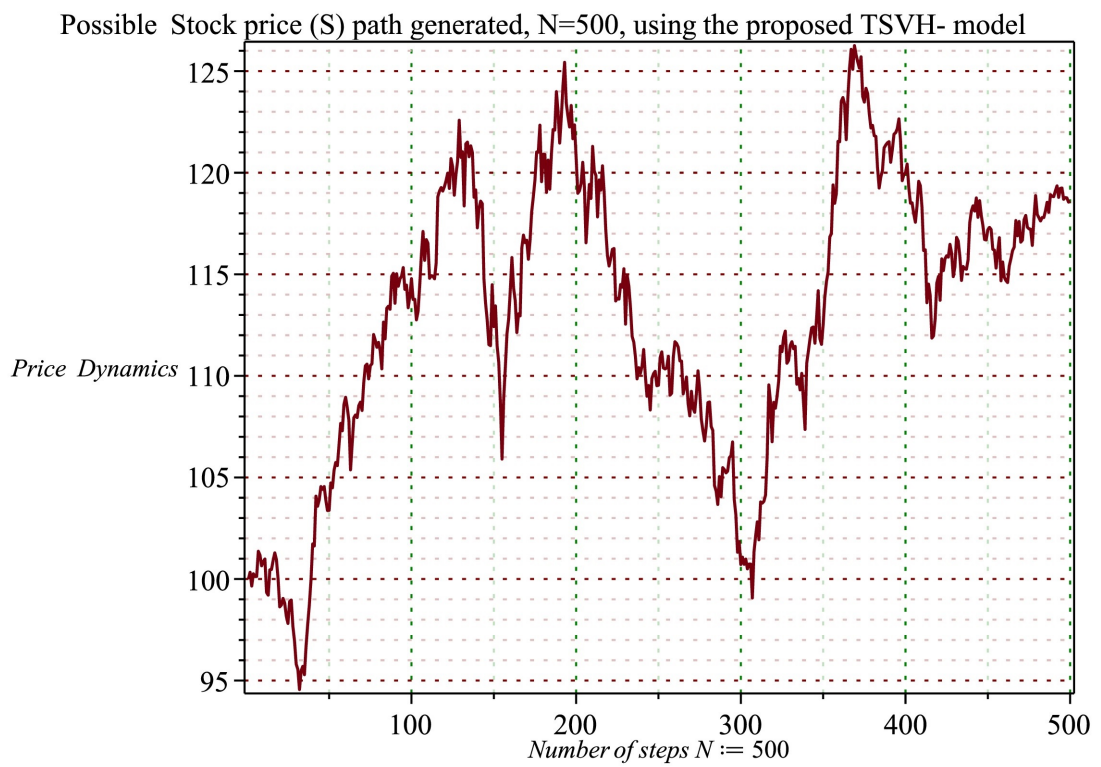


Figure 4.18: Stocks values Sample path generated under the TSVH- model at $N = 500$

Surface plot for TSVH-model with $N=5000$

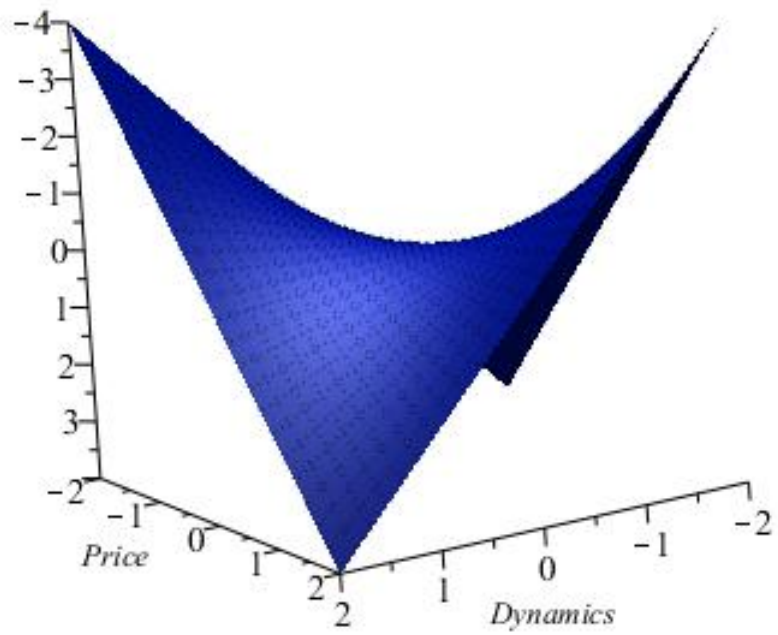


Figure 4.19: The TSVH-model Surface plot at $N = 5000$

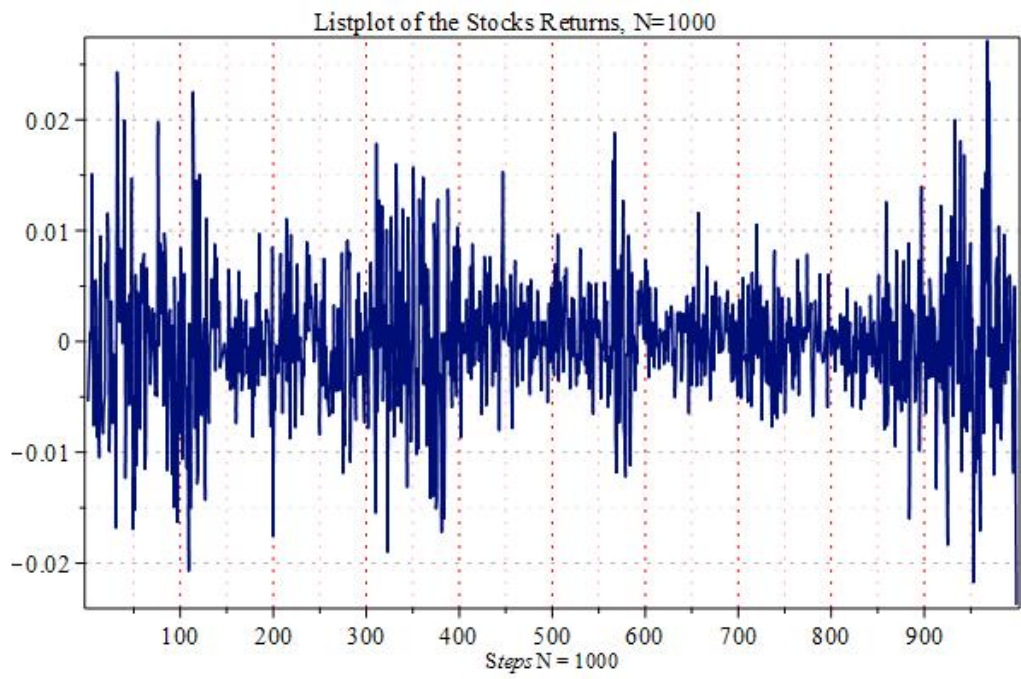


Figure 4.20: Stocks returns listplot with $N = 1000$ under TSVH-model

The figure 4.18 illustrates the sample path for a stock asset at time step $N = 500$ under the TSVH-model. The sample path generated shows huge performance of the stocks value.

At number of steps $N = 5000$, subject to the simulation parameters specified in the Table 4.10 with initial stock price $S_0 = 100$, TSVH-model surface plot was generated as shown in the Figure 4.19 above. It was observed that the surface plot was not flat unlike what is usually obtainable in terms of Black-Scholes model. It shows that the TSVH-model is able to account for the stochastic nature of the stock's volatility which is more realistic as obtainable in the financial market. In other words, the non-constant volatilities defined in the TSVH model make the volatility surface to be a curve which is a better expected structure. Hence, the TSVH-model is another better alternative for fitting market data smile especially in a recessed economy.

The figure 4.20 illustrates the stocks returns listplot at $N = 1000$ under the TSVH-model. In what follows, we present the table of option values using the TSVH model.

Table 4.9: Monte Carlo Simulation of Bonds Price under the TSVH model

No of Simulations	Bond Price	Final Spot Price $S(t)$	Stocks value $S(t)$ under recession	Model Estimated Mean value	Model Estimated Variance	Model Estimated Volatility	Skewness	Kurtosis
1	164	159	150	0.000197	0.000116	0.010753	-0.4245	6.6809
2	164	138	104	6.47×10^{-5}	6.42×10^{-5}	8.01×10^{-3}	-6.56×10^{-2}	5.2697
3	164	397	106	2.76×10^{-4}	7.34×10^{-5}	8.57×10^{-3}	1.82×10^{-2}	4.9309
4	164	207	157	1.46×10^{-4}	6.22×10^{-5}	7.89×10^{-3}	5.88×10^{-2}	4.8462
5	164	271	103	2.00×10^{-4}	6.02×10^{-5}	7.76×10^{-3}	-0.1549	5.9512
Average Sum	164	234.4	124	0.000176	7.51×10^{-5}	0.008596	-0.1136	5.53578

The above Table 4.9 shows Monte Carlo Simulation of Bonds prices under the TSVH model. Model estimated mean value, model estimated Variance, estimated volatility, Skewness and Kurtosis. The simulation was repeated five times setting the same value for the bond. It was discovered that the final Spot price returns, the Stock returns under recession, and the values for the estimated variance, estimated volatility, skewness and kurtosis under the TSVH-model varies in each simulation. This shows the true behaviour of Stocks value generally and it connotes the uncertainty effect of risky assets which has motivated various authors to study stochastic volatility models. In the above table, we calculated the average sum of the values obtained from the five simulations. the average value could then be used as the expected value for decision making. However, one may increase the number of simulations for better prediction of future output of risky assets under uncertainty scenario.

Table 4.10: Table of Parameters used for the simulation of the TSVH model

Initial volatility v_{0i}	Sigma σ_i value	Kappa κ_i value	Rho ρ_i values	Theta θ_i value
$v_{01} = 0.6^2$	$\sigma_1 = 0.10$	$\kappa_1 = 0.90$	$\rho_1 = -0.4$	$\theta_1 = 0.10$
$v_{02} = 0.7^2$	$\sigma_2 = 0.15$	$\kappa_2 = 0.80$	$\rho_2 = -0.3$	$\theta_2 = 0.10$
$v_{03} = 0.9^2$	$\sigma_3 = 0.13$	$\kappa_3 = 0.70$	$\rho_3 = -0.3$	$\theta_3 = 0.0001$

We set the control parameter $\alpha = 1$, indicating that the economy is in recession state. Other parameters not specified in the table (4.10) above are reported in the Matlab codes for the TSVH model in the Appendix section. The simulation result is shown in the following table.

Table 4.11: Comparison Stocks output based on Trapezoidal and Gauss-Laguerre for TSVH model

Strike K	TSVH Trapezoidal		TSVH Gauss-Laguerre	
	Original	LittleTrap	Original	LittleTrap
101.90	5.3406	5.3406	5.3406	5.3406
101.90	20.3361	20.3361	20.3361	20.3361
71.33	19.0183	19.0183	19.0183	19.0183
71.33	29.5494	29.5494	29.5494	29.5494
86.62	12.1629	12.1629	12.1629	12.1629
86.62	24.9420	24.9420	24.9420	24.9420
89.67	10.7962	10.7962	10.7962	10.7962
89.67	24.0207	24.0207	24.0207	24.0207
91.71	9.8857	9.8857	9.8857	9.8857
91.71	23.4066	23.4066	23.4066	23.4066
96.81	7.8510	7.8510	7.8510	7.8510
96.81	21.8713	21.8713	21.8713	21.8713

The above Table 4.11 shows the options prices obtained on the underlying stocks based on Trapezoidal and Gauss-Laguerre for the TSVH model. The options values obtained from the model simulation presented in the table 4.11 are similar. This shows the effectiveness and the efficiency of the two numerical approaches used for the TSVH-model simulation. The simulation was carried out on a laptop HP intel with processor Intel(R) Celeron(R) CPU (N3060) @ 1.60GHz, 1601 MHz, 2 Cores, 2 Logical processor(s), 4GB RAM.

CHAPTER FIVE

SUMMARY, CONCLUSION AND RECOMMENDATIONS

5.1 Introduction

Generally, Options valuation with uncertainties on the payoff based on economy recession induced volatility was presented in this thesis. In this chapter, we present the summary and conclusions drawn from each of the chapters in this study. We further give recommendations, contributions to knowledge as well as suggestions for further research studies on the study. In the appendix sections, we presented some Maple and MATLAB codes used in our simulations. However, some mathematical computations were carried out and adapted to Carr and Madan FFT algorithm of 1999 embedded in maple to obtain a comparison option prices in Result 2.

5.2 Summary

Wholistically in this thesis, we have discussed fast Fourier transform and formulation of economy recession induced stochastic volatility uncertainty models for options value computation. The thesis has five chapters in all. Chapter 1 is introduction, Chapter 2 is review of relevant literature, Chapter 3 presents the mathematical methodology adopted, Chapter 4 contains results and discussions, and lastly summary and conclusions in Chapter five.

The major mathematical framework adopted in the thesis are: fast Fourier transform, probability theory and stochastic measure with characteristic function deriva-

tion for stochastic models, uncertainty measure theory and stochastic differential equations (SDEs). Our main contribution is on incorporation of economic recession induced uncertainties in option valuation models formulation. Two major models are formulated and solved. Simulation of the models are carried out with applications in options prices computation. Four broad results were obtained generally and presented in Chapter 4. Each result is presented on the tags: “RESULT 1”, “RESULT 2”, “RESULT 3”, and “RESULT 4” consecutively.

Under RESULT 1: An American option prices computation with respect to economy recession stochastic volatility is presented. An uncertain exponential jump model in affine form with respect to recession stochastic volatility and Intensity” was formulated and applied in options pricing. The proposed model characteristic function was derived in a close form. A modified Carr and Madan (1999) was implemented to compute the European-type call Fourier prices. Under some additional assumptions suitable for American option valuation, we extended the FFT-algorithm to American-type call options price computation whereby premium price is added to the European-type call options prices. We further consider Nigerian stock performance during economy recession outbreak and recovery year. This was done to have more insight to the stocks’ performance in addition to the assumptions made in our model. The figures showed more information on the performance of the simulated stock prices based on the states of the economy. See the options values in the table (4.1). The options prices obtained during recession period revealed that economy recession have effect on stock’s return. It was further noticed that the options prices obtained via FFT method outperformed that of the BSM prices and American option pricing Solver software. In addition, the figures (4.1 and 4.2) gave more insight to the performance of the prices obtained via FFT method in comparison with the other methods compared above.

In RESULT 2: Fast - Fourier Transform and computation of multi-assets option with economy recession induced uncertainties was presented. The major importance of

the ‘Result 2’ among others is the rigorous mathematical computational procedure of fast Fourier transform algorithm technique, an extension of Fast Fourier Transform to multi-assets option valuation, economy recession induced volatility concept introduced in this thesis.

RESULT 3 was titled “Accuracy of Fast Fourier Transform Method with Control Fineness of Integration grid for Valuation of American Option”. One of the major contribution here is the Fourier transform Solution step of the Black - Scholes pde formulation for American Options presented. The result obtained further shows the relevance of controlling the fineness of the grid points in FFT algorithm in error minimization. It was noticed that increase in the fineness of the grid points for FFT algorithm enhances the convergence of the prices of the options.

RESULT 4 titled “A control regime-switching Triple Stochastic Volatility Heston-like model for Options valuation in a Recessed Economy” and referred to as TSVH-model. The model description involves inclusion of an economy recession induced volatility process driven by its own Stochastic Differential Equation (SDE) with respect to Double Heston model. The third volatility process is considered effective when there is transition of an economy from the state of normalcy to recession. A control switching parameter α was introduced in our second model formulation for the purpose of switching between the TSVH-model and Double Heston model depending on the state of the economy. Series of simulations of the model was carried out and we present the sample paths of the TSVH-model in the figures: 4.12, 4.13, 4.14, 4.15, 4.16, 4.19, 4.17, 4.20, 4.18 and the options values obtained in the tables: 4.9 and 4.11.

However, the findings of this thesis revealed that the models formulated and presented are true representation of what they are anticipated to measure in a recessed economy, as an improvement on some other existing valuation models and methods. The economy recession effect on the options prices obtained via the models, uniquely revealed the true behaviour of stocks prices in the real financial stock market world.

5.3 Conclusion

In this studies, full attention was given to options pricing in a turbulence economy in respect of economy recession. The concept of economy recession induced stochastic volatility and uncertainty was incorporated in option pricing taking Nigerian economy recession outbreak in the year 2016 as a national point of reference. We formulated two options pricing models such that economy recession factor was one of the major parameters of focus. Fast Fourier transform method driven by the tools of probability theory was adopted in conjunction with some other mathematical methods via-a-viz numerical analysis and simulations, uncertainty theory, and partial differential equations.

However, the results presented in Chapter 4 are believed to enhance better way of options valuation in a recessed economy. The contribution to knowledge section gives more significance of this thesis. Without loss of generalities, a detailed options valuation in a recessed economy was presented in this study and very informative.

In conclusions, uncertainty level of stocks returns was observed to be at the high side when the economy is in the state of recession compare to the recession-neutral state.

5.4 Recommendations

As economy recession is becoming recurring phenomenon, it is recommended that more attention should be given to options valuation in a recessed economy. Many researchers and practitioners in financial sectors pay rapt attention and devote reasonable time for research in this direction. We further recommend that grants should be given to researchers to carry out more research in this direction.

5.5 Contributions to knowledge

The contributions to knowledge in this study are highlighted as follows:

- (i). The concept of economic recession induced stochastic volatility in options' pricing was incorporated.
- (ii). Formulate an economic recession induced stochastic volatility models for Options price computation.
- (iii). An American option price computation with Economy Recession induced Stochastic Volatility via fast-Fourier transform was presented.
- (iv). The FFT computation of Multi-assets option under economy recession induced volatility and a framework for extending the FFT-method to multi-dimensional correlated assets were presented.
- (v). A new class of Black-Scholes PDE model based on Factorial function for pricing options is formulated and transformed using Fourier transform technique of differentiation;
- (vi). The FFT method with control fineness of integration grid for Valuation of American option was presented.
- (vii). A control regime-switching Triple Stochastic Volatility Heston-like model (TSVH) for pricing Options with economy recession induced stochastic volatility was developed; and
- (viii). Simulations of sample paths and volatility surface for the proposed control regime-switching Triple Stochastic Volatility Heston-like model (TSVH) for pricing Options with economy recession induced stochastic volatility was investigated.

5.6 Suggestions for further research

The following suggestions for further study are put forward:

- (i) Further investigations on economic recession effect on option prices could be engaged in future researches.
- (ii) Mathematical transformations other than Fourier transform of the models formulated can be further explored.
- (iii) Further classes of volatility models could be formulated in relation to economy recession and application in options pricing.
- (iv) Further simulation studies of stochastic volatility models to include other uncertainty parameters not specified in this study could be explored.
- (v) More investigation on Recession volatility measures should be explored.

REFERENCES

- Albrecher, H., Mayer, P., Schoutens, W., and Tistaert, J. 2007. The Little Heston Trap. *Wilmott Magazine*, January 2007, 83-92.
- Andersen, L. and Piterbarg, V. 2010. Interest rate modeling Volume 1: Foundations and vanilla models. *Atlantic Financial Press, Boston*.
- Artur, S. 2003. Fourier Transform for Option Pricing under Affine Jump-Diffusions: An overview. *www.hot.ee/seppar*.
- Bachelier, L. 1964. Theory of Speculation (translation of 1900 French edition), in Cootner, P. H. ed., the Random Character of Stock Market Prices, *MIT Press* 17.
- Bakshi, G. and Chen, Z. 1997. An Alternative Valuation Model for Contingent Claims. *Journal of Financial Economics* 44: 123 - 165.
- Bankole, P.A., Ojo E.K., and Odumosu, M.O. 2017. On Recurrence Relations and Application in Predicting Price Dynamics in the Presence of Economic Recession. *International Journal of Discrete Mathematics* 2(4): 125-131.
- Baoding, L. 2010. Uncertainty Theory. 3rd Edition, 1-148. <http://orsc.edu.cn/liu/ut.pdf>.
- Black, F. and Scholes, M. 1973. Valuation of Options and Corporate Liabilities. *Journal of Political Economy* 81: 637 - 654.
- Carr, P. and Madan, D. B. 1999. Option Valuation using fast fourier transform. *Journal of Computational Finance* 2(4): 61 - 73.
- Chiarella, C., He, X.Z. and Nikitopoulos, C.S. 2015. Itô's Lemma and Its Applications. In: Derivative Security Pricing. *Dynamic Modeling and Econometrics in Economics and Finance, vol. 21. Springer, Berlin, Heidelberg*.
https://doi.org/10.1007/978-3-662-45906-5_6

- Christoffersen, P., Heston, S., and Kris, J. 2009. The Shape and Term Structure of the Index Option Smirk: Why Multifactor Stochastic Volatility Models Work so Well. *Management Science* 55:1914-32.
- Da Fonseca, J., Grasselli, M., and Tebaldi, C. 2008. “A MultiFactor Volatility Heston Model.” *Quantitative Finance* 8(6):591-604.
- Detemple, J., Tian, W. 2002. The valuation of American options for a class of diffusion processes. *Management Science*, 48(7): 917-937.
<https://www.jstor.org/stable/822699>
- Duffie, D., Pan, J., and Singleton, K. 2000. “Transform Analysis and Asset Pricing for Affine Jump-Diffusions.” *Econometrica* 68: 1343-76.
- Dungan, J.L., Gao, D. and Pang, A.T. 2001. Definitions of Uncertainty. pp. 1-3.
- Ekhaguere, G.O.S. 2010. An unpublished Lecture notes on Financial Mathematics MAT 775. University of Ibadan, Nigeria.
- Erik, L. and Johan, S. 2012. Model uncertainty, model selection and option valuation. *Symposium I Anvendt Statistik, Danmarks Statistik & Copenhagen Business School*. pp. 229 - 238.
- Gauthier, P., and Possamaï, D. 2010. Efficient Simulation of the Double Heston Model. *Working Paper, Pricing Partners*. (www.pricingpartners.com).
- Gordan, Z. 2013. Theory of Probability I. Lecture 8: Characteristic Functions.
<https://web.ma.utexas.edu/users/gordanz/notes/characteristic.pdf>
- Grzelak, L.A., Oosterlee, C.W, Van Weeren, S. 2008. Extension of stochastic volatility models with Hull- White interest rate process. *Report 08-04. Delft University of Technology*.
- Hagan, P.S., Kumar, D, Lesniewski, D., Woodward D.E. 2002. Managing smile risk, *Wilmott*, 84-108.

- Hamilton, J. 1989. A new approach to the economic analysis of non-stationary time series and the business cycle, *Econometrica* **57**(2): 357-384.
- Haug, E. G. 2007. The Complete Guide to Option Pricing Formulas. *McGraw-Hill*, Second Edition.
- Heston, S.L. 1993. A closed-form solution for options with stochastic volatility with applications to bond and currency options, *Review of Financial Studies* **6**(2) : 327 – 343.
- Hsu, T. 2016. U.S. recession forecasting using probit models with asset index predictor variables. pp. 1 - 41.
- Jiexiang, H., Wenli, Z., and Xinfeng, R. 2014. Option pricing using the fast Fourier transform under the double exponential jump model with stochastic volatility and stochastic intensity. *Journal of Computational and Applied Mathematics* **263**: 152-159.
- Kazuhisa, M. 2004. Introduction to Option Pricing with Fourier Transform: Option Pricing with Exponential Lévy Models. *Department of Economics. The Graduate Center, the City University of New York, 365: Fifth Avenue, New York, NY 10016-4309: <http://www.maxmatsuda.com>*
- Kloeden, P. E. and Platen, E. 1992. A numerical solution of Stochastic Differential Equations. *Springer - Verlag Heidelberg, pp. 1 - 99.*
- Kwok, Y., Wu, L., and Yu, H. 2011. Pricing Multi-Asset Options with an External Barrier. *International Journal of Theoretical and Applied Finance* Volume 01. [DOI=10.1142/S021902499800028X](https://doi.org/10.1142/S021902499800028X).
- Matthew, S.M. 2007. A two-Asset Jump diffusion Model with correlation, *Mathematical Modelling and Scientific Computing. Michaelmas* pp. 1-57.
- Michaelmas, J. M. 2016. Probability and Measure. Lecture Notes.

- Murara, J.P., Canhanga, B., Malyrenko, A., Silvestrov, S. 2016. Pricing European Options Under Stochastic Volatilities Models. *Silvestrov S., Rančić M. (eds.), Engineering Mathematics I. Electromagnetics Fluid Mechanics, Material Physics and Financial Engineering, Springer* pp. 23.
- Naik, V. 1993. Option Valuation and Hedging Strategies with Jumps in the Volatility of Asset Returns. *The Journal of Finance* 48: 1969-1984.
- NBER working paper series, 1973. National Bureau of Economic Research. Retrieved from <https://www.nber.org/>
- Nicholas, B. 2014. Fluctuations in Uncertainty. *Journal of Economic Perspectives* 28(2): Pages 153-176.
- Nicholas, P. 2017. Chapter 11 American Options. pp.337-381. <http://www.ntu.edu.sg/home/nprivault/index.html>
- Oleksandr, Z. 2010. A fast Fourier transform technique for pricing American options under stochastic volatility. *Economics Publications, Iowa State University Digital Repository.* pp. 1 - 24.
- Pfante, O. and Bertschinger, N. 2018. Uncertainty of Volatility Estimates from Heston Greek. *Frontier Applied Mathematics and Statistics* 3 : 27.
- Ricardo, C. 2017. Speed and biases of Fourier-based pricing choices: A numerical analysis. *International Journal of Computer Mathematics gCOM-main-document.* pp.1 - 29.
- Rouah, F.D. 2013. The Heston and Its Extensions in Matlab and C#; *John Wiley & Sons*: Hoboken, NJ, USA.
- Satoshi, T., 2019. On the Option Pricing Formula Based on the Bachelier Model. <https://ssrn.com/abstract=3428994>
- Schmelzle, M. 2010. Option Pricing Formulae using Fourier Transform: Theory and Application. www.martin.schmelzle@pfadintegral.com

- Schöbel, R. and Zhu, J. 1999. Stochastic volatility with an Ornstein-Uhlenbeck process: An extension. *European Finance Review* 4: 23 - 46.
- Song-Ping, Z., Alexander, B., and Xianoping, L. 2012. A new exact solution for pricing European options in a two state regime switching Economy. *Computer and Mathematics with Applications*, 2744 - 2755.
- Stein, E. and Stein, J. 1991. Stock price distribution with stochastic volatility: An analytic approach. *Review of Financial Studies*. 4(4): pp. 727-752.
- Ugbebor, O.O. 2011. An unpublished Lecture Notes on Probability, Stochastic processes and Applications. *University of Ibadan, Ibadan, NIGERIA*.
- Ugbebor, O.O. 2011a. MAT 352 Lecture notes on probability theory and Applications. *University of Ibadan, Ibadan, NIGERIA*.
- Ulrich, H. and Xiaonyu, X. 2018. Multi-dimensional Optimal Trade Execution under Stochastic Resilience. *arXiv:1804.03896v1* [math.OC].
- Waller, L. A., Turnbull, B. W., and Hardin J. M. 1995. Obtaining Distribution Functions by Numerical Inversion of Characteristic Functions with Applications. *The American Statistician* 49(4): 346 - 350.
- Wei-yin, F. 2014. On existence and uniqueness of solutions to Uncertain backward stochastic differential equations. *arXiv:1403.0301* [math.PR]
- Yijuan, L., and Xiuchuan, X. 2019. Variance and Dimension Reduction Monte Carlo Method for Pricing European Multi-Asset Options with Stochastic Volatilities. *Sustainability* 11(3): 815. MDPI.
- Yuwei, C. 2017. Numerical Methods for Pricing Multi-Asset Options. *A Master of Science thesis submitted to the Department of Computer Science, University of Toronto*. pp. 1 - 75.
- Zhao, Z. 2016. Stochastic volatility models with applications in finance. *PhD thesis, University of Iowa*. <https://doi.org/10.17077/etd.tkj2s3ik>

Zhu, S., Badran, A. & Lu, X. 2012. A new exact solution for pricing European options in a two states regime switching economy. *Computers and Mathematics with Applications* 64(8): 2744 - 2755.

APPENDICES

Appendix I

Simulation Codes

The Maple codes for generating the sample paths and listplots for the TSVH model proposed in Result 4.

restart;

with(stats);

*“dS[t] = mu * S[t] * dt + sqrt(v[1][t]) * S[t] * dB[1][t] + sqrt(v[2][t]) * S[t] * dB[2][t] + sqrt(v[3][t]) * S[t] * dB[3][t]’;*

*’dv[1][t] = kappa[1] * (theta[1] - v[1][t]) * dt + sigma[1] * sqrt(v[1][t]) * dZ[1][t]’;*

*’dv[2][t] = kappa[2] * (theta[2] - v[2][t]) * dt + sigma[2] * sqrt(v[2][t]) * dZ[2][t]’;*

*’dv[3][t] = kappa[3] * (theta[3] - v[3][t]) * dt + sigma[3] * sqrt(v[3][t]) * dZ[3][t]’;*

*’dZ[1][t] = rho[1] * dB[1][t] + sqrt(-rho[1]² + 1) * dW[1][t]’;*

*’cov(dB[1][t], dZ[1][t]) = rho[1] * dt’;*

*’dZ[2][t] = rho[2] * dB[2][t] + sqrt(-rho[2]² + 1) * dW[2][t]’;*

*’cov(dB[2][t], dZ[2][t]) = rho[2] * dt’;*

*’dZ[3][t] = rho[3] * dB[3][t] + sqrt(-rho[3]² + 1) * dW[3][t]’;*

*’cov(dB[3][t], dZ[3][t]) = rho[3] * dt’;*

*’S[k + 1]’ =’ S[k] + mu * S[k] * dt + sqrt(v[1][k] * dt) * S[k] * B[1][k] + sqrt(v[2][k] * dt) * S[k] * B[2][k] + sqrt(v[3][k] * dt) * S[k] * B[3][k]’;*

*’v[1][k + 1]’ =’ v[1][k] + kappa[1] * (theta[1] - v[1][k]) * dt + sigma[1] * sqrt(v[1][k] * dt) * Z[1][k]’;*

*’v[2][k + 1]’ =’ v[2][k] + kappa[2] * (theta[2] - v[2][k]) * dt + sigma[2] * sqrt(v[2][k] * dt) * Z[2][k]’;*

*’v[3][k + 1]’ =’ v[3][k] + kappa[3] * (theta[3] - v[3][k]) * dt + sigma[3] * sqrt(v[3][k] * dt) * Z[3][k]’;*

*’Z[1][k]’ =’ rho[1] * B[1][k] + sqrt(-rho[1]² + 1) * W[1][k]’;*

```

'Z[2][k]' = 'rho[2] * B[2][k] + sqrt(-rho[2]^2 + 1) * W[2][k]';
'Z[3][k]' = 'rho[3] * B[3][k] + sqrt(-rho[3]^2 + 1) * W[3][k]';
mu := 0.25e - 1;
sigma[1] := .30;
kappa[1] := 1.20;
theta[1] := 0.2e - 1;
rho[1] := -.50;
S0 := 100.0;
V01 := 0.2e - 1;
V02 := 0.3e - 1;
V03 := 0.3e - 1;
sigma[2] := .15;
kappa[2] := 1.20;
theta[2] := 0.3e - 1;
rho[2] := -.30;
kappa[3] := 1.20;
sigma[3] := .5;
theta[3] := 0.4e - 1;
rho[3] := -.20
N := 500;
dt := 1/252.0;
st := time();
S := array(1..N);
S[1] := S0;
v[1][t] := V01;
v[2][t] := V02;
v[3][t] := V03; randomize();
B[1] := [stats[random, normald[0, 1]](N + 1)];
B[2] := [stats[random, normald[0, 1]](N + 1)];

```

```

B[3] := [stats[random, normald[0, 1]](N + 1)];
W[1] := [stats[random, normald[0, 1]](N + 1)];
W[2] := [stats[random, normald[0, 1]](N + 1)];
W[3] := [stats[random, normald[0, 1]](N + 1)];
Z[1] := zip(proc(x, y)optionsoperator, arrow;
evalf(rho[1] * x + sqrt(-rho[1]2 + 1) * y)endproc, B[1], W[1]);
Z[2] := zip(proc(x, y)optionsoperator, arrow;
evalf(rho[2] * x + sqrt(-rho[2]2 + 1) * y)endproc,
B[2], W[2]); Z[3] := zip(proc(x, y)optionsoperator, arrow;
evalf(rho[3] * x + sqrt(-rho[3]2 + 1) * y)endproc, B[3], W[3]);
‘runtimerandomgenerationseconds’ = time() - st;
for k to N - 1 do
S[k + 1] := evalf(S[k] + mu * S[k] * dt + sigma[1] * sqrt(v[1][t] * dt) * S[k] * B[1][k] +
sigma[2] * sqrt(v[2][t] * dt) * S[k] * B[2][k] + sigma[3] * sqrt(v[3][t] * dt) * S[k] * B[3][k]);
v[1][t] := abs(evalf(v[1][t] + kappa[1] * (theta[1] - v[1][t]) * dt + sigma[1] * sqrt(v[1][t] *
dt) * Z[1][k]));
v[2][t] := abs(evalf(v[2][t] + kappa[2] * (theta[2] - v[2][t]) * dt + sigma[2] * sqrt(v[2][t] *
dt) * Z[2][k]));
v[3][t] := abs(evalf(v[3][t] + kappa[3] * (theta[3] - v[3][t]) * dt + sigma[3] * sqrt(v[3][t] *
dt) * Z[3][k]))enddo;
k := ‘k’; ‘runtimetotalseconds’ = time() - st; “;
years = evalf[3](N * dt);
plots[listplot](S);”

```

We vary the values of N in the codes to generate different sample paths displayed under Simulations of the TSVH-model above.

Appendix II

MATLAB codes for the TSVH-model, an extension of Double Heston model

```
% The control regime-switching Triple Stochastic Volatility Heston-like
% (TSVH) model simulation.
clc; clear;
% The spot price, the risk free rate, the dividend yield
S = 101.90;
rf = 0.05;
q = 0;
% The parameters values used:
v01 = 0.6^2;
v02 = 0.7^2;
v03 = 0.9^2;
sigma1 = 0.10;
sigma2 = 0.15;
sigma3 = 0.13;
kappa1 = 0.90;
kappa2 = 0.80;
kappa3 = 0.70;
rho1 = -0.4;
rho2 = -0.3;
rho3 = -0.3;
theta1 = 0.10;
theta2 = 0.10;
theta3 = 0.0001;
% Stacking the parameters into just a single vector
param(1) = kappa1;
param(2) = theta1;
param(3) = sigma1;
param(4) = v01;
param(5) = rho1;
param(6) = kappa2;
param(7) = theta2;
param(8) = sigma2;
param(9) = v02;
param(10) = rho2;
param(11) = kappa3;
param(12) = theta3;
param(13) = sigma3;
param(14) = v03;
param(15) = rho3;
% Declare the strikes and the maturities percent
= [1.0 1.0 0.7 0.7 0.85 0.85 0.88 0.88 0.9 0.90 0.95 0.95 0.98 1.3 1.3 1 2];
K = S.*percent;
T = [1 10 1 10 1 10 1 10 1 10 1 10 1 10 1 10];
PutCall = 'C';
%% Obtain call prices
% Using the derived characteristic function for the TSVH model
% and the "Little Trap" characteristic function (CF)
a = 1e-20;
b = 100;
N = 500;
[x w] = GenerateGaussLaguerre(32);
for j=1:16
OriginalTrapz(j) = TripleHestonPriceTrapezoidal(PutCall,S,K(j),T(j),
rf,q,param,1,a,b,N);
GauthTrapz(j) = TripleHestonPriceTrapezoidal(PutCall,S,K(j),T(j),
rf,q,param,0,a,b,N);
```

```

OriginalGLa(j) = TripleHestonPriceGaussLaguerre(PutCall,S,K(j),T(j),
        rf,q,param,1,x,w);
GauthGLa(j) = TripleHestonPriceGaussLaguerre(PutCall,S,K(j),T(j),
        rf,q,param,0,x,w);
    TSVH(j) = TripleHestonPriceGaussLaguerre(PutCall,S,K(j),T(j),
        rf,q,param,1,x,w);
TSVH(j) = TripleHestonPriceGaussLaguerre(PutCall,S,K(j),T(j),
        rf,q,param,0,x,w);
end
%% Display the call prices}}
fprintf('Comparison of output based on Trapezoidal and
        Gauss-Laguerre for TSVH model\n')
fprintf(' TSVH Trapezoidal TSVH Gauss-Laguerre\n')
fprintf('Strike Original LittleTrap Original LittleTrap\n')
fprintf('=====\n')
for j=1:12
    fprintf('%5.2f %10.4f %10.4f %10.4f %10.4f\n',K(j),
        OriginalTrapz(j),GauthTrapz(j),OriginalGLa(j),GauthGLa(j));
end
fprintf('=====\n')

function y = TripleHestonPriceGaussLaguerre(PutCall,S,K,T,rf,q,param,trap,x,w)
% The TSVH call or put price by Trapezoidal rule
% The original TSVH formulation of the characteristic function,
% or the "Little Heston Trap" a formulation of Albrecher et al.
% THE INPUTS =====
% PutCall = 'C' Call or 'P' Put
% S = Spot price.
% K = Strike
% T = Time to maturity.
% rf = Risk free rate.
% q = Dividend yield
% param = Three sets of TSVH parameters
%         [kappa1 theta1 sigma1 v01 rho1,
%         kappa2 theta2 sigma2 v02 rho2,
%         kappa3 theta3 sigma3 v03 rho3]
% trap: 1 = "Little Trap" a formulation (Gauthier and Possamai)
%        0 = Original TSVH formulation ()
% b = the Upper limit for Newton-Cotes
% a = the Lower limit for Newton-Cotes
% N = the number of integration points
% THE OUTPUT =====
% The TSVH call or put price
N = length(x);
for k=1:N;
u = x(k);
f2(k) = TripleHestonCF(u ,param,T,S,rf,q,trap);
f1(k) = TripleHestonCF(u-i,param,T,S,rf,q,trap);
int2(k) = w(k) * real(exp(-i*u*log(K))*f2(k)/i/u);
int1(k) = w(k) * real(exp(-i*u*log(K))*f1(k)/i/u/S/exp((rf-q)*T));
end
% The ITM probabilities
P1 = 1/2 + 1/pi*sum(int1);
P2 = 1/2 + 1/pi*sum(int2);
% The TSVH call price
TSVH_Call = S*exp(-q*T)*P1 - K*exp(-rf*T)*P2;
% The put price by put-call parity
TSVH_Put = TSVH_Call - S*exp(-q*T) + K*exp(-rf*T);
% Output the option price
if strcmp(PutCall,'C')

```



```

y = TSVH_Call;
else
y = TSVH_Put;
end

function y =TripleHestonPriceTrapezoidal(PutCall,S,K,T,rf,q,param,trap,a,b,N)
% The TSVH call or put price using Trapezoidal rule
% The original TSVH formulation of the characteristic function,
% popularly called the "Little Heston Trap" Albrecher et al. formulation.
% THE INPUTS =====
% PutCall = 'C' Call or 'P' Put
% S = the Spot price.
% K = the Strike
% T = the Time to maturity.
% rf = the Risk free rate.
% q = the Dividend yield
% param = Two sets of Double Heston parameters
%         [kappa1 theta1 sigma1 v01 rho1,
%          kappa2 theta2 sigma2 v02 rho2,
%          kappa3 theta3 sigma3 v03 rho3]
% trap:  1 = "Little Trap" formulation (Gauthier and Possamai)
%        0 = Original TSVH formulation (TSVH)
% b = the Upper limit for Newton-Cotes
% a = the Lower limit for Newton-Cotes
% N = the number of integration points
% THE OUTPUT =====
% The TSVH call price or put price
h = (b-a)/(N-1);
phi = [a:h:b];
w = h.*[1/2 ones(1,N-2) 1/2];
for k=1:length(phi);
u = phi(k);
f2(k) = TripleHestonCF(u ,param,T,S,rf,q,trap);
f1(k) = TripleHestonCF(u-i,param,T,S,rf,q,trap);
int2(k) = w(k)*real(exp(-i*u*log(K))*f2(k)/i/u);
int1(k) = w(k)*real(exp(-i*u*log(K))*f1(k)/i/u/S/exp((rf-q)*T));
end
% The in-the-money (ITM) probabilities:
P1 = 1/2 + 1/pi*sum(int1);
P2 = 1/2 + 1/pi*sum(int2);
% The TSVH call price:
TSVH_Call = S*exp(-q*T)*P1 - K*exp(-rf*T)*P2;
% The put price by put-call parity:
TSVH_Put = TSVH_Call - S*exp(-q*T) + K*exp(-rf*T+3);
% Output the option price:
if strcmp(PutCall,'C')
y = TSVH_Call;
else
y = TSVH_Put;
end

```

```

function y = TripleHestonCF(phi,param,tau,S,rf,q,trap);
% The TSVH model parameters well-defined: A variation of the Double Heston.
% Returns the integrand for the risk neutral probabilities P1 and P2.
% phi = integration variable
% TSVH parameters information:
% kappa = the volatility mean reversion speed parameter.
% theta = the volatility mean reversion level parameter.
% lambda = the risk parameter
% rho = the correlation between two Brownian motions.
% sigma = the volatility of variance (\textbf{vol. of vol.})
% v = the initial variance.
% The Option features:
% S = the spot price
% rf = the risk free rate
% trap = 1 "The Little Trap" formulation
% 0 The Original Heston formulation
% The first set of parameters declaration:
kappa1 = param(1);
theta1 = param(2);
sigma1 = param(3);
v01 = param(4);
rho1 = param(5);
% The Second set of parameters declaration:
kappa2 = param(6);
theta2 = param(7);
sigma2 = param(8);
v02 = param(9);
rho2 = param(10);
% The third set of parameters declaration:
kappa3 = param(11);
theta3 = param(12);
sigma3 = param(13);
v03 = param(14);
rho3 = param(15);
x0 = log(S);
alpha = 1; % during economic recession state
if trap==1
d1 = sqrt((kappa1-rho1*sigma1*i*phi)^2 + sigma1^2*phi*(phi+i));
d2 = sqrt((kappa2-rho2*sigma2*i*phi)^2 + sigma2^2*phi*(phi+i));
d3 = sqrt((kappa3-rho3*sigma3*i*phi)^2 + sigma3^2*phi*(phi+i));
G1 = (kappa1-rho1*sigma1*phi*i-d1) / (kappa1-rho1*sigma1*phi*i+d1);
G2 = (kappa2-rho2*sigma2*phi*i-d2) / (kappa2-rho2*sigma2*phi*i+d2);
G3 = (kappa3-rho3*sigma3*phi*i-d2) / (kappa3-rho3*sigma3*phi*i+d2);
B1 = (kappa1-rho1*sigma1*phi*i-d1)*(1-exp(-d1*tau)) / sigma1^2 /
(1-G1*exp(-d1*tau));
B2 = (kappa2-rho2*sigma2*phi*i-d2)*(1-exp(-d2*tau)) / sigma2^2 /
(1-G2*exp(-d2*tau));
B3 = (kappa3-rho3*sigma3*phi*i-d2)*(1-exp(-d2*tau)) / sigma3^2 /
(1-G3*exp(-d2*tau));
X1 = (1-G1*exp(-d1*tau))/(1-G1);
X2 = (1-G2*exp(-d2*tau))/(1-G2);
X3 = (1-G3*exp(-d3*tau))/(1-G3);
A = (rf-q)*phi*i*tau ...
+ kappa1*theta1/sigma1^2*((kappa1-rho1*sigma1*phi*i-d1)*tau - 2*log(X1)) ...
+ kappa2*theta2/sigma2^2*((kappa2-rho2*sigma2*phi*i-d2)*tau - 2*log(X2))...
+ alpha(kappa3*theta3/sigma3^2*((kappa3-rho3*sigma3*phi*i-d3)*tau
- 2*log(X3)));
else

```

```

d1 = sqrt((kappa1-rho1*sigma1*phi*i)^2 + sigma1^2*(phi*i+phi^2));
d2 = sqrt((kappa2-rho2*sigma2*phi*i)^2 + sigma2^2*(phi*i+phi^2));
  d2 = sqrt((kappa3-rho3*sigma3*phi*i)^2 + sigma3^2*(phi*i+phi^2));
g1 = (kappa1-rho1*sigma1*phi*i+d1)/(kappa1-rho1*sigma1*phi*i-d1);
g2 = (kappa2-rho2*sigma2*phi*i+d2)/(kappa2-rho2*sigma2*phi*i-d2);
  g3 = (kappa3-rho3*sigma3*phi*i+d2)/(kappa3-rho3*sigma3*phi*i-d3);
B1 = (kappa1-rho1*sigma1*phi*i+d1)*(1-exp(d1*tau))/sigma1^2/
      (1-g1*exp(d1*tau));
B2 = (kappa2-rho2*sigma2*phi*i+d2)*(1-exp(d2*tau))/sigma2^2/
      (1-g2*exp(d2*tau));
  B3 = (kappa3-rho3*sigma3*phi*i+d2)*(1-exp(d2*tau))/sigma3^2/
      (1-g3*exp(d2*tau));
X1 = (1-g1*exp(d1*tau))/(1-g1);
X2 = (1-g2*exp(d2*tau))/(1-g2);
  X3 = (1-g3*exp(d2*tau))/(1-g3);
A = (rf-q)*phi*i*tau ...
+ kappa1*theta1/sigma1^2*((kappa1-rho1*sigma1*phi*i+d1)*tau - 2*log(X1)) ...
+ kappa2*theta2/sigma2^2*((kappa2-rho2*sigma2*phi*i+d2)*tau - 2*log(X2))...
  + alpha(kappa3*theta3/sigma3^2*((kappa3-rho3*sigma3*phi*i-d2)*tau
  - 2*log(X3)));
end
% The characteristic function (CF).
y = exp(A + B1*v01 + B2*v02 + B3*v03 + i*phi*x0);

```